Identification of innate immune components as biomarkers of early liver inflammation

DISSERTATION ZUR ERLANGUNG DES
DOKTORGRADES DER NATURWISSENSCHAFTEN (DR. RER. NAT.)
DER FAKULTÄT FÜR BIOLOGIE UND VORKLINISCHE MEDIZIN
DER UNIVERSITÄT REGENSBURG

vorgelegt von

Jordi Yang Zhou

Aus Spanien

im Jahr 2023

Das Promotionsgesuch wurde eingereicht am: 23. Mai 2023

Die Arbeit wurde angeleitet von: Prof. Dr. Edward K. Geissler

Unterschrift:

_____

(Jordi Yang Zhou)

Table of Contents

A. Summary

The liver is a strong innate immune organ with a repertoire of liver-resident immune cells. The innate immune system operates as the first-line defense against pathogens but also induces tolerance to harmless antigens. Innate-like immune cells, namely, invariant Natural Killer T cells (iNKT), Type II NKT cells (T2NKT), Mucosal-associated invariant T cells (MAIT) and γδ T cells, contribute to liver homeostasis and pathogenesis (Figure 1). Liver diseases originate from excessive inflammation but it is unlikely to be diagnosed until the late stages. This represents a gap in the clinical management of patients.

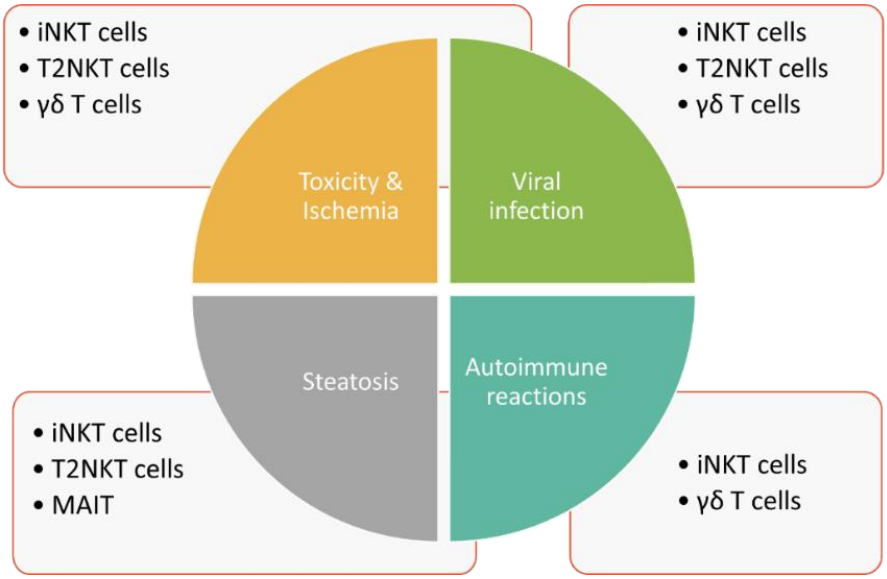

Figure 1. The contribution of different subsets of hepatic innate-like immune cells in liver diseases.

In this thesis, I address in Chapter 1 the role of innate immune cells in early liver inflammation and the patterns of inflammation according to liver pathology. Chapter 2 presents a case report of a patient with a liver transplant and recurrent hepatocellular carcinoma. Traditional liver function tests and immune cell biomarkers are discussed as poor biomarkers of therapy response and graft rejection. From Chapters 3-5, I evaluate the use of innate immune cells as biomarkers. Chapter 3 tackles T2NKT cells as potential biomarkers and their limitations. Chapter 4 explores iNKT cells as biomarkers of steatosis. Chapter 5 studies a receptor in hepatocytes that modulates iNKT cells' function. The dysregulation of the receptor in steatosis is explored as a biomarker of early liver pathogenesis. Chapter 6 integrates the findings of my work in a broader context and discusses the contributions to the field.

- PUBLISHED ARTICLE –

Published in: Frontiers in Immunology. 2023 May;

https://doi.org/10.3389/fimmu.2023.1175147

1. Introduction: Innate Immunity and Early Liver Inflammation

Jordi Yang Zhou[1,2]

1. Department of Surgery, University Hospital Regensburg, Regensburg, Germany
2. Leibniz Institute for Immunotherapy, Regensburg, Germany

* *Corresponding author*: Jordi Yang Zhou PhD(c)
Department of Surgery
University Hospital Regensburg,
Franz-Josef-Strauß-Allee 11
93053 Regensburg, Germany
Tel: 0049 941 944 6961
Email: Jordi.Yang-Zhou@klinik.uni-regensburg.de

1.1 Abstract

The innate system constitutes a first-line defence mechanism against pathogens. 80 % of the blood supply entering the human liver arrives from the splanchnic circulation through the portal vein, so it is constantly exposed to immunologically active substances and pathogens from the gastrointestinal tract. Rapid neutralization of pathogens and toxins is an essential function of the liver, but so too is avoidance of harmful and unnecessary immune reactions. This delicate balance of reactivity and tolerance is orchestrated by a diverse repertoire of hepatic immune cells. In particular, the human liver is enriched in many innate immune cell subsets, including Kupffer cells (KCs), innate lymphoid cells (ILCs) like Natural Killer (NK) cells and ILC-like unconventional T cells – namely Natural Killer T cells (NKT), γδ T cells and Mucosal-associated Invariant T cells (MAIT). These cells reside in the liver in a memory-effector state, so they respond quickly to trigger appropriate responses. The contribution of aberrant innate immunity to inflammatory liver diseases is now being better understood. In particular, we are beginning to understand how specific innate immune subsets trigger chronic liver inflammation, which ultimately results in hepatic fibrosis. In this review, we consider the roles of specific innate immune cell subsets in early inflammation in human liver disease.

1.2 Introduction

Understanding the liver´s architecture and the niches formed by the different hepatic immune cells is equally important to deciphering their immune roles. The liver is subdivided into hepatic lobules, which consist of a portal triad (hepatic artery, portal vein and bile duct), hepatocytes arranged in linear cords between a capillary network (sinusoids) and a central vein (Figure 1). The blood flows from the portal triad to the central vein. The vascular system connecting the portal triad to the central vein is mainly constituted by liver sinusoidal endothelial cells (LSECs). Large fenestrae allow the exchange of macromolecules and components from the sinusoids with hepatocytes [1, 2]. Interestingly, hepatocytes have different functions based on their zoning. Close to the portal triad, hepatocytes are the first to interact with gut-derived antigens whereas hepatocytes in proximity to the central vein are associated with detoxification [3]. The gradual change in blood nutrients, oxygen and antigen load is correlated with significant changes in hepatocytes´ gene expression signature [3, 4]. Immune cells could also perform different functions according to their position within the liver. The distribution of innate cells in the liver is based on different chemokines, adhesion molecules and surface receptors [5]. KCs are located adherent in the sinusoids and emit extensions into the Disse space. KCs along with LSECs constitute part of the reticuloendothelial system, which clears debris and harmful compounds in the blood. 65 % of intrahepatic lymphocytes consist of NK cells, NKT cells, MAIT cells and γδ T cells [6–8] (Figure 2A, B). NK cells are in close proximity to KCs in both mouse and human models, suggesting a physical co-dependence [9, 10]. NKT cells are constantly surveilling the liver sinusoids and stop when they detect inflammatory signals [9]. CXCR6 was identified as a receptor to regulate mouse intrahepatic NKT cell frequencies and its ligand CXCL16 is overexpressed in macrophages and endothelium near injury areas [10]. Human γδ T cells were identified in portal sections and in association with biliary epithelium [11]. Human MAIT cells are reported to reside predominantly

around bile ducts [12]. However, the distribution and frequency of innate cells during inflammation are drastically changed with the recruitment of immune cells to the site of inflammation [9].

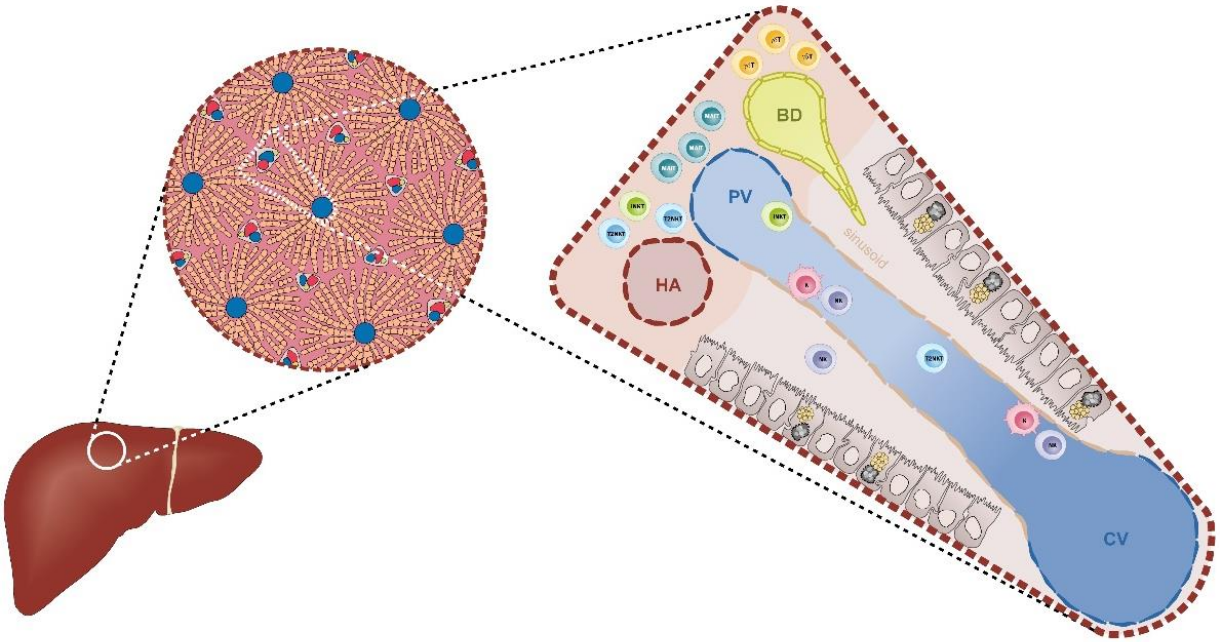

Figure 1. Diagrammatic representation of the liver architecture. The classical hexagonal lobule constitutes the anatomic unit of the liver. The lobule´s parenchyma is mainly formed by hepatocytes that are distributed along the sinusoids. The portal triad, formed by the hepatic artery (HA), the portal vein (PV) and the biliary duct (BD), carries the blood supply towards the centroid of the lobule where it is collected by the central vein (CV). Within the sinusoids, Kupffer cells (K) and Natural Killer cells (NK) are located in close proximity to the endothelium (beige). Other ILC-like cells such as iNKT cells and T2NKT cells are constantly surveying the sinusoids. Closer to the triad, especially near the BDs, there is a high frequency of MAIT cells and γδ T cells.

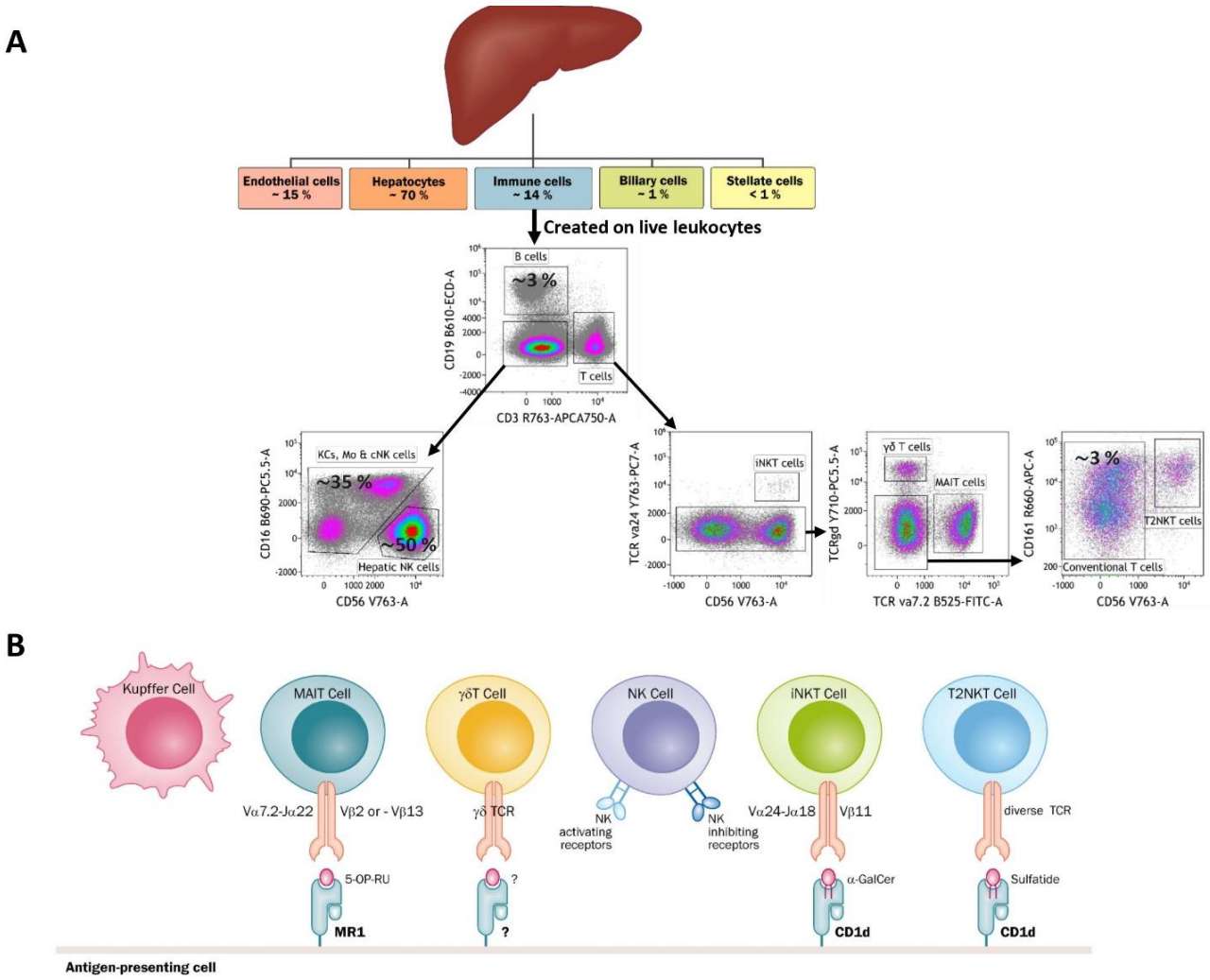

Figure 2. (A) Diagram tree of the approximate frequency of liver-resident cells and a FACS-based gating strategy to identify each cell type. The liver is mainly constituted by parenchyma (hepatocytes) and ILCs. Among ILCs, Kupffer cells and NK cells are the most abundant immune cells. The liver is also characteristic for having a niche of unconventional T cells, namely iNKT cells, T2NKT cells, γδ T cells and MAIT cells. (B) The main types of antigen recognition by unconventional T cells through their T-cell receptors (TCRs), Kupffer cells and NK cells. Kupffer cells and NK cells are activated through pattern recognition receptors. Additionally, NK cells have receptors that can sense healthy and stressed or dead cells.

1.2.1 Kupffer cells

KCs are liver-resident macrophages that constitute 15 % of the total human non-parenchymal liver cell count [13]. They represent the primary barrier against pathogens and toxic compounds coming from portal circulation [14]. KCs are antigen-presenting cells (APC) and play a crucial role in inducing liver tolerance through cell-to-cell contact, cytokines and other mechanisms such as dioxygenase-dependent sequestration of tryptophan [15]. Under physiological conditions, KCs are the major reservoir of macrophages in the liver and can self-renew independently from the bone marrow [16]. Upon activation, KCs secrete chemokine ligand 2 (CCL2) which promotes the infiltration of human circulating monocyte-derived macrophages. Increased frequency of CCR2+ monocytes participates in liver fibrosis in mouse models [17, 18] and is indicative of pathology in human acetaminophen-induced acute liver injury [19]. However, it is not yet clear whether liver-resident and circulating macrophages are two distinguished populations with different functions. The majority of pathogens coming from portal circulation are trapped in the liver by KCs phagocytosis. KCs cooperate with other non-parenchymal liver cells to clear potential infections [20]. KCs can also sense damage-associated molecular patterns (DAMPs) expressed in hepatocytes that induce the secretion of a variety of cytokines and chemokines to efficiently restore homeostasis [20]. When liver diseases compromise KCs function, aggravation of the diseases can be foreseen due to secondary infections [21].

1.2.2 Mucosal-associated invariant T cells

MAIT cells are an abundant subset of hepatic T lymphocytes. They constitute up to 30-40 % of human hepatic $CD8^+$ T cells [6, 7]. Their roles in pathogen defense and tissue repair have been previously reported [22–24]. MAIT cells have an invariant T cell receptor (TCR) that recognizes the nonpolymorphic class Ib major histocompatibility (MHC) class I-related protein (MR1) when loaded with antigens. MAIT cells recognize riboflavin derivatives which are necessary for

metabolism of many bacteria. These cells are considered an evolutionary system to defend hosts from pathogens since mammals do not produce these metabolites. Under inflammatory conditions, hepatocytes present the riboflavin derivative 5-A-RU to MAIT cells and also secrete IL-7 which is known to shape MAIT cells towards a pro-inflammatory state [7, 25]. Upon activation, MAIT cells secrete large amounts of pro-inflammatory and pro-fibrogenic cytokines such as IFN-γ, TNF-α and IL-17 [26]. Studies in humans demonstrated that triggering MAIT cells in the absence of co-stimulation with cytokines induces wound repair and tissue regeneration [24]. These studies suggest that under physiological conditions, MAIT cells probably contribute to tissue repair and regeneration since there is a constant influx of 5-A-RU present in human sera [27] but promote inflammation under acute inflammation. The high sensitivity for cytokines indicates that MAIT cells might be one of the first contributors to early inflammatory responses.

1.2.3 Gamma-delta T cells

γδ T cells are non-conventional subset of T lymphocytes with a limited non-MHC-restricted TCR repertoire. They constitute around 1-10 % of human circulating T cells [28]. They can recognize a wide variety of antigens and can be activated via pathogen-associated molecular patterns (PAMPs), DAMPs or cytokines alone. Upon activation, cells can execute cytotoxic as well as effector functions. Moreover, γδ T cells also play a role in tissue homeostasis [29]. In humans, the stratification of γδ T cells is based on the Vδ gene segments used to produce their TCR. $Vδ1^+$ T cells are abundant in the epithelium [30] and protect tissues via recognition of non-classical MHCs such as CD1a, CD1c and CD1d [31]. $Vδ2^+$ T cells are the most abundant subtype in circulation and can clear infections in periphery organs [28, 32]. They recognize phosphoantigens, which are non-peptide low molecular weight antigens. $Vδ2^+$ T cells respond rapidly in a Th1-like fashion to high amounts of self-phosphoantigens (for example in tumor cells) or microbial phosphoantigens [33, 34]. The butyrophilin 3A (BTN3A) family can trigger activation of $Vδ2^+$ T

cells upon stimulation with phosphoantigens [35]. The heterodimer BTNL3/BTNL8 expressed in APC was reported to mediate the TCR-dependent activation of Vδ2$^+$ T cells by binding of the intracellular domain of BTNL3 with phosphoantigens [36]. Interestingly, the expression of *BTNL8* was not detectable in human PBMC but it was highly expressed in regulatory T cells after polyclonal stimulation [37]. This suggests further investigation into the role of the butyrophilin family in the development of hepatitis and potential role in influencing Vδ2$^+$ T cells. Vδ3$^+$ T cells are a heterogeneous group of T lymphocytes enriched in the liver and also in some diseases such as leukaemia or chronic viral infection [38]. They recognize antigens presented by CD1d molecules and respond by producing cytokines and killing of CD1d$^+$ cells [38]. Recent evidences suggest that γδ T cells may be involved in liver diseases as previously shown in other autoimmune diseases [28], especially due to the rapid and large secretion of IL-17 [39].

1.2.4 Natural Killer T cells

NKT cells are a rare subset of T lymphocytes comprising less than 1 % of human peripheral blood T lymphocytes but enriched in the liver [8, 40]. NKT cells are known to express NK cell markers like CD56, CD16 and CD161, and produce granzyme [40, 41]. Their restricted TCR repertoire recognizes antigenic lipids presented by the MHC class I-like molecule CD1d [42, 43]. Based on their TCR, NKT cells have been divided into two subsets. Type I NKT, or invariant (i)NKT cells, are the most studied group because they are enriched in mouse liver and have a semi-invariant TCR. The prototype ligand for iNKT cells is α-galactosylceramide (α-GalCer) [44]. Type II NKT cells (T2NKT) consist of a subset with more diverse TCR. The major ligand recognized by T2NKT cells is sulfatide, which is a glycolipid enriched in the myelin of the central nervous system, pancreas, kidney and liver [45]. It is difficult to study T2NKT cells because there is a lack of tools to identify and characterize them. Recently, we proposed a novel strategy to isolate and characterize T2NKT cells in humans but the low number of cells in blood is still a limitation [40].

The role of iNKT cells and T2NKT cells in liver diseases have been mainly studied using transgenic mice models of CD1d-knockouts or TCRVα14-knockouts, which lack iNKT cells. These studies suggest that, in general, iNKT cells play a pro-inflammatory phenotype whereas T2NKT cells suppress inflammation through direct and indirect inhibition of inflammatory cells, including iNKT cells [46–49]. We described a novel subpopulation of T2NKT cells that expresses regulatory T cell markers such as FoxP3 and CD25 [40]. FoxP3^{+} T2NKT cells were found both in the periphery and in the liver and may explain some of the regulatory functions reported previously.

1.2.5 Natural Killer cells

NK cells are a major component of the liver's innate immune cell compartment. They account for almost 50 % of human intrahepatic lymphocytes [50]. Human hepatic NK cells are classified into three different subsets based upon their transcriptional, phenotypical and functional features [50]. Liver-resident NK cells are CD56^{bright} CD69^{+} CXCR6^{+} CCR5^{+} and highly cytotoxic [51–54]. These cells are long-lived tissue-resident subsets [55]. Interestingly, a subset of liver-resident CXCR6^{+} NK cells was described as having a memory-like responsiveness against - vesicular stomatitis virus (VSV), human immunodeficiency virus (HIV) and influenza [56]. Memory-like NK cells produce higher amounts of IFN-γ after rechallenge with the virus. The third NK cell subset is transient circulating NK cells, which are CD56^{dim} CD69^{-} CXCR6^{-} CCR5^{-} and show less cytotoxic activity. They can secrete high amounts of pro-inflammatory cytokines such as TNF-α and GM-CSF [57–59]. The regulation of NK cell activity consist on a balance between activating and inhibitory receptors displayed on their surface [60]. NK cells survey the liver and induce apoptosis in infected or aberrant cells via different mechanisms such as FasL or TRAIL [61, 62]. Under inflammatory conditions, NK cells kill hepatic stellate cells (HSCs) to resolve inflammation and limit liver fibrosis via granzyme-induced apoptosis and IFN-γ secretion [62, 63]. NK cells are fundamental for the proper protection of the liver and aberrant functions have been reported in

several liver diseases. Over the past decade, studies on NK cells suggest very heterogeneous populations with distinctive transcriptomes and cellular interactions [64].

1.3 Innate immune cell subsets and early liver inflammation

Liver inflammation is the first step to resolving and healing from different hepatocellular stress. When not effective, inflammation can become pathogenic. Hepatitis is a hallmark of liver disease [65] (Figure 3). It is important to identify which cells are precursors of early liver inflammation to avoid unnecessary harm. A recent report highlights the importance of the inflammasome in early inflammation [66]. KCs express a variety of pathogen recognition receptors (PRRs) to cover a wide range of dangers. Some of these dangers overactivate the inflammasome, which triggers pyroptosis, a form of cell death accompanied by cell membrane rupture and release of pro-inflammatory IL-1β and IL-18 [67]. These cytokines are responsible for the recruitment and activation of innate immune cells [68, 69]. The direct cytotoxic and effector functions of innate immune cells can restore homeostasis. However, innate immune cells can also have early involvement in disease processes when the danger is not resolved (e.g. chronic viral infection) or because of repeated insults (e.g. alcohol or drug abuse) (Table 1). Innate immune cells can also recruit other immune cells from the liver and peripheral circulation. Overall, innate immune cells are suggested to be the precursors of the inflammatory niche because of their optimal location, preactivated state, enrichment in the liver and strong effector functions.

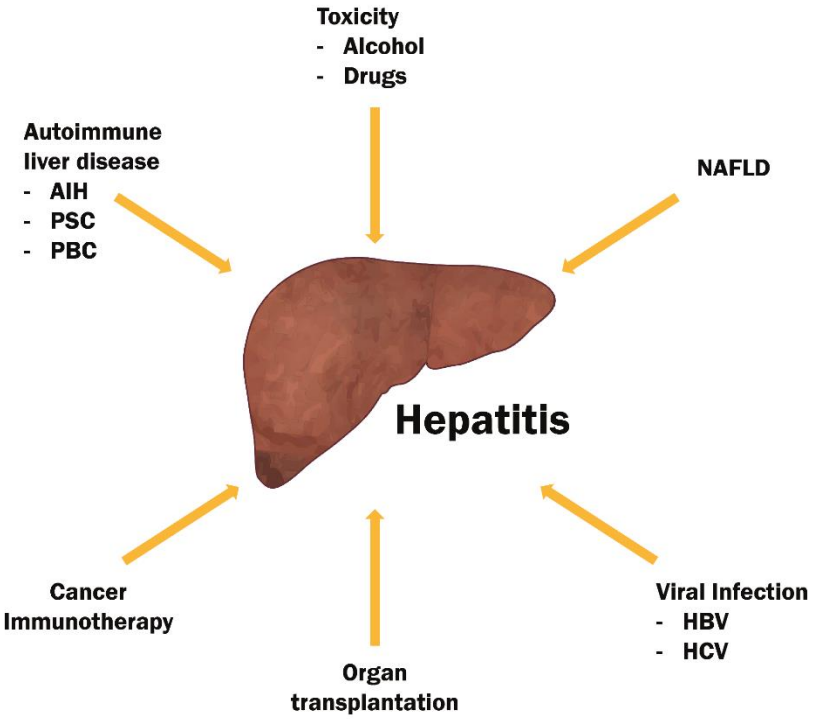

Figure 3. Hepatitis is a hallmark of the majority of liver diseases.

1.3.1 Viral hepatitis

Hepatotropic viruses such as hepatitis A, B, C, D and E (HAV, HBV, HCV, HDV and HEV) possess mechanisms to escape from the hosts´ antiviral immunity. When the viruses replicate, often the innate immunity detects viral components, hence triggering an acute inflammatory response resulting in the killing of infected hepatocytes. Since the infection is not properly resolved, viruses remain in a latent state and replicate opportunistically. This progressively leads to chronic liver inflammation [70]. In particular, HBV and HCV are the main causes of chronic liver disease and are estimated to affect 257 million (data from WHO 2015) and 115 million people [71], respectively. Together they represent the most common cause of liver cirrhosis, liver cancer and viral hepatitis-related deaths [72].

HBV is directly mutagenic and induces low-grade inflammation progressing into HCC [73]. HBV-infected hepatocytes release PAMPs such as glycoproteins, secreted HBsAg or free viral nucleic acids that are recognized by the innate immune system. Human KCs release pro-inflammatory cytokines to orchestrate an antiviral response which also arrests hepatocyte replication, hence viral replication [74]. Studies in mice demonstrated the antiviral roles of NK cells and NKT cells [75, 76]. HBV patients present higher levels of NK cells in blood compared to HBV-negative controls [77, 78] and are deemed as the major contributors to HBV clearance [79]. A positive correlation was found between NK cell activation levels and HBV clearance [79]. NK and NKT cell numbers from peripheral blood correlated to the frequency of HBcAg-specific cytotoxic T lymphocytes (CTLs) [80]. However, infiltration of circulating NK cells can contribute to liver injury [81]. NK cells from HBV patients produced higher levels of TNF-α and induced in vitro expression of TRAIL in hepatocytes [82]. This study showed that infiltrated circulating NK cells could induce apoptosis of non-infected hepatocytes via TRAIL [82]. Additional studies in mice and patients show that NK cells could also exacerbate liver injury via TNF-α, Fas/FasL and NKG2D/NKG2DL pathways [83, 84]. NKT cells and KCs secrete induced nitric oxide synthase (iNOS) as a viral eradication mechanism [85, 86]. Moreover, the frequency of NKT cells was increased to normal values with virus clearance [80]. These results suggest that circulating NK cells and NKT cells are recruited in the liver causing a reduction in their frequencies in blood. In contrast, peripheral MAIT cells were significantly decreased in HBV-related liver failure patients compared with chronic HBV patients [87]. The study suggested that MAIT cells are recruited in the liver and promote a strong inflammatory response damaging the liver. MAIT cells were also reduced in patients with middle/late-stage compared with early-stage liver failure [87]. Similar to NK cells and NKT cells, patients that showed disease improvement had an increment in the frequency of MAIT cells [87]. In another two studies exploring changes in peripheral γδ T cells in HBV patients, γδ T cells were less abundant in liver failure patients and correlated with disease severity [88]. Activation of γδ T

cells with PMA/Ionomycin induced the greatest amount of pro-inflammatory TNF-α and IL-17 in liver failure patients [89]. However, another study indicated that γδ2 T cells exhibited impaired proliferation and chemotaxis [90]. The same study showed in vitro that γδ2 T cells inhibit Th17 T cells through cell-to-cell contact and produce high amounts of IFN-γ [90]. These results suggest that NK cells and NKT cells are the first-line of defense against HBV infection. Failing to clear the infection, MAIT cells and γδ T cells contribute to chronic inflammation. IFN-α therapy is effective in 20-30 % of chronic HBV patients [91]. The low response rates may be attributed to the wide spectrum of different clinical conditions. Based on the current understanding of the role of NK cells in HBV clearance, IFN-α is likely to improve the cytotoxic function of liver-resident NK cells by targeting HSC cells and reduce fibrosis [92]. It is necessary to investigate whether IFN-α therapy response is subjected to the frequency of circulating NK cell infiltration.

HCV-induced inflammation is partly triggered by non-structural proteins of the virus [93] but the major contributor to HCV-hepatitis are the inflammatory immune cells. In vitro studies show that HCV-infected hepatocytes produce several pro-inflammatory cytokines including IL-6, IL-8, MIP-1α and MIP-1β as a response to IL-1β secreted by HSCs [94] or IL-1β and TNF-α by KCs [95]. Similar to HBV infection, human circulating MAIT cells were generally reported to be depleted with markers of exhaustion and hyperactivation [96–98]. Additional studies suggest that hepatic MAIT cells are major contributors to hepatitis and fibrosis given the nature of the cells. Repetitive IL-12 stimulation or IL-7 secretion by hepatocytes was a sufficient stimulus to induce secretion of the pro-inflammatory cytokines IFN-γ, TNF-α and IL-17 [7, 26]. Intrahepatic γδ T cells were shown to be cytotoxic against human hepatocytes in culture [99]. We have recently identified a subset of $CD8^+$ γδ T cells that were more abundant in baseline peripheral blood of melanoma patients that had hepatitis after ICI therapy versus non-hepatitis cohort. ICI therapy might induce γδ T cells cytotoxic activity against hepatocytes as observed in HCV infection. NK cells were shown to be compromised in HCV patients allowing the virus to replicate [78, 100]. IFN-α therapy induced

activation of NK cells and further improved the clearance of the virus [101]. NKT cells were also reported to play a role in HCV resolution and progression. The frequency of activated $CD38^+$ or $CD69^+$ iNKT cells strongly correlated with alanine transaminase levels [102]. Increased levels of activated iNKT cells were observed during acute inflammation and chronic HCV infection without apparent functional differences [102]. The frequency of activated iNKT cells declined spontaneously in resolving patients [102]. These data suggest that HCV infection could be mainly managed by NK and NKT cells. Viral clearance also involves other ILC-like cells such as MAIT cells and γδ T cells. Under inflammatory conditions, host hepatocytes switch to an antiviral state to prevent further viral replication. If the infection is not properly resolved, we propose a model where NK cells and MAIT cells have an exhausted phenotype while iNKT cells and γδ T cells promote pathogenesis by targeting infected hepatocytes.

1.3.2 Alcohol-induced hepatitis and drugs

The liver is vital for the detoxification of substances that are harmful to the body. Liver detoxification consists mainly of converting ingested drugs into water-soluble metabolites via xenobiotic biotransforming enzymes [103]. This allows drugs to be efficiently secreted through urine. However, in an attempt to solubilize drugs, some compounds are converted into their active form. Acetaminophen, also known as paracetamol, leads to reactive metabolites causing apoptosis and necrosis of hepatocytes [104]. In the case of alcohol, free radicals and acetaldehyde are harmful by-products that can lead to significant liver damage over time. Drugs and alcohol can also damage the intestine barrier leading to more bacteria translocation to the bloodstream [105, 106]. The influx of gut microbiota and its metabolites activate the immune system through PAMPs and DAMPs [107–110]. KCs were reported to be major contributors to the development of alcohol-related liver disease (ALD). Intestine permeability is directly associated with KC activation [111, 112]. Exposing mice to LPS and alcohol-derived reactive

oxygen species (ROS) has shown to induce TNF-α secretion by KCs [113, 114]. In a paracrine manner, IL-1ß secretion by KCs had a significant effect on the pathological progression of ALD [115]. A rat model of ALD with depletion of KCs resulted in impaired progression of the pathology suggesting a key role of KCs [116]. NK cells were less frequent in alcoholic patients [117] and were less cytotoxic compared to healthy individuals [118]. A reduced expression of the activating receptor NKG2D and production of IFN-γ in mice suggests that NK cells cannot efficiently kill activated HSCs [119]. Chronic ethanol feeding in mice increased CD1d by enterocytes [120]. Similarly, patients affected by alcohol misuse also show increased expression of CD1d in the small intestine [120]. An in vitro study showed that CD1d increased the loading of αGalCer following increasing concentrations of ethanol and thus, could increase stimulation of iNKT cells [121]. Many studies in mice suggest that iNKT cells have a pathogenic role in the development of ALD. It was reported that iNKT cells crosstalk with KCs through IL-1β, promote inflammation and recruit neutrophils [122, 123]. CD1d blocking antibodies could partially prevent liver injury [123]. Intestinal iNKT cells were observed to migrate to the liver and, collectively with liver iNKT cells, showed a chronic activated phenotype with downregulation of TCR, increased apoptosis and FasL expression [120]. In vitro experiments from the same study confirmed that iNKT cells could kill hepatocytes via Fas-FasL mechanism [120]. Activation of T2NKT cells by sulfatide inhibited iNKT cell hepatic damage [124, 125]. In a concanavalin A-induced hepatitis mouse model, injection of lysophosphatidylcholine (LPC) activated T2NKT cells and prevented liver injury by iNKT cells [125]. Another study described the crosstalk of T2NKT cells with plasmacytoid dendritic cells and recruitment of anergic iNKT cells to the mouse liver via IL-12 and MIP-2 [126]. As mentioned above, our group recently identified a novel population of human FoxP3$^+$ T2NKT cells that might exert immunoregulatory functions in this scenario [40]. Alcoholic-related cirrhosis and severe alcoholic hepatitis patients had a dramatic depletion and hyperactivated circulating MAIT cells [127, 128]. Dysfunctional MAIT cells could explain the susceptibility to infection of these

patients [127, 128]. In another study, MAIT cells had an exhausted phenotype and partially recovered with patient´s alcohol abstinence [129]. MAIT cells may contribute to the pathogenesis of ALD via IL-17 secretion [129]. Surprisingly, only a few reports have described the role of γδ T cells in ALD. In a mouse study following binge ethanol drinking, γδ T cells were described to produce higher amounts of IL-17A than non-binge ethanol-drinking mice [130]. The activation of γδ T cells was IL-1ß-dependent, possibly by KCs [130]. However, under acute-on-chronic ethanol consumption, γδ T cells did not produce further IL-17A. Instead, CD4+ T cells were the major contributors. This suggests that KCs could play a predominant role in the development of ALD. KCs orchestrate an inflammatory response that involves pro-inflammatory iNKT cells and γδ T cells. Alcohol could directly affect MAIT cells and NK cells causing depletion and impaired functions such as the inactivation of HSCs by NK cells, and tissue repair by MAIT cells.

1.3.3 Non-alcoholic fatty liver disease

Non-alcoholic fatty liver disease (NAFLD), characterized by an excessive accumulation of fat in hepatocytes, is the most common indication for liver transplant in Western countries and the leading cause of liver transplantation in women [131, 132]. It is estimated that 23-25 % of the global population have NAFLD to some degree [133]. Etiologically, it is suggested that the adipose tissue from patients with NAFLD predisposition release free fatty acids (FFA) and pro-inflammatory mediators into the circulation [134, 135]. As a result, an inflammatory response is triggered in the liver. Lipotoxicity, mitochondrial dysfunction and endoplasmic reticulum stress are key inducers of the inflammatory cascade [136]. Higher frequencies of KCs were observed in liver biopsies of non-alcoholic steatohepatitis (NASH) patients [137]. Depletion of KCs in rats exposed to a high-fat diet (HFD) prevented the development of steatosis [138]. In vitro experiments showed that TNF-α was responsible for the increased accumulation and the reduced oxidation of fatty acids in hepatocytes [139]. Immunohistological stainings revealed a complex crown-like structure

consisting of KCs surrounding dying steatotic hepatocytes. Cholesterol crystals are accumulated in the center of these structures [140]. Interestingly, previous exposure of KCs to cholesterol crystals showed to precondition the cells towards a pro-inflammatory innate memory-like state [141]. Similar observations were taken from macrophages cultured with oxidized low-density lipoproteins [142]. Likewise to the effect of alcohol, NK cells of obese individuals had lower NKG2D expression [143] and impaired cytotoxicity [144, 145]. Another study showed that there were no differences between NK cells from healthy individuals and NAFLD, while higher expression of NKG2D in NK cells was found in NASH patients [146]. Data from mice and humans suggest that iNKT cells have a dual role in NAFLD. More specifically, it is hypothesized that iNKT cells have a protective role during early stages of simple steatosis. In different mouse models of hepatosteatosis, like ob/ob mice, animals fed with HFD or a choline-deficient diet, iNKT cells were apoptotic and showed decreased intrahepatic frequency [147–149]. Adoptive transfer of hepatic mononuclear cells but not $CD1d^{-/-}$ mononuclear cells regulated hepatic steatosis via IL-10 [150]. However, in other instances, opposite results were reported. Mice fed with HFD developed adipose tissue inflammation and glucose intolerance [151]. This was significantly exacerbated by αGalCer-dependent activation of iNKT cells [151]. In the liver, iNKT cells could be directly activated via hepatic CD1d molecules, exacerbate steatosis and decrease insulin sensitivity by promoting a pro-inflammatory cytokine environment [152]. This could suggest that iNKT cells play a protective role during early stages of simple steatosis but exacerbate the disease in chronic steatosis. It would also be interesting to study the potential effect of iNKT cell migration from tissues like the intestines as discussed earlier. T2NKT cells might also play dual roles. In HFD mice, T2NKT cells initiate inflammation in the liver and adipose tissue and promote obesity and insulin resistance [153]. However, adoptive transfer of T2NKT cells in HFD obese mice induced prolonged weight loss and glucose tolerance [154]. The heterogeneity and impact of fat in intrahepatic T2NKT cell populations remains unclear. The frequency of human NKT cells is

decreased in steatosis [155] but increased accordingly to the progression of NAFLD, especially IFN-γ^{+} and IL-4^{+} cells [156–158]. NASH patients had a 4-5 fold relative increase in liver NKT cells [158]. CD1d expression was reported to be increased in liver immunohistochemical samples of NAFLD and correlated with disease progression [156]. Taken together, NKT cells are reduced in the early stages of simple steatosis. A pro-inflammatory response is protective against obesity. In advanced NAFLD, NKT cells are increased and pathogenic. Circulating MAIT cell frequency was reported to decrease while the number of intrahepatic MAIT cells was increased in NAFLD patients' livers and it tended to be greater with disease progression [159]. MAIT cells from NAFLD patients had increased secretion of IL-4 and reduced expression of IFN-γ and TNF-α [159]. The current knowledge about the role of γδ T cells in NAFLD is mostly based on mice models. γδ T cells can recognize molecules presented by CD1d and its differentiation is dependent on hepatocyte CD1d [160]. γδ T cells are high producers of IL-17A in steatohepatitis [161], a key cytokine known to induce fibrosis and ROS production [162, 163]. In HFD mice, IL-17^{+} γδ T cells are elevated [164]. Additionally, adoptive transfer and gene knockout experiments in HFD mice demonstrated that γδ T cells exacerbate steatohepatitis and liver damage [160, 161]. In humans, NAFLD patients showed decreased frequencies of Vδ2^{+} T cells, but elevated frequencies of Vδ2^{-} T cells compared to healthy controls [143]. Overall, the progression of NAFLD to NASH is a process derived from the increased cellular oxidative stress that leads to the activation of inflammatory pathways [165]. Accumulation of ROS induces the expression of TNF-α which can trigger necrotic cell death [166]. In line with these results, NK cells were suppressed by ROS [167]. KCs develop an apparent pro-inflammatory immune memory state by contact with cholesterol crystals. γδ T cells promote pathogenesis through IL-17 secretion, while NKT cells and MAIT cells exacerbate steatosis by secretion of Th2 cytokines which also contributes to fibrosis [168].

1.3.4 Liver autoimmunity

The three main autoimmune liver diseases are autoimmune hepatitis (AIH), primary biliary cirrhosis (PBC) and primary sclerosing cholangitis (PSC). AIH affects portal tracts and liver lobules by lymphoplasmacytic infiltrates while PSC and PBC mainly affect bile ducts. The etiologies of these diseases are yet unknown, but several studies suggest a common immune-mediated liver injury. The dysregulation of immune regulatory networks causes the activation and expansion of autoreactive T cells and B cells [169, 170]. The innate system plays an important role in the regulation of the adaptive system. In AIH, an increased frequency of cytotoxic circulating NK cells in the liver was observed in an experimental mouse model of AIH [171]. In humans, the frequency of circulating $CD56^{bright}$ NK cells was higher in untreated AIH, while the frequency of circulating $CD56^{dim}$ NK cells was reported to be reduced in active AIH patients or while in remission [171, 172]. Our knowledge about NKT cells in liver autoimmunity is mainly based on mouse models. In AIH, concanavalin-induced hepatitis is the preferred model. iNKT cells were reported to upregulate FasL expression to mediate cytotoxicity against hepatocytes [173]. Activation of iNKT cells via α-GalCer exacerbates the disease and is suggested to be carried out via IL-4 and TNF-α secretion [174, 175]. Inflammation was also promoted via the secretion of IL-17 [176]. MAIT cells were reported to be depleted and exhausted in the periphery in patients [177]. Chronic stimulation of MAIT cells due to an increased influx of bacteria antigens and chronic inflammation may lead to MAIT cell function impairment. Induction of the exhausted state by repetitive stimulation with IL-12 and IL-18 showed that MAIT cells reduced IFN-γ production but maintained expression of the proinflammatory cytokine IL-17 [177]. The frequency of circulating γδ T cells was increased in patients with AIH, PSC and PBC [8]. $V\delta1^+$ T cells, known to produce high levels of IFN-γ and granzyme B, were especially incremented in patients with AIH [178]. Another study showed that γδ T cells with low expression of TOX were enriched in AIH patients and had prediction potential [179]. TOX deficiency was suggested to promote the

expression of IL-17A in γδ T cells [179]. In general, IL-17 secretion was reported in iNKT cells, MAIT cells and γδ T cells. Although the clinical profile of the distinctive autoimmune liver diseases is different, current studies support common immunological pathways. Taking for instance the role of circulating NK cells, the frequency of these cells was reported to be increased and a higher expression of cytotoxic molecules such as perforin was found in PBC and PSC patients compared to healthy individuals [180, 181].

1.3.5 Liver transplantation

Liver transplantation represents a major hepatic injury. One of the unavoidable injuries is caused by oxygen deprivation. After liver resection, blood flow is restricted for a period of time and the organ becomes hypoxic. This leads to different forms of cell death like apoptosis, ferroptosis, pyroptosis and necrosis [182]. After reperfusion, innate immune cells from the recipient migrate to the liver and induce inflammation or tolerance [183]. The degree of ischemia-reperfusion injury (I/R) is correlated to the risk of liver rejection [184, 185]. I/R injury increased the expression of monocyte chemoattractant protein-1 (MCP-1) and it was associated with poorer graft function [186]. This observation was correlated with the increased recruitment of monocytes 2 hours after reperfusion [186]. The role of NK cells is dependent on activating and inhibitory receptors expressed in hepatocytes as well as cytokines secreted by neighbour cells. In I/R injury, components of the inflammasome in KCs like NLRP3 and AIM2 are hyper-activated [187, 188]. Inflammasome-derived IL-18 secretion can induce FasL [189] and IFN-γ production in NK cells [190]. IFN-γ was reported to induce expression of Fas receptor in hepatocytes and neutralization of IFN-γ secretion by NK cells could protect mice from tissue damage [191]. Due to the increased demand for livers and the increasing prevalence of NAFLD, the debate of using steatotic livers for transplant is on the table [192]. Steatosis is deemed to cause oxidative stress in the liver, which worsens the graft´s condition with I/R injury. In a retrospective, exploratory study, steatotic

livers showing signs of I/R had a significantly worse one-year survival rate, while the survival rate was not conditioned in healthy livers´ by I/R injury [193]. In this study, γδ T cells were suggested to exacerbate liver rejection in steatotic livers [193]. NKT cells were reported to promote I/R injury. After reperfusion, NKT cells rapidly expand in the liver and produce IFN-γ [194, 195]. Depletion of NKT cells with antibodies or both NKT cells and NK cells significantly reduced I/R injury [196]. The role of MAIT cells in liver I/R injury remains to be elucidated. In focal cerebral ischemia, MAIT cells were reported to play a pro-inflammatory role [197].

1.3.6 Immunotherapy-associated liver reactions

Cancer immunotherapies, especially immune checkpoint inhibitor (ICI) therapy, have opened new clinical perspectives for cancer patients and is fast becoming one of the main pillars of cancer treatment. ICI therapy uses monoclonal antibodies blocking T cell receptors that are used by cancer cells to evade the immune system. Immune-related adverse events (irAEs) are the result of immune activation derived from ICI therapy. The incidence of ICI-derived hepatitis is approximately 1-3 % for programmed cell death 1 (PD1) inhibitors and 3-9 % in cytotoxic T-lymphocyte-associated protein 4 (CTLA4) inhibitors [198]. The combination of α-PD1/CTLA4 increases the rate of hepatitis [198]. CTLA4 plays an important role in downregulating the immune response. The expression of CTLA4 is upregulated in T cells after activation and competes with the costimulatory receptor CD28 to bind to its ligand CD80/CD86 on APC [199]. PD-1 is expressed on T cells and B cells and it promotes self-tolerance. Upon binding to its ligand PD-L1, it drives T cell apoptosis or regulatory phenotype. Thus, ICI therapy can arguably impair liver immunotolerance. In acute liver injury, α-PD1 therapy improved the bacterial clearance function of KCs [200]. A study treating melanoma patients with α-PD1 showed that NK cell frequency in blood was not affected while NKT frequency was significantly increased [201]. Another study observed no changes in either the number or function of MAIT cells in melanoma patients treated

with α-PD1 therapy [202]. γδ T cells showed no apparent functional changes upon PD-1 blockade in vitro [203]. The frequency of γδ T cells in melanoma patients treated with a combination of α-PD1/CTLA4 remained unchanged [204]. Overall, these data suggest that innate immune cells are not drastically affected by ICI therapies, with the exception of KCs and NKT cells. Immune-suppressive KCs expresses PD-1 to suppress T lymphocytes in acute liver injury [200]. α-PD-1 therapy has shown to invigorate bacteria clearance, but it also suggests that KCs may have impaired tolerogenic function to self-antigens reactive T cells. NKT cells also responded to α-PD-1 therapy and exert increased anti-tumor functions by secretion of IFN- γ secretion of inflammatory cytokines [205].

1.4 Innate immune cells as diagnostic and therapeutic targets

The innate immune system is also involved in immune homeostasis and healthy tissue turnover. This is accomplished via three steps consisting of early inflammation, amplification of the inflammatory signal and resolution. Liver fibrosis is a consequence of inflammation and inefficient resolution. Liver biopsy is the gold standard for diagnosing cirrhotic liver disease, yet it is estimated to miss 10-30 % of cases [169]. Additionally, biopsy is not ideal because of invasiveness, pain, hypertension and bleeding [206]. An optimal approach would be to identify early inflammation before fibrosis development. This could improve patient's treatment and prognosis. Blood markers bring promising perspectives to detect liver damage and abnormal functions [207]. The current scoring system for diagnosis and prognosis of fibrosis includes serum proteins (albumin), bilirubin, liver enzymes (aminotransferases, alkaline phosphatase, γ-glutamyl transferase) and direct markers of extracellular matrix turnover (type IV collagen, matrix metalloproteinases). However, there is room for improvement regarding specificity (etiology) and sensitivity (disease stages) [206]. The immune system has emerged as an interesting diagnostic and therapeutic target in liver inflammation. Innate immune cells are the frontline defenders in the

liver and participate in the initiation, amplification and resolution of inflammation. Identifying immune changes in innate immune cell´s surface expression markers and frequencies can bring future perspective to the diagnosis of low-grade inflammation and also novel therapies. As discussed in this review, depletion of innate immune cells in mice models with hepatitis was able to attenuate several liver diseases. Noteworthy, the close relationship between innate immune cells with DAMPs and cytokines signaling suggests taking into consideration all three factors for the future of liver immunomonitoring and therapies.

Author contributions

JYZ performed literature search and wrote the manuscript. The author confirms being the sole contributor of this work and has approved it for publication.

Acknowledgements

We are very grateful to Dieter Pirner from the Department of Surgery, University Hospital Regensburg, for his contribution to the design of the illustrations.

The Supplementary Material for this article can be found online at:

https://www.frontiersin.org/articles/10.3389/fimmu.2023.1175147/full#supplementary-material

- CASE REPORT -

Manuscript submitted

2. Predictability of Clinical Response and Rejection Risk After Immune Checkpoint Inhibition in Liver Transplantation

Jordi Yang Zhou[1,2], Dominik Eder[1], Florian Weber[3], Philipp Heumann[4], Katharina Kronenberg[1], Jens M. Werner[1], Edward K. Geissler,[1] Hans J. Schlitt[1], James A. Hutchinson[1] & Florian Bitterer[1*]

[1] Department of Surgery, University Hospital Regensburg, Regensburg, Germany

[2] Leibniz Institute for Immunotherapy, University Hospital Regensburg, Regensburg, Germany

[3] Institute for Pathology, University of Regensburg, Regensburg, Germany

[4] Department for Internal Medicine I, University Hospital Regensburg, Regensburg, Germany

2.1 Abstract

Background: The approval of Atezolizumab/Bevacizumab therapy (Atezo/Bev) in 2020 opened up a promising new treatment option for patients with end-stage hepatocellular carcinoma (HCC). However, liver transplant (LTx) patients with HCC are still denied this therapy owing to the risk of ICI-induced organ rejection and lack of regulatory approval. **Methods**: A prospective observational study at a tertiary liver transplant centre monitored the compassionate, off-label use of Atezo/Bev in a single, stable LTx recipient with non-resectable HCC recurrence. Close clinical, laboratory and immunological monitoring of the patient were performed throughout a four-cycle Atezo/Bev treatment. Measured parameters were selected after a systematic review of the literature on predictive markers for clinical response and risk of graft rejection caused by ICI therapy. **Results**: 19 articles describing 20 unique predictive biomarkers were identified. The most promising negative prognostic factors were the baseline values and dynamic course of IL-6, alpha-fetoprotein (AFP) and the AFP/CRP ratio. The frequency of regulatory T cells (Treg) reportedly correlates with the success of ICI therapy. PD-L1 and CD28 expression level with the allograft, peripheral blood $CD4^+$ T cell numbers and Torque Teno Virus (TTV) titre may predict risk of LTx rejection following ICI therapy. No relevant side effects or acute rejection occurred during Atezo/Bev therapy; however, treatment did not prevent tumor progression. Absence of PD-L1 expression in pre-treatment liver biopsies, as well as a progressive downregulation of CD28 expression by $CD4^+$ T cells during therapy, correctly predicted absence of rejection. Furthermore, increased IL-6 and AFP levels after starting therapy, as well as a reduction in blood Treg frequency, correctly anticipated a lack of therapeutic response. **Conclusion**: Atezo/Bev therapy for unresectable HCC in stable LTx patients remains a controversial strategy because it carries a high-risk of rejection and therapeutic response rates are poorly defined. Although previously described biomarkers of rejection risk and therapeutic response agreed with clinical outcomes in the described case, these immunological parameters are difficult to reliably interpret. Clearly, there is an important unmet need for standardized assays and clinically validated cut-offs before we use these biomarkers to guide treatment decisions for our patients.

2.2 Introduction

Hepatocellular carcinoma (HCC) represents the third leading cause of cancer deaths worldwide [208]. Therapeutic options for advanced HCC that cannot be treated curatively by surgical resection, liver transplantation or radiofrequency ablation are limited. In end-stage cases, apart from transarterial chemoembolisation and radioembolisation, available drug therapies include the multikinase inhibitors (MKI) sorafenib and lenvatinib for first-line treatment, cabozantinib and regorafenib for second-line treatment after progression on sorafenib; and the anti-angiogenesis drug ramucirumab as second-line after progression on sorafenib. Beyond its limited oncological effectiveness, use of MKI therapy has been restricted by its pronounced side effects [209]. Consequently, advanced HCC still carries a poor prognosis and represents a significant unmet medical need.

Approval of cancer immunotherapies, especially immune checkpoint inhibitor (ICI) therapy, has opened new clinical perspectives for cancer patients and is fast becoming one of the main pillars of cancer treatment. Early studies in advanced HCC suggested that only 15-20 % of patients benefited from anti-PD-1 monotherapy, including Checkmate040 (NCT01658878) [210, 211] and KEYNOTE-224 (NCT02702414) [212, 213]. More recently, combination therapy using atezolizumab, an anti-PD-L1 immune checkpoint inhibitor, plus bevacizumab, an anti-VEGF neoangiogenesis inhibitor, showed promising results in the randomized phase 3 IMbrave150 trial (NCT03434379). Compared to sorafenib, advanced HCC patients had superior overall survival (OS) (19.2 months vs 13.4 months, HR=0.66, 95 % CI=0.52-0.85, P=0.0009) and progression-free survival (PFS) (6.9 months vs 4.3 months, HR=0.65, 95 % CI=0.53-0.81, P=0.0001) [214]. In 2020, the United States Food and Drug Administration (FDA) and the European Medicines Agency (EMA) approved Tecentriq (Atezolizumab) in combination with Avastin (Bevacizumab) as the new standard of care for patients with unresectable or metastatic HCC who have not received

prior systemic therapy. Critically, the approved indication excludes liver transplant (LTx) patients owing to the potential risk of acute graft rejection.

Immune-related adverse events (irAEs) are the result of dysregulated immune activation following ICI therapy. Checkmate040 and KEYNOTE-224 indicated that around 25 % of advanced HCC patients develop grade 3 or 4 irAEs, including severe or life-threatening pneumonitis, colitis, hepatitis, dermatitis, arthritis, encephalitis and other complications [210–213]. With the goal of sparing unnecessary toxicity and comorbidity, as well as offering therapeutic alternatives to LTx patients with recurrent HCC, efforts have been made to identify biomarkers that predict therapeutic responses and risk of irAEs [207, 215, 216]. Unfortunately, success has been limited despite the characterization of novel mechanisms for ICI-induced hepatitis. In particular, in a cohort of melanoma patients treated with a combination of anti-PD-1 and anti-CTLA-4, patients with a chronic or recurrent immune response against cytomegalovirus (CMV) showed an expansion of effector memory $CD4^+$ T cells that predisposed to hepatitis [217]. However, it is not presently clear whether such biomarkers and preventative strategies can be directly translated to liver transplant recipients with unresectable recurrent HCC. In a comprehensive review of 28 cases of ICI therapy in LTx heavily pre-treated patients, mostly HCC recurrent patients, graft rejection was observed in 32 % of the cases and only 25 % responded to therapy [218]. Based upon the limited number of reported ICI-treated HCC cases in LTx recipients, it is hard for clinicians to assess the potential risks and benefits of off-label treatment in individual cases; therefore, we urgently need reliable clinical markers to guide effective treatment decisions [219].

2.3 Case description

2.3.1 History of recurrent HCC after liver transplantation

A 62-year-old man presented in 2021 to our liver transplant outpatient clinic with a first HCC recurrence in liver segment IVa/VIII. The patient was the recipient of an orthotopic liver transplant

in 2010, necessitated by alcohol-related liver cirrhosis with intrahepatic, multilocular HCC. At the time of recurrence in the graft, radiofrequency ablation was started with curative intent, but was ineffective. At short-term re-staging, several new intrahepatic HCC foci were identified, as well as new pulmonary metastases (Figure 1A-B). The presence of extrahepatic metastases meant that therapies limited to the liver, such as TACE, SIRT or multiple ablations, were inappropriate. With no other potentially curative options, the transplanted patient was considered for off-label treatment with Atezo/Bev therapy as an alternative to the guideline-recommended 'standard of care' with an MKI.

An extensive risk assessment was undertaken, including clinical and laboratory investigations. The patient's general clinical condition was normal for age, with an ECOG status of 0 and Karnofsky index of 100 %. We further excluded comorbidities as contraindications for immunotherapy, including synchronous tumors, autoimmune diseases, and occult infections (suppl. Figure 2). Liver transplant function was stable under triple immunosuppression with Sirolimus (target trough levels of 3-5 µg/l), mycophenolate mofetil (1000 mg twice a day). Balancing the potential oncological success of ICI therapy against its risk of causing rejection, we added low-dose prednisolone (2.5 mg once daily), knowing that it may be associated with reduced tumor response [220]. No clinically validated investigations provided an estimate of rejection risk; therefore, the patient was offered Atezo/Bev therapy with a 32 % attendant risk of transplant failure and 25 % therapy response rate [218]. The patient provided full, informed consent to treatment.

Four cycles of 1200 mg Atezolizumab plus 15 mg/kg Bevacizumab were administered at three-week intervals. The patient was kept under close surveillance for signs of acute transplant rejection. In the first week after Atezo/Bev infusion, we reviewed the patient at least every second day; during the breaks in therapy, he was seen at least once per week. The patient never developed clinical or biochemical signs of a serious irAEs. Over time, the patient complained of

mild symptoms, including moderate fatigue, mild diarrhea, and sleeping problems. Transplant function remained stable throughout and following Atezo/Bev therapy. Specifically, liver enzyme values were stable after each cycle (Figure 3) and ultrasound imaging revealed no signs of acute liver rejection. Unfortunately, interim CT scans revealed further HCC progression with multiple intrahepatic foci and new pulmonary metastases (Figure 1C-D). Hence, despite completing a full course of Atezo/Bev therapy without a serious irAE or acute rejection occurring, the treatment was ultimately ineffective.

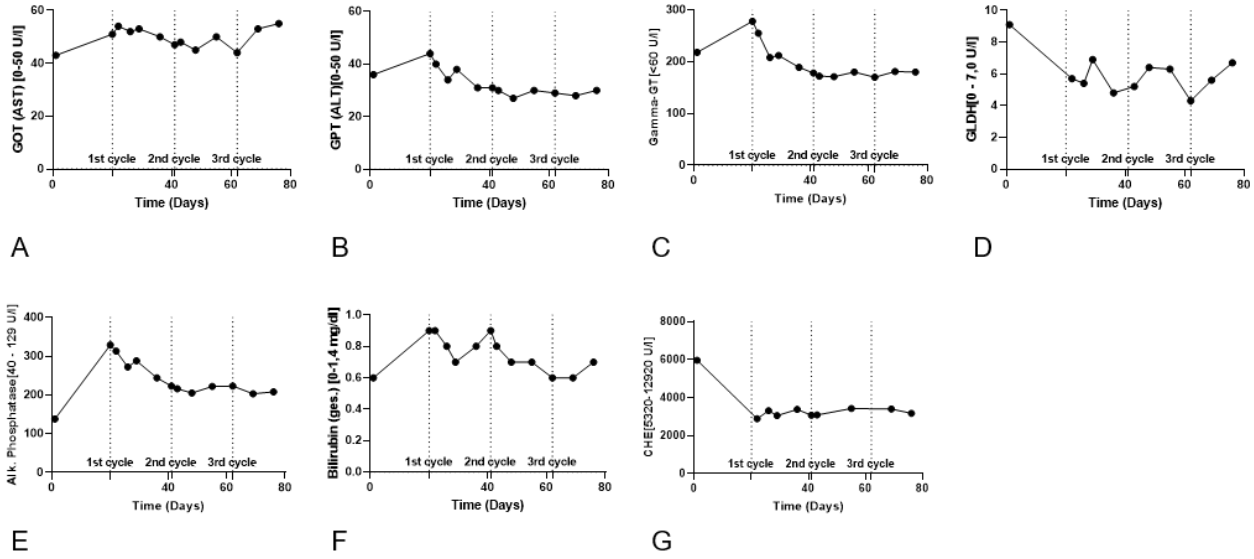

Figure 3. Routine biochemical liver parameters in the course of ICI therapy. (A & B) Liver enzymes (GOT & GPT) to assess the vitality of the hepatocytes. (C – E) Cholestasis parameters (γGT, GLDH & AP) to assess the vitality of the cholangiocytes. (F & G) Bilirubin and CHE for assessing metabolic functionality of the transplant liver.

This case illustrates the difficult clinical decision of whether to offer immunotherapy to liver transplant recipients with recurrent HCC. At the present time, neither the risk of irAE or rejection, nor the likelihood of clinical response can be accurately predicted using clinically validated tests. Therefore, we next asked what experimental methods could be of use.

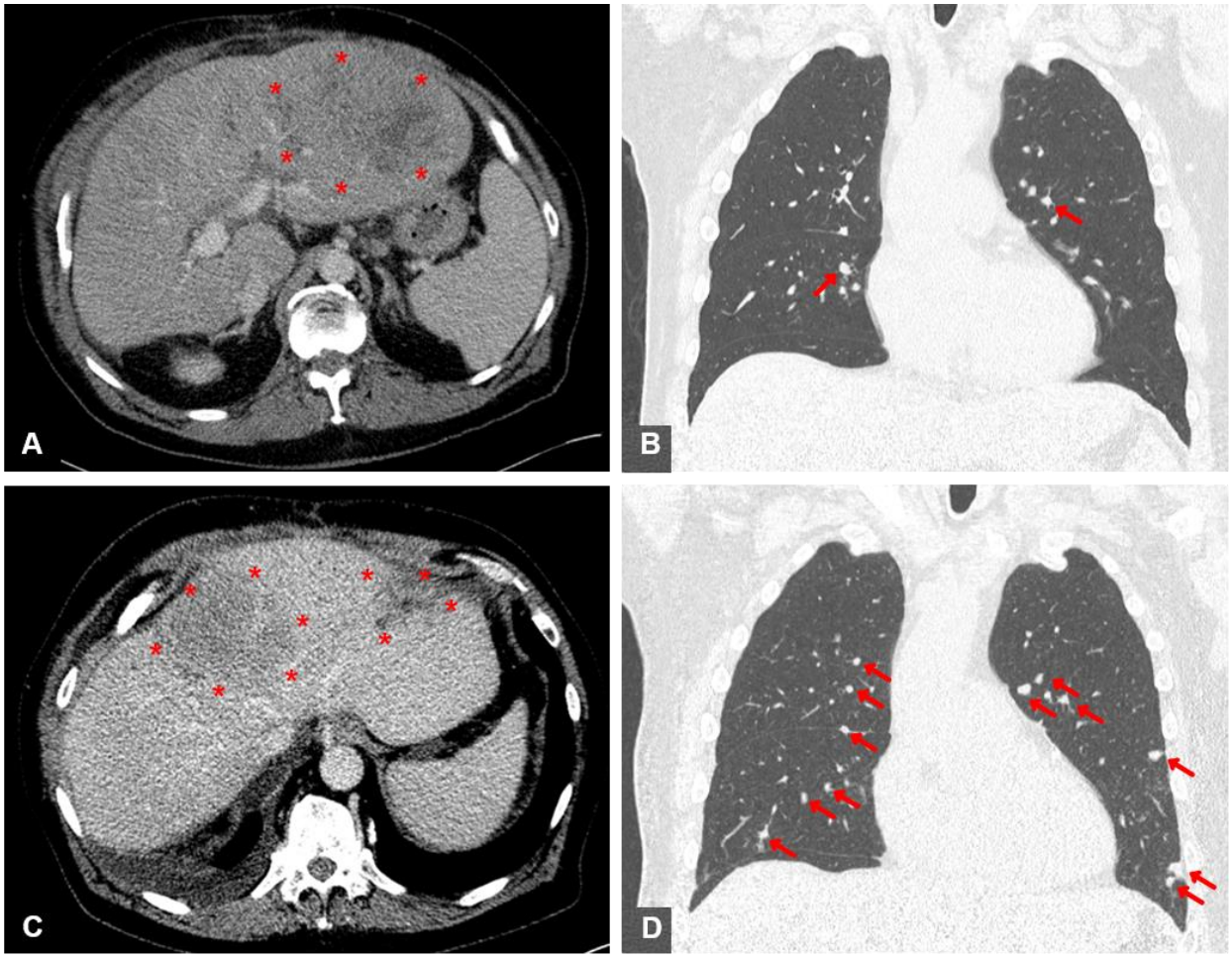

Figure 1. Contrast-enhanced CT scans before initiation of ICI therapy and as interim examination after 3 cycles of atezolizumab/bevacizumab treatment. Both intrahepatic (A+C) and intrapulmonary (B+D) HCC metastases are marked in colour. (A) Pretherapeutic, axially reconstructed abdominal CT scan showing exemplarily a large recurrence of HCC in the left liver lobe. (B) Pretherapeutic, coronary reconstructed thoracic CT scan showing exemplarily a pulmonary metastasis of HCC. (C) Axial reconstructed abdominal interim CT scan showing an example of a pronounced progression of intrahepatic HCC. (D) Coronary reconstructed thoracic interim CT scan showing marked progression of pulmonal HCC metastases.

2.3.2 Hepatic PD-L1 expression as a marker of rejection risk

Programmed death-ligand 1 (PD-L1) is a cell-surface ligand widely expressed on tumor cells. Binding of Atezolizumab to PD-L1 blocks its interaction with PD-1, an inhibitory receptor expressed by T cells, which releases them from functional inhibition by tumors. In HCC, PD-L1 is expressed by approximately 10 – 20 % of tumor cells and higher levels are generally associated

with tumor aggressiveness and poor survival [221]. A phase I trial of Atezo/Bev therapy in HCC patients concluded that high expression of PD-L1 within tumors correlated with better responses and longer progression-free survival (PFS) times [222].

In many experimental models of transplant acceptance, disrupting PD-L1 interactions leads to acute allograft rejection [223]. Likewise, transcriptomic profiling of tolerated and stably accepted liver transplants has revealed the importance of PD-L1 in controlling T cell alloimmunity in patients [224]. In the context of ICI after liver transplantation, a retrospective study investigated intragraft PD-L1 expression as a marker of acute transplant rejection risk in liver-transplanted patients with recurrent HCC who underwent anti-PD-1 therapy [225]. PD-L1 expression by hepatocytes was associated with a greater risk of acute rejection. Similarly, a prospective single-arm study of anti-PD-1 for recurrent malignancy after liver transplantation found that 5 patients lacking PD-L1 expression in their grafts remained stable during therapy, whereas a single PD-L1^{+} patient underwent acute rejection [226]. Given the limited available data, hepatic PD-L1 expression is an interesting, but unvalidated biomarker of rejection risk.

Histopathological examination of a liver biopsy taken before starting Atezo/Bev therapy revealed acute steatohepatitis with distinct fatty degeneration of the hepatocytes (70 %) and fibrosis (Ishak fibrosis grade 3-4) (Figure 2A). There were no signs of rejection. A biopsy from the tumor showed solid and trabecular infiltrates of malignant and moderately-differentiated hepatocellular carcinoma (G2) with typical shift of the nuclear-plasma relation, small-foci necrosis and marked fragmentation (Figure 2D). Immunohistochemical staining of tumor-free liver specimens for PD-L1 and PD-1 was completely negative in hepatocytes. The intrahepatic immune cells, especially the lymphocytes, showed minimal expression of PD-L1 (< 1 %) and about 5 % positivity for PD-1 (Figure 2B-C). Immunohistochemistry from the tumor biopsy indicated a Tumor Proportion Score (TPS) of 0 %, an Immune Cell Score (ICS) <1 % and a Combined Positive Score (CPS) <1 % (Figure 2E), registering a scattered CD3-positive intra/peritumoral T lymphocyte infiltrate (Figure

2F). Thus, we add another case of a stable LTx patient lacking histological PD-L1 expression that safely underwent ICI therapy without rejection.

The question of whether to start of anti-PD-L1 treatment knowing there is minimal PD-L1 expression (<1 %) is important. Unfortunately, we cannot conclusively answer whether treatment failure was predictable in this case. In contrast to other tumor entities such as melanoma, HNSCC or urothelial carcinoma, where intratumoral expression of PD-L1 or PD-1 has been shown to be predictive, this is not consistent in HCC. For example, in Checkmate040, response rates were comparable across all subgroups (PD-L1 < or ≥1 %) [210, 211]. On the other hand, KEYNOTE-224 correlated ICI response with PD-L1 expression under certain conditions [212, 213]. All of these limitations of using PD-L1 expression as a stand-alone biomarker are reflected in the FDA's deliberate disregard of PD-L1 expression for ICI approval in the treatment of HCC [227].

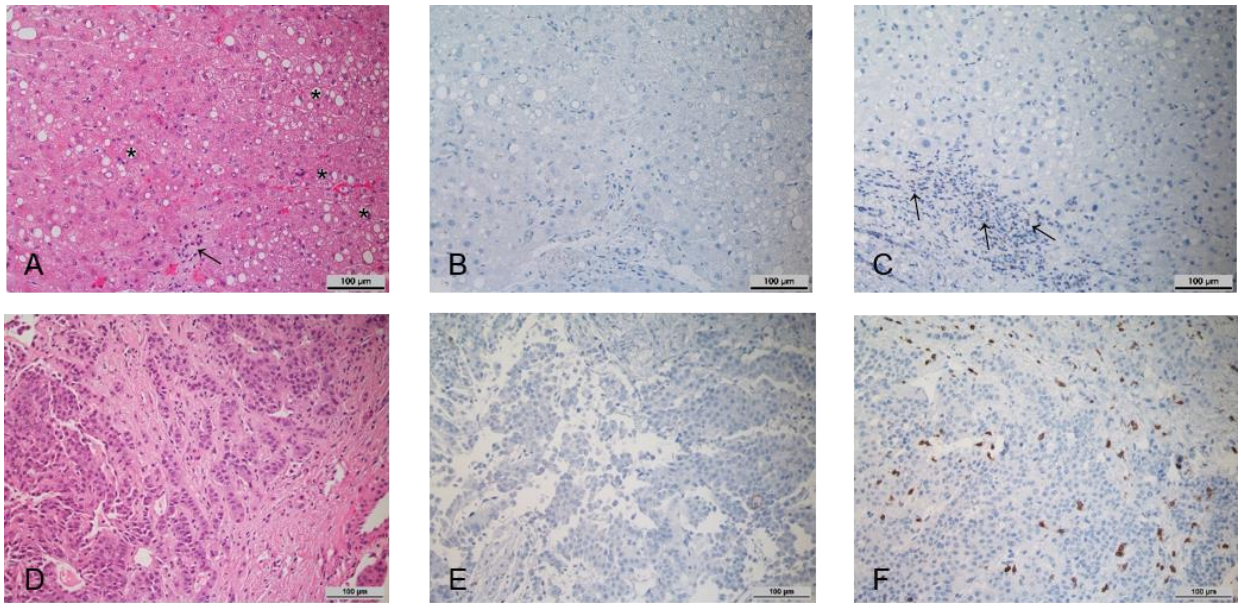

Figure 2. Histopathology of biopsies of the transplant liver (A-C) as well as intrahepatic HCC foci (D-E) prior to initiation of immune checkpoint therapy (20x magnification). (A) HE-stained representative section of the transplant liver biopsy. * intrahepatic fat vacuoles, → inflammatory infiltrate. (B) Corresponding immunohistochemical staining for PD-L1. (C) Corresponding immunohistochemical staining for PD-1. Arrows indicate inflammatory infiltrate with scattered PD-1 positive lymphocytes. (D) HE-stained representative section of HCC-infiltrated liver biopsy. (E) Corresponding immunohistochemical staining for PD-L1. (F) Immunohistochemical staining for CD3.

2.3.3 Plasma markers of clinical response

IL-6 has been proposed as a predictor of therapeutic response in patients receiving Atezo/Bev therapy [228]. In a recent study, patients with elevated baseline IL-6 levels (>4.77 pg/ml) were significantly disposed to shorter PFS. IL-6 mediates inflammation and promotes T cell infiltration of tumors. On the other hand, in some cancers, including HCC, IL-6 can suppress tumor immunity by recruiting myeloid-derived suppressor cells (MDSCs) [228]. When IL-6 levels were measured in our patient, they exceeded the cut-off associated with a positive clinical responses. We observed a persistent ~4-fold increase in IL-6 levels after starting immunotherapy (Figure 4C).

Presently, alpha-fetoprotein (AFP) is widely applied as a non-invasive monitoring biomarker of HCC tumor burden and aggressiveness. AFP ≥ 400 ng/mL is a negative prognostic factor for overall survival (OS) and is used as a stratification factor for unresectable HCC patients in clinical trials. In the context of Atezo/Bev therapy, AFP might be a useful marker for monitoring clinical effectiveness. It was recently reported that a ≥75 % decrease or ≤10 % increase in AFP levels from baseline to 6 weeks has been associated with improved OS and PFS [229]. Our patient presented with an AFP of 731 ng/mL at baseline, and 6 weeks after the start of therapy there was a progressive increase in AFP levels by ~7.5-fold (5435 ng/ml) (Figure 4E).

Combining AFP and C-Reactive Protein (CRP) serum levels has been suggested as an scoring system to predict clinical responses and survival in advanced HCC patients treated with Atezo/Bev therapy [230, 231]. Lower scores are associated with better PFS and OS. A maximum score of 2 is assigned to patients with baseline AFP ≥ 100 ng/ml and CRP ≥ 1 mg/dL. Based on this parameter, our patient had a score of 1 (AFP 731 ng/ml; CRP 0.46 mg/dL), indicative of inferior OS and inferior PFS (Figure 4B, E). In relation to our patient, the IL-6 and AFP/CRP scores lead to contradictory prognoses, suggesting that further aspects need to be considered.

2.3.4 Torque Teno Virus as a marker of rejection risk

Torque Teno Virus (TTV) load is widely used to monitor the intensity of general immunosuppression in transplant recipients. In healthy individuals, TTV load is controlled by T cell responses; therefore, adequately immunosuppressed transplant recipients have higher viral titers. A normalized TTV load in a transplant recipient suggests under-immunosuppression and an elevated risk of rejection [232]. Our patient showed a consistent reduction in TTV load after each cycle of Atezo/Bev therapy, suggesting intensified T cell activity; however, TTV titers recovered quickly after each cycle (Figure 4D). TTV values should be interpreted with caution. In the context of graft tolerance, Atezo/Bev did not lead to a stable increase in TTV titers indicating adequate immunosuppression. As for the efficacy of the therapy, TTV load has not been established as an indicator of therapy responsiveness in LTx patients. In the absence of a validated normal TTV titer range in this particular constellation of ICI therapy plus low dose of prednisolone, it may be mechanistically interesting, but is currently unhelpful in guiding clinical decisions.

2.3.5 Flow cytometry markers of clinical response and rejection risk

A study analyzing samples from the G030140 phase 1b study found that higher numbers of regulatory T cells (Treg) in blood was associated with longer PFS in patients treated with Atezo/Bev therapy compared to atezolizumab alone. Furthermore, Treg frequencies tended to decline after immunotherapy. In our patient, baseline Treg frequency was 1.6 % and we observed a reduction to 0.9 % Tregs after starting therapy, which did not recover during follow-up (Figure 4G).

Acutely increased CD28 expression by peripheral blood $CD4^+$ T cells has been reported as a predictive marker for risk of acute liver transplant rejection [233]. Our flow cytometry results

indicated a progressive downregulation in CD28 MFI during Atezo/Bev therapy, suggesting our patient did not have an elevated risk of rejection (Figure 4F).

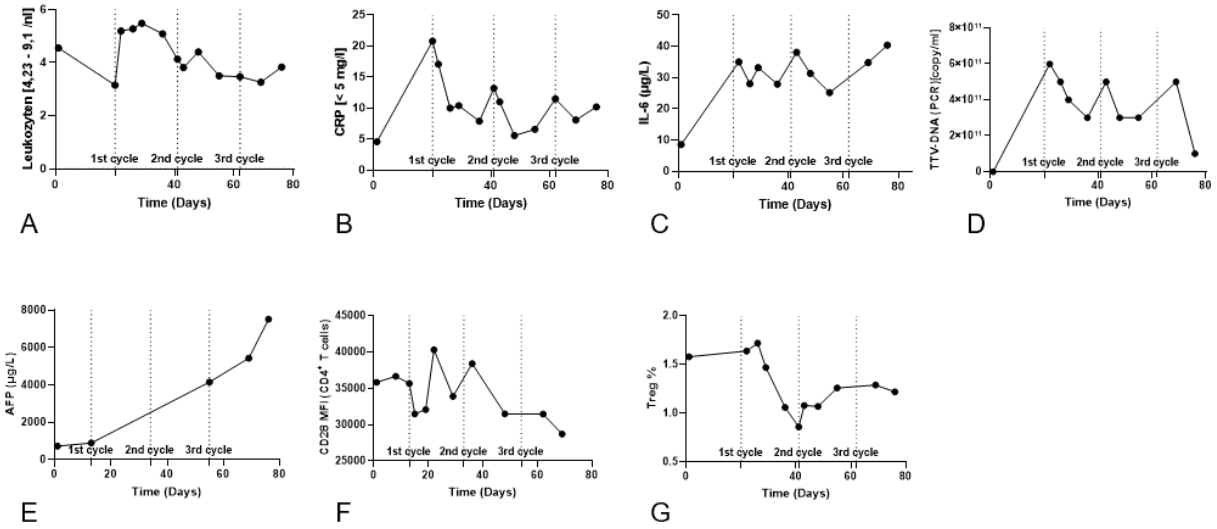

Figure 4. Immunomonitoring data in the course of ICI therapy. (A – C) Clinical routine Inflammatory parameters. (D) Torque Teno Virus level (TTV) as a surrogate parameter for the patient's immunocompetence. (E) AFP tumor marker level. (F) CD28 expression level in $CD4^+$ T cells in peripheral blood. (G) Frequency of Tregs in the peripheral blood.

2.4 Diagnostic assessment

2.4.1 Case Study

We report the case of a single liver transplant recipient who presented to the liver transplant outpatient clinic at University Hospital Regensburg with recurrent HCC. According to German Pharmaceutical Law, the patient was treated off-label with atezolizumab plus bevacizumab as a compassionate-use case. The patient provided full, informed written consent to laboratory investigations and collection of case details for publication.

2.4.2 Systematic review protocol and data extraction

Selection of publications and data extraction were performed in a standardized manner. We searched Medline at the National Library of Medicine through the NCBI website on 20-OCT-2022. Our search terms were ‘immunotherapy’, ‘atezolizumab’, ‘bevacizumab’, ‘HCC’, ‘biomarkers’, ‘liver’, ‘response’, ‘acute cellular rejection´ and synonyms. We followed up on relevant citations from articles returned in our original search. In total, we found 19 articles describing 20 unique biomarkers (Supplementary Figure 1).

2.4.3 Clinical laboratory investigations

Before starting ICI therapy, tissue biopsies were taken under sonographic guidance from both the transplanted liver and intrahepatic foci of HCC recurrence. An in-house accredited pathology laboratory (Institute of Pathology, UKR) performed histopathological investigations. For immunohistochemical staining, PD-L1 was detected with antibody clone 22C3 (DAKO, Denmark), PD-1 was detected with NAT105 (abcam, UK) and CD3 was detected with #A0452 (DAKO, Denmark). Routine Biochemistry and Haematology were performed by an in-house accredited diagnostic laboratory (Institute of Clinical Chemistry and Laboratory Medicine, UKR). Blood samples for this purpose were part of routine clinical examinations that occurred several times a week.

2.4.4 Flow cytometry

Whole blood samples were collected in EDTA tubes by peripheral venipuncture and stored at 4 °C until processing began within 4 h. Samples were prepared for flow cytometry analysis according to previously published methods [217]. Detailed step-by-step protocols are available through Protocol Exchange [234]. Briefly, whole blood samples were stained with DURAClone IM antibody panels (DURAClone IM Count Tube, C00162; DURAClone IM phenotyping BASIC Tube, B53309; DURAClone IM B cells Tube, B53318; DURAClone IM Dendritic Cell Tube, B53351;

DURAClone IM Granulocytes Tube, B88651; DURAClone IM T cell Subsets Tube, B53328; DURAClone IM TCRs Tube, B53340; DURAClone IM Treg Tube, B53346; all from Beckman Coulter, Germany). Data were recorded with a Navios™ cytometer running Cytometry List Mode Data Acquisition from Beckman Coulter. Analyses were performed using Kaluza version 2.1 (suppl. Figure 3).

2.5 Discussion

Recurrent hepatocellular carcinoma is a significant problem after liver transplantation with few satisfactory treatment options. Immunotherapy for HCC in non-transplant patients is a promising approach, but its translation to liver transplant recipients raises critical questions about likely effectiveness and the risk of precipitating acute rejection. With sparse evidence, transplant clinicians are forced to make challenging decisions about using off-label immunotherapies in their patients. Achieving an optimal balance between immunosuppression and cancer immunotherapy is crucial to a successful outcome. Faced with this dilemma, we asked ourselves whether previously reported markers of clinical efficacy or rejection risk could help in decision-making. Of the parameters described in the literature, some, such as IL-6, AFP or CRP, are routinely measured in the clinic, while others require flow cytometry or invasive immunohistochemistry.

Although our measurements of parameters that predict rejection risk and clinical response broadly agreed with the observed clinical outcome in this case, we must be cautious about the general utility of these markers. Because of the non-validated discriminatory cut-off values of these markers, as well as the small numbers of reported patient outcomes, a final answer to the question regarding their prognostic value is not yet possible. The fact that the dynamic course of some parameters during ICI therapy, rather than baseline measurements, is important for prediction complicates decision-making.

This clinical challenge of deciding about ICI therapy in transplant patients will become even more complex in the future as new agents or combinations besides Atezo/Bev gain regulatory approval for treatment of non-resectable HCC. Recently, the FDA approved of the combination of durvalumab, an anti PD-L1 antibody, and tremelimumab, an anti-CTLA-4 antibody, after the HIMALAYA Study showed an improvement in overall survival for patients with non-resectable HCC [235]. Similarly the LEAP002 study [236, 237] demonstrated the benefit of pembrolizumab, a PD-1 inhibitor, used together with the TKI lenvatinib. Because of fast-paced advances in ICI therapy for HCC is fast, it is unclear whether a single predictive marker or marker combination is capable of predicting efficacy and rejection risk in all circumstances. All this underlines the importance of further clinical studies.

Author Contributions

FB, HJS and JAH designed study. JYZ and FB performed literature search and wrote together with JAH the manuscript. DE collected the clinical course as well as the biochemical and haematological data. FW provided expert pathological opinion. PH was responsible for oncological patient care and provided expert oncological opinion. KK organized and performed immune monitoring. HJS, EKG and JMW provided infrastructural support and critical feedback. All authors contributed to the article and approved the submitted version.

Acknowledgments

The authors thank all colleagues from Surgery and Internal Medicine I involved in this case. We thank Erika Ostermeier for her outstanding technical support.

2.6 Supplementary material

Biomarker	Author	Year	Type of study	Cancer type	Cohort size	Treatmen	Timepoint	PMID	Respo nse	Graft toleranc e	Comment
NLR	Eso et al.	2021	Prospective	HCC	40	Atezo/Bev	Baseline	346772 70	Yes	NA	Patients with disease control had a significantly lower NL ratio
% CD4+ CD154+ T cells	Boix et al.	2021	Prospective	NA	30	LTx	Baseline, 7d post-transplant & 14d post-transplant	330256 22	NA	Yes	Significantly higher percentage in ACR
% CD8+ CD154+ T cells	Boix et al.	2021	Prospective	NA	30	LTx	Baseline, 7d post-transplant & 14d post-transplant	330256 22	NA	Yes	Significantly lower percentage in ACR
HLA-DRB1 mismatch	Boix et al.	2021	Prospective	NA	30	LTx	Baseline	330256 22	NA	Yes	Higher risk of ACR
CD28 expression in CD4+ T cells	Minguela et al.	1997	Prospective	NA	55	LTx	Baseline vs after transplant	912310 2	NA	Yes	CD28 MFI increased in ACR patients
% IL-2+ CD3+ CD8+ T cells	Boleslawski et al.	2004	Prospective	NA	21	LTx	Baseline	152238 97	NA	Yes	Higher risk of ACR
% IFNg+ CD8+ T cells	Millán et al.	2013	Prospective	NA	47	LTx	Baseline	232659 66	NA	Yes	>55.8% identified as cut-off for high risk of ACR
% IL-17+ CD4+ T cells	Fan et al.	2012	Prospective	NA	76	LTx	Acute rejection	232326 31	NA	Yes	Higher in ACR group vs NACR
AEC	Barnes et al.	2003	Prospective	NA	112	LTx	On the day or one day before biopsy	126940 65	NA	Yes	Elevated AEC is a risk factor for ACR
Vδ1/ Vδ2 ratio	Zhao et al.	2013	Prospective	NA	34	LTx	After transplant	232228 96	NA	Yes	Higher ratio in graft tolerated patients
Vδ1/ Vδ2 ratio	Martínez-Llordella et al.	2007	Prospective	NA	16	LTx	After transplant	172411 11	NA	Yes	Higher numbers in tolerant recipients compared to non-tolerant patients or healthy individuals.
Vδ1/ Vδ2 ratio	Puig-Pey et al.	2010	Prospective	NA	314	LTx	After transplant	204779 99	NA	Yes	Expansion of Vδ1 T cells is a common finding in transplant recipients
NLR	Tada et al.	2022	Retrospective	HCC	249	Atezo/Bev	Baseline	351705 29	Yes	NA	Lower ratio had better prognosis
PD-L1+ in TILs	Cheng et al.	2022	Retrospective	HCC	135	Atezo/Bev	Prior to therapy	349025 30	Yes	NA	≥1% associated with greater PFS & OS
T-effector signature	Zhu et al.	2022	Prospective	HCC	90	Atezo/Bev	Prior to therapy	357392 68	Yes	NA	High expression of T effector signature (GZMB, PRF1, CXCL9) associated with clinical response and longer PFS
CD274	Zhu et al.	2022	Prospective	HCC	91	Atezo/Bev	Prior to therapy	357392 68	Yes	NA	High expression associated with higher PFS & OS
Intratumoral CD8+ T cells	Zhu et al.	2022	Prospective	HCC	86	Atezo/Bev	Prior to therapy	357392 68	Yes	NA	Higher density in IHC associated with higher PFS & OS
Treg signature	Zhu et al.	2020	Prospective	HCC	91	Atezo/Bev	Prior to therapy	NA	Yes	NA	Higher expression of Treg signature (CCR8, BATF, CTSC, TNFRSF4, FOXP3, TNFRSF18, IKZF2 & IL2RA) associated with longer PFS
PD-L1+ in tumor cells	Munker et al.	2018	Retrospective	HCC	5	LTx + anti-PD-1	After transplant	302288 83	NA	Yes	Liver biopsies without evidence of PD-L1 expression are indicative of graft tolerance
PD-L1+ in tumor cells	Shi et al.	2021	Prospective	HCC	18	LTx + anti-PD-1	After transplant	328976 57	NA	Yes	Liver biopsies without evidence of PD-L1 expression are indicative of graft tolerance
VEGFR expression	Zhu et al.	2020	Prospective	HCC	91	Atezo/Bev	Prior to therapy	NA	Yes	NA	Higher expression associated with longer PFS
Myeloid inflammation signature	Zhu et al.	2020	Prospective	HCC	91	Atezo/Bev	Prior to therapy	NA	Yes	NA	Higher expression associated with longer PFS
TREM1/MDSC signature	Zhu et al.	2020	Prospective	HCC	91	Atezo/Bev	Prior to therapy	NA	Yes	NA	Higher expression associated with longer PFS
AFP	Yavuz et al.	2021	Prospective	HCC	208	Atezo/Bev	6 weeks after treatment	345951 40	Yes	NA	≥75% decrease or ≤10% increase associated with improved OS & PFS
AFP	Finn et al.	2020	Prospective	HCC	336	Atezo/Bev	Baseline	324021 60	Yes	NA	AFP<400ng/ml associated with improved OS & PFS
PD-L1+ in tumor cells	Cheng et al.	2022	Retrospective	HCC	135	Atezo/Bev	Prior to therapy	349025 30	Yes	NA	≥1% associated with greater PFS & OS
Anti-drug antibody	Galle et al.	2021	Prospective	HCC	336	Atezo/Bev	Baseline	NA	Yes	NA	ADA negative patients had improved OS vs sorafenib
IL-6	Myojin et al.	2022	Prospective	HCC	64	Atezo/Bev	Baseline	352056 31	Yes	NA	IL-6 high group had shorter PFS & OS vs IL-6 low group

Supplementary Figure 1. Overview of the results of the systematic literature review to identify parameters for predicting treatment response and induction of graft rejection by ICI therapy in HCC recurrence after liver transplantation.

Routine laboratory parameters	pre-therapeutic baseline	Range
Leukocytes	4,55 /nl	4,23 – 9,1
Haemoglobin	12,7 g/dl	13,7 – 17,5
Platelets	78 /nl	163 - 337
Sodium	140 mmol/l	136 – 145
Potassium	4,0 mmol/l	3,4 – 4,5
Creatinine	1,35 mg/dl	0,67 – 1,17
GFR (CKD-EPI) Crea	54 ml/min/1,73 qm	
Urea	60 mg/dl	16,6 – 48,5
TSH (basal)	3,61 mIU/l	0,27 – 4,2
LDH	163 U/l	0 – 250
Lipase	83 U/l	13 – 60
CK	124 U/l	< 190
Ferritin	48,2 ng/ml	30 – 400
Transferrin	293 mg/dl	200 – 360
NT-proBNP	116 pg/ml	< 376

Graft liver function	pre-therapeutic baseline	Range
GOT (AST)	43 U/l	0 – 50
GPT (ALT)	36 U/l	0 – 50
GLDH	9.1 U/l	0 – 7,0
Gamma-GT	218 U/l	< 60
Alk. Phosphatase	138 U/l	40 – 129
CHE	5968 U/l	5320 – 12920
Bilirubin (total)	0.6 mg/dl	0 – 1,4
Bilirubin (direct / conjugated)	0.3 mg/dl	0 – 0,3
Bilirubin (indirect / unconjugated)	0.3 mg/dl	
Total protein	82.5 g/l	66 – 87
Albumin	43.8 g/l	35 – 52
Quick	>100 %	> 70
INR	0.98	0,85 – 1,15
PTT	34.6 sec.	25,9 – 36,6
Fibrinogen	392.9 mg/dl	210 – 400
Sirolimus	3.9	
Faktor II	92 %	70 – 120
Faktor V	123 %	70 – 120
Faktor VII	104 %	70 – 120
Faktor VIII	169 %	70 – 150
Protein C	74 %	70 – 140
freies Protein S (immunolog.)	96.2 %	66 – 149

Tumour markers	pre-therapeutic baseline	Range
AFP	731.0 ng/ml	< 7,0
CA 19-9	53.1 U/ml	< 27
CEA	2.2 ng/ml	< 3,8
PSA (total)	0.19 ng/ml	< 4,1
PSA (free)	0.07 ng/ml	
beta-HCG	0.63 mIU/ml	< 2,0

Infectiological parameters	pre-therapeutic baseline	Range
Anti-HAV-IgG	0.50 S/co	< 1,0
Anti-HAV-IgM	0.08 S/co	
HBsAg	0.20 S/co	
Anti-HBc	0.23 S/co	
Anti-HBs	0 IU/l	< 10
Anti-HCV	0.17 S/co	
Anti-HEV-IgG-ELISA	61.7 U/ml	0 – 24
Anti-HEV-IgM-ELISA	2.2 U/ml	0 – 24
Anti-HIV/p24-Antigen	0.13 S/co	< 1,0
TBC-Elispot	negative	
Anti-CMV-IgG (CMIA)	1.40 AU/ml	< 6
Anti-CMV-IgM (CMIA)	0.14 index	
CMV-DNA (PCR, stool)	0 copy/ml	
CMV-DNA (PCR, serum)	0 copy/ml	
Anti-Varizella Zoster-Virus, IgG	>2000 mIU/ml	
Anti-EBV-IgG-Immunoblot	positive	
Anti-EBV-IgM-Immunoblot	negative	

Autoimmune / rheumatologic parameters	pre-therapeutic baseline	Range
ANA (Titer)	1:320 Titre	< 1:40
autoimmunity against mitochondria	<1:40 Titre	< 1:40
AMA-M2	negative	
PCNA	negative	
Jo 1	negative	
Ro-52	negative	
SS-A	negative	
Sm	negative	
IgG	1809 mg/dl	700 – 1600
IgG-4	30.60 mg/dl	3,0 - 201
alpha1-Globulin	3.1 %	2,9 – 4,9
alpha2-Globulin	7.9 %	7,1 – 11,8
beta1-Globulin	4.3 %	4,7 – 7,2
beta2-Globulin	3.5 %	3,2 – 6,5
gamma-Globulin	16.8 %	11,1 – 18,8

Supplementary Figure 2. Overview of the routine clinical and laboratory examinations performed to exclude comorbidities such as secondary tumours, autoimmune diseases and occult infections. In order, routine laboratory parameters, biochemical graft liver function, tumour markers to exclude secondary tumours, infectiological parameters to exclude occult infections and autoimmune / rheumatologic parameters

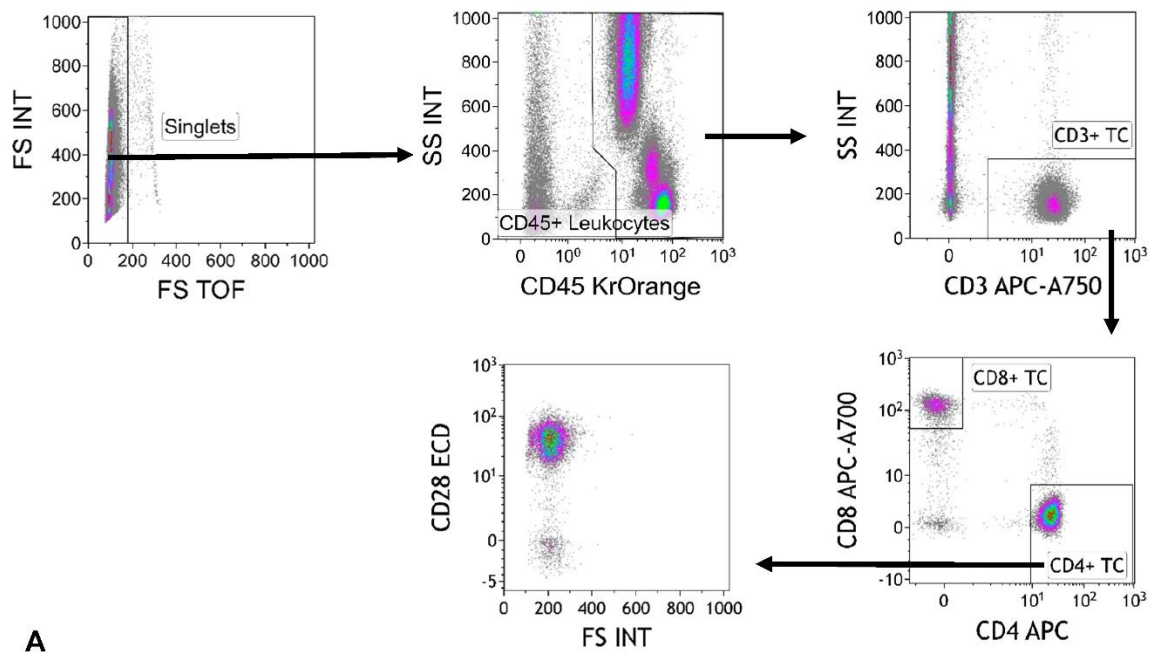

A

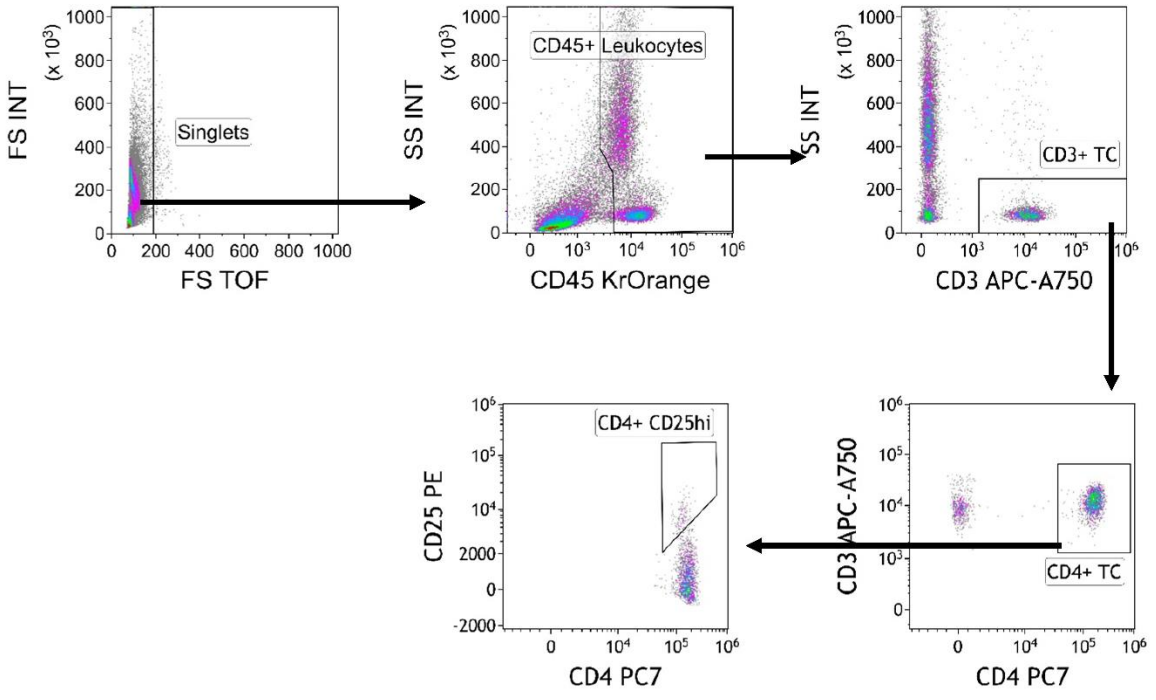

B

Supplementary Figure 3. Gating strategies used for immunomoditoring, as recommended by the manufacturer, to determine the CD28 expression level in $CD4^+$ T cells (A) and the frequency of regulatory T cells (B).

- Published Article –

Published in: Frontiers in Immunology. 2022 June;

https://doi.org/10.3389/fimmu.2022.898473

3. Identification and Isolation of Type II NKT Cell Subsets in Human Blood and Liver

Jordi Yang Zhou,[1,2] Jens M. Werner,[1] Gunther Glehr,[1]

Edward K. Geissler,[1,2,3,4] James A. Hutchinson[1] and Katharina Kronenberg[1†]

1. Department of Surgery, University Hospital Regensburg, Franz-Josef-Strauß-Allee 11, 93053 Regensburg, Germany
2. Leibniz Institute for Immunotherapy, Franz-Josef-Strauß-Allee 11, 93053 Regensburg, Germany
3. Fraunhofer-Institute for Toxicology and Experimental Medicine ITEM-R, AmBiopark 9, 93053 Regensburg, Germany
4. Regensburg International Graduate School of Life Sciences, University of Regensburg, Universitätsstraße 31, 93053 Regensburg, Germany

3.1 Abstract

Background: Steatotic livers are more prone to rejection, but are often transplanted owing to the shortage of available organs. Type II NKT (T2NKT) cells are liver-resident lymphocytes that react to lipids presented by CD1d. The role of T2NKT cells in rejection of fatty liver transplants is unclear, partly because of a lack of T2NKT cell markers and their very low frequency in blood. Here, we quantify human T2NKT cells in blood and liver tissue by flow cytometry and provide a strategy for their enrichment and expansion. **Methods:** Human T2NKT cells were identified as $CD3^+$ $CD56^+$ $CD161^+$ TCR-$\gamma\delta^-$ $TCRV\alpha7.2^-$ and $TCRV\alpha24^-$ cells. T2NKT cells were enriched from blood by sequential positive selection using CD56 and CD3 microbeads. These were subsequently FACS-sorted to purity then expanded in vitro for 3 weeks using anti-CD3/CD28 beads and TGF-β1. **Results:** The frequency of human T2NKT cells in blood was very low (0.8 ± 0.4 % of $CD3^+$ T cells) but they were a more abundant population in liver (6.3 ± 0.9 %). Enriched T2NKT cells expressed the transcription factor PLZF. A novel subset of $FoxP3^+$ T2NKT cells was discovered in blood and liver tissue. T2NKT cells were expanded in culture by 15- to 28-fold over 3 weeks, during which time they maintained expression of all identifying markers, including PLZF and FoxP3 (16.9 ± 3.6 %). **Conclusions:** Our work defines new strategies for identifying and isolating T2NKT cells from human blood and liver tissue. We showed that this rare population can be expanded *in vitro* in order to obtain experimentally amenable cell numbers. Further, we identified a novel T2NKT cell subset that stably expresses FoxP3, which might play a role in regulating innate-like lymphocyte responses in steatotic liver transplants.

3.2 Introduction

Demand for liver transplants has significantly increased over the past decade [131]. Approximately 25 % of the global population is affected by nonalcoholic fatty liver disease, which is characterized by excessive accumulation of fat in hepatocytes, a condition known as steatosis. Thus, a high proportion of livers available for transplant are steatotic [238]. Unfortunately, a significantly higher rate of primary graft dysfunction is observed after transplantation of steatotic livers [239]. Moreover, moderate and severe steatosis of donor livers is associated with inferior post-transplant outcomes [240].

Natural Killer T (NKT) cells are non-conventional T cells that share common features with NK cells. NKT cells are rare in peripheral blood, but represent a larger fraction of liver, spleen, lung, and intestine resident T cells [241]. Expression of T Cell Receptor (TCR)-αβ enables NKT cells to recognize antigenic lipids presented by CD1d, an MHC class I-like molecule [242]. NKT cells express the promyelocytic leukemia zinc finger protein (PLZF) transcription factor as a prerequisite for their development [241]. Among T cells, only innate-like γδ T cells and MAIT cells otherwise express PLZF [241]. NKT cells are subclassified into invariant NKT (iNKT) cells and type II NKT (T2NKT) cells according to their TCR specificity. iNKT cells possess an invariant TCR Vα24-Jα18α chain paired with TCR Vβ11, which mainly responds to α-galactosylceramide glycopeptide (αGalCer). By contrast, T2NKT cells utilize different TCR rearrangements to recognize diverse lipids [243].

Our understanding of T2NKT cells in transplant immunology has been limited by the technical challenges of studying them, especially the very low frequency of these cells in blood and lack of exclusive markers. Human T2NKT cells are conventionally detected with sulfatide-loaded CD1d tetramers [244]; however, this method is noisy and fails to identify T2NKT cells that recognize other lipids. Here, we report a strategy to detect and isolate T2NKT cells from human blood and

liver tissue. We further develop an expansion strategy to increase cell numbers, making it possible to conduct *in vitro* experiments.

3.3 Methods

3.3.1 Study approval and human samples

Human peripheral blood leucocytes were collected from healthy individuals as a by-product of thrombocyte donation with the approval of the Ethics Committee of the University of Regensburg (approval number 19-1403-101). Intrahepatic lymphocytes (IHL) were isolated from resected liver tissues with the approval of the Ethics Committee of the University of Regensburg (approval number 13-257-101). All cell and tissue donors gave full, informed, written consent to the study.

3.3.2 Isolation of mononuclear leucocytes from apheresates and liver

Peripheral blood mononuclear cells (PBMC) were isolated by Ficoll gradient centrifugation as previously described [37]. IHL were isolated from surgically resected liver. Briefly, samples were washed with Hank's balanced salt solution (HBSS) (H9394, Gibco, UK), minced with a sterile blade, and incubated in HBSS supplemented with 0.5 mg/ml collagenase type IV (C4-28-BC, Sigma-Aldrich, Germany) and 0.05 µg/ml DNase I (A37880, AppliChem, Germany) for 10 mins at 37 °C. The suspension was filtered through a 100 µm nylon mesh filter, then through a 30 µm nylon mesh filter to remove cell clumps and hepatocytes. IHL were isolated by Ficoll gradient centrifugation and subsequently frozen in RPMI (72400-021, Gibco) with 10 % DMSO at -160 °C liquid nitrogen. For thawing, cryovials were placed in 37 °C water bath for 1 min and then cells were transferred into a 15 ml Falcon tube with 1 ml prewarmed RPMI supplemented with 100 µg/ml DNase I. Cells were rested for 4 mins and incubated with 2 ml RPMI for 2 mins before adding 4 ml RPMI and incubating for 2 mins.

3.3.3 Magnetic bead selection of T2NKT cells

Starting with a single-cell suspension of PBMC or IHL, a two-step process was used to enrich T2NKT cells. In the first step, a typical starting number of 1 – 7 x 10^8 cells were sorted with the REAlease CD56 MicroBead Kit (130-117-033, Miltenyi, Germany) according to the manufacturer's instructions, using LS columns (130-042-401, Miltenyi) and Separation Buffer (PBS, 0.5 % Albunorm (00200331, Octapharma, Germany), 0.4 % UltraPure 0.5M EDTA (15575-038, Invitrogen, USA)). In the second step, after "de-labelling" of CD56-selected cells, a second magnetic bead isolation was performed with CD3 MicroBeads (130-050-101, Miltenyi). Typically, 0.1 – 5 x 10^7 recovered cells were positively selected according to the manufacturer's instructions using the "Possel" selection routine on an AutoMACS Pro Separator (Miltenyi). After selection, enriched cells were resuspended in 2 ml NKT medium (500 ml RPMI Medium 1640 supplemented with 2 mM GlutaMAX^{TM}, 50 ml FCS, 5 ml Pen/Strep, 5 ml sodium pyruvate, 15 ml 7.5 % $NaHCO_3$, and 55 µl β-ME). Cells were then stored at 4 °C overnight before further processing.

3.3.4 Purification of T2NKT cells by flow cytometry sorting

Enriched cells were resuspended in 50 µl Cell Staining Buffer (CSB) (420201, Biolegend, USA) plus 10 % FcR-Block (130-059-901, Miltenyi) then incubated for 15 mins at 4 °C. Cells were labelled with biotinylated antibodies against TCR-γδ (130-113-502, Miltenyi), TCR-Vα24 (130-117-958, Miltenyi) and TCR Vα7.2 (130-110-957, Miltenyi) in a total volume of 100 µl of CSB for 15 mins at 4 °C. After washing in 2 ml CSB, cells were stained for 30 mins at 4 °C with α-biotin FITC (130-110-957, Miltenyi), αCD161 PE (339904, BioLegend), αCD25 PC5.5 (356112, BioLegend), αCD56 APC (318310, BioLegend), αCD3 APC-H7 (560176, BD Biosciences, USA) and αCD4 BV421 (344632, BioLegend) in a final volume of 100 µl/sample comprising CSB plus 50 µl Brilliant Staining Buffer (563794, BD). Cells were washed with 2 ml CSB then resuspended in 500 µl PBS prior to sorting on a FACSAria Fusion (BD).

3.3.5 Expansion of T2NKT cells in culture

On day 0, 0.5 – 1 x 10^5 flow-sorted T2NKT cells were resuspended in 100 µl/well TexMACS medium (130-097-196, Miltenyi) supplemented with 500 U/ml recombinant human IL-2 (P30-2901, Peprotech, USA), and 5 % human AB serum (P30-2901, PAN-Biotech, Germany) in U-bottom 96-well plates (3799, Costar, USA). Anti-CD3/CD28 MACSiBeads were prepared following the manufacturer's instructions and added into the wells at a bead:cell ratio of 4:1. To promote expansion of $FoxP3^+$ T2NKT cells, 5 pg/µl TGF-β1 (240-B-010/CF, R&D Systems, USA) was added to cultures. On day +1, wells were topped up with 100 µl TexMACS medium containing 5 pg/µl TGF-β1. Medium was changed every 3 days by replacing 100 µl consumed media with fresh TexMACS medium containing 5 pg/µl TGF-β1. After 2 weeks expansion, cells were harvested and resuspended in 1 ml TexMACS medium. A 10 µl aliquot of cells was counted using Precision Count Beads (424902, BioLegend). Remaining cells were maintained in culture for another 1 week with medium supplementation every 3 days.

3.3.6 Identification of T2NKT cells by flow cytometry

Samples were prepared for analysis by flow cytometry according to previously published methods [217]. Briefly, 10^6 cells were transferred into V-bottom 96 well microplates (651201, Greiner, Germany) with 50 µl/well CSB plus 10 % FcR-Block for 15 mins at 4 °C. Biotin-labelled antibodies against TCR-Vα24, TCR-vα7.2, and TCR-γδ were added and adjusted with CSB to 100 µl/well. Samples were incubated for 15 mins at 4 °C and washed with 150 µl/well CSB. Samples were resuspended in 50 µl Brilliant Staining Buffer with following antibodies and adjusted to a total volume of 100 µl with CSB: α-CD161 PE (339904, Biolegend); α-CD25 PC5.5 (356112, BioLegend); α-CD127 BV421 (351332, BioLegend); α-CD56 BV510 (318340, BioLegend); α-Biotin FITC (130-110-957, Miltenyi); CD3 APC-H7 (560176, BD). Samples were incubated for 30 mins at 4 °C then washed twice with 200 µl/well CSB. Cells were then stained for intracellular

markers using the eBioscience FOXP3/Transcription Factor Staining Buffer Set (00-5523-00, Invitrogen, USA) according to the manufacturer's instructions. After fixation and permeabilization, samples were stained with α-PLZF PC7 (25-9322-82, Invitrogen, Germany) and α-FoxP3 (320213, Biolegend) for 30 mins at 4 °C. Cells were washed in CSB then resuspended in 1X Fixative Solution IOTest3 solution (A07800, Beckman Coulter, Germany) prior to measurement with a Canto-II (BD) or CytoFlex LX (Beckman Coulter) cytometer.

Sulfatide-loaded CD1d tetramers were prepared as previously described [244]. Briefly, 1.7 µg sulfatide (1049, Matreya) were incubated with 11 µg human CD1d Unloaded Biotinylated Monomer (kindly provided by the *NIH* Tetramer Core Facility) in a total volume of 20 µl PBS at 37 °C overnight. The next day, 1 µl, 10 µl, or 100 µl of 1:10 PE streptavidin (405203, Biolegend) in sterile PBS was mixed with the complex and incubated for 2 h at RT in a total volume of 110 µl. 10^6 PBMC or IHL were incubated with 50 µl/well PBS plus 10 % FcR-Block in V-bottom 96 well microplates for 15 mins at 4 °C. Cells were then stained with 1 µl, 5 µl or 10 µl of each sulfatide-CD1d preparation with gentle mixing and incubated for 30 mins at 4 °C. Cells were then stained for flow cytometry as described above without an intervening washing step.

3.4 Results

3.4.1 Establishing a flow cytometry panel to quantify T2NKT cells

T2NKT cells are challenging to study because of a lack of positive markers and their very low frequency in blood [241]. Although NKT cells can be positively identified using CD1d tetramers loaded with lipids (such as α-GalCer, sulfatide and lysosulfatides) this is neither a convenient nor reliable approach for quantifying total T2NKT cells in a single sample [245] (Supplementary Figure 1). Therefore, we propose a working definition of T2NKT cells as $CD3^+$ $CD56^+$ $CD161^+$ T cells after excluding TCR-Vα24$^+$ iNKT cells, TCR-γδ$^+$ T cells and TCR-Vα7.2$^+$ MAIT cells (Figure 1A & B). It is useful to further subdivide T2NKT cells into $CD4^+$, $CD8^+$ and double-negative (DN)

subpopulations, which may reflect functional differences in cytokine production [246]. Our panel also included two members of the NKG2 (CD159) C-type lectin-like receptor family that are commonly expressed in NK cells and other innate-like lymphocytes [245]. $CD4^-$ iNKT cells reportedly express NKG2D, enabling them to respond to MHC Class I-like molecules (*eg*. H60, RAE, MULT1 and MIC families) [247]. By contrast, NKG2A has an inhibitory function. We anticipate that NKG2A and NKG2D will be useful markers of T2NKT cell activation in future immune monitoring studies. To improve the accuracy of our cell type identification, particularly when also using CD1d tetramers, we included CD16 and CD19 to exclude monocytes and B cells [248]. Using this assay panel, we identified a $CD3^+$ $CD56^+$ $CD161^+$ TCR-Vα24$^-$ TCR-γδ$^-$ TCR-Vα7.2$^-$ living T2NKT cell population that represented 0.8 ± 0.4 % of $CD3^+$ T cells from PBMC and 6.3 ± 0.9 % of $CD3^+$ T cells from IHL preparations (Figure 1C).

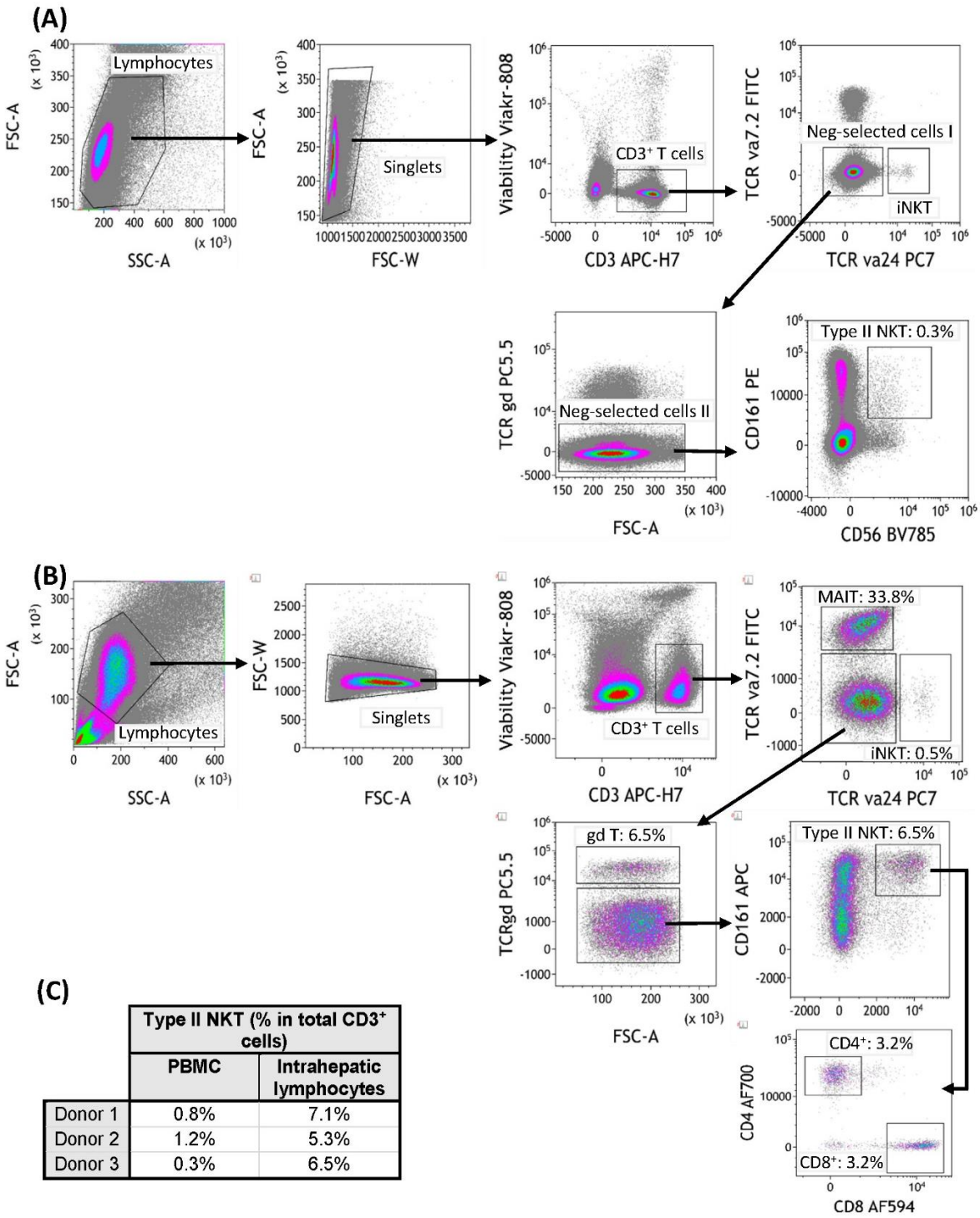

(C)

	Type II NKT (% in total CD3⁺ cells)	
	PBMC	Intrahepatic lymphocytes
Donor 1	0.8%	7.1%
Donor 2	1.2%	5.3%
Donor 3	0.3%	6.5%

Figure 1. Flow cytometry gating strategy for quantification of human type II NKT cells. (A) Human T2NKT cells were defined as $CD3^+$ $CD56^+$ $CD161^+$ $TCR\gamma\delta^-$ $TCRV\alpha7.2^-$ $TCRV\alpha24^-$ lymphocytes. Gating of human PBMC resulted in a very low frequency of circulating T2NKT cells (0.3 % of total $CD3^+$ T cells). (B) Gating of human intrahepatic lymphocytes (IHL) revealed a higher frequency of T2NKT cells in non-steatotic liver (6.5 % of total $CD3^+$ T cells). Intrahepatic T2NKT cells could be subdivided into $CD4^+$ and $CD8^+$ cells. (C) Frequency of human T2NKT cells with respect to $CD3^+$ T cells from 3 PBMC and 3 liver (steatosis 0 %, n=2; steatosis 15 %, n=1) samples.

3.4.2 Pre-enriching $CD3^+$ $CD56^+$ NKT cells by positive selection

Because circulating T2NKT cells are so rare, we next developed a magnetic bead-based protocol to pre-enrich $CD3^+$ $CD56^+$ innate lymphocytes prior to immunophenotyping by flow cytometry or further purification by flow-sorting (Figure 2A). We compared alternative separation strategies (Supplementary Figure 2 & 3), namely: (1) Sorting for $CD3^+$ cells then $CD56^+$ cells; (2) sorting for $CD56^+$ cells then $CD3^+$ cells; (3) sorting using a $CD3^+$ $CD56^+$ NKT Cell Isolation Kit from Miltenyi Biotec; (4) sorting for $CD56^+$ cells, then $CD3^+$ cells and then depleting TCR-$V\alpha24^+$ iNKT cells, TCR-$\gamma\delta^+$ T cells and TCR-$V\alpha7.2^+$ MAIT cells; (5) sorting for $CD56^+$ cells, then $CD3^+$ cells, then depleting TCR-$V\alpha24^+$ iNKT cells, TCR-$\gamma\delta^+$ T cells and TCR-$V\alpha7.2^+$ MAIT cells and then enriching for $CD161^+$ cells. We found that enriching $CD3^+$ cells prior to $CD56^+$ selection (Strategy 1) led to poorer yields than first enriching $CD56^+$ cells (Strategy 2) (Supplementary Figure 2A-C). Miltenyi's $CD3^+$ $CD56^+$ NKT Cell Isolation Kit (Strategy 3) performed well in enriching $CD3^+$ $CD56^+$ NKT cells, but led to a disproportionate loss of T2NKT compared to iNKT cells (Supplementary Figure 3A). We attempted to increase the purity of our enriched samples by depleting TCR-$V\alpha24^+$ iNKT cells, TCR-$\gamma\delta^+$ T cells and TCR-$V\alpha7.2^+$ MAIT cells without (Strategy 4) or with (Strategy 5) positive selection of $CD161^+$ cells. Both methods had unacceptably low yields (Supplementary Figure 3B & C). Hence, we determined that enriching $CD56^+$ cells using REAlease CD56 MicroBead Kit from Miltenyi prior to positive selection of $CD3^+$ cells using CD3 MicroBeads from Miltenyi is an optimally efficient method for pre-enriching human T2NKT cells from blood (Figure 2B & C).

3.4.3 Expression of PLZF and FoxP3 in $CD3^+$ $CD56^+$ $CD161^+$ T2NKT cells

The transcription factor PLZF is primarily expressed by innate-like lymphocytes, especially NK cells, MAIT cells and NKT cells. Intracellular staining of pre-enriched NKT cells from blood revealed an intermediate level of PLZF in T2NKT cells, which was similar to PLZF expression in

NK cells, but less than PLZF expression in iNKT cells and greater than PLZF expression in conventional T cells (Figure 2D).

We hypothesize that distinct subsets of human T2NKT cells play inflammatory or regulatory roles in steatotic livers after transplantation; therefore, we next investigated expression of Treg-associated markers in pre-enriched NKT cells. This revealed a previously undescribed subset of $CD3^+$ $CD56^+$ $CD161^+$ $CD4^+$ $CD25^+$ $CD127^{low}$ $PLZF^+$ $FoxP3^+$ T2NKT cells that represented 4.8 ± 1.3 % (n=3) of T2NKT cells from PBMC (Figure 2E). Additionally, among other innate-like lymphocytes, we identified a $FoxP3^+$ MAIT cell population, but not a $FoxP3^+$ iNKT cell or γδ T cell population (Supplementary Figure 4).

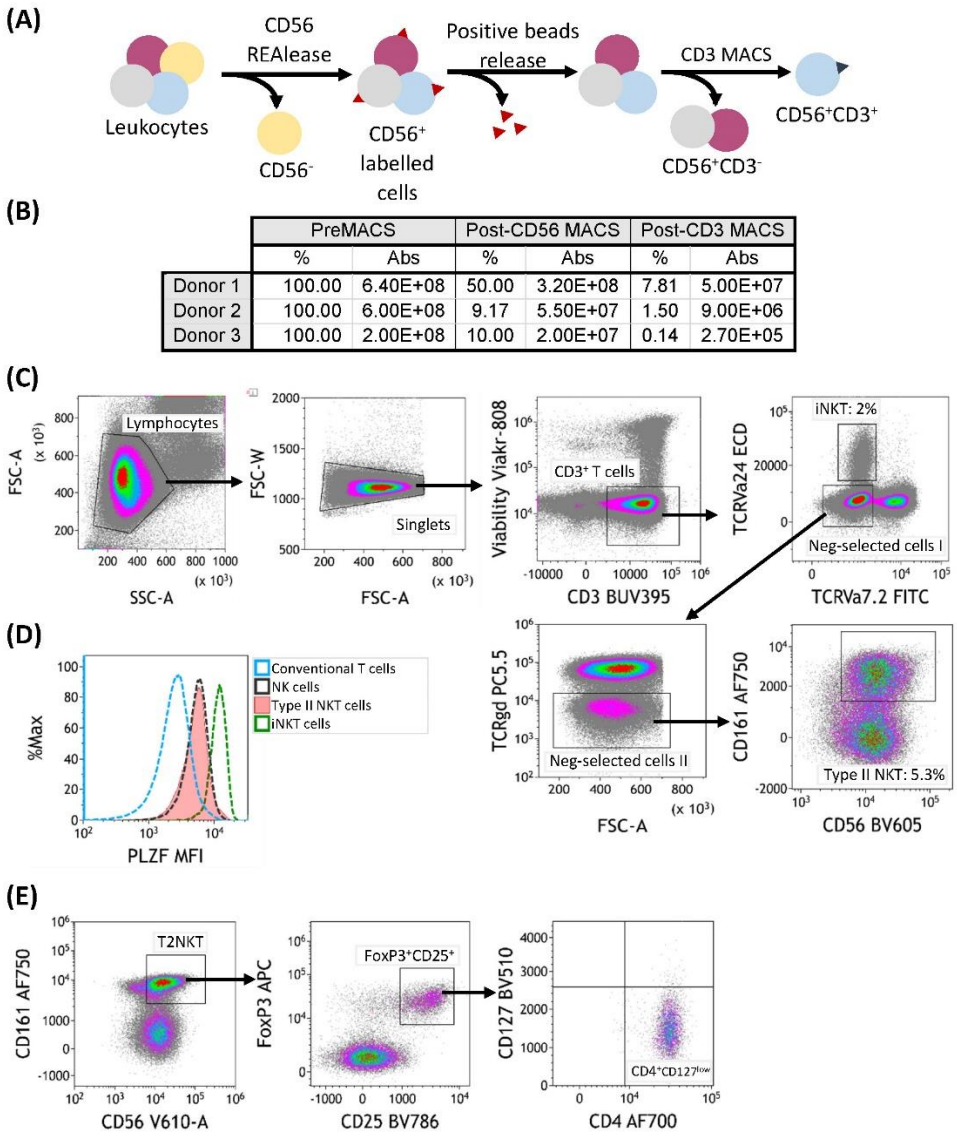

	PreMACS		Post-CD56 MACS		Post-CD3 MACS	
	%	Abs	%	Abs	%	Abs
Donor 1	100.00	6.40E+08	50.00	3.20E+08	7.81	5.00E+07
Donor 2	100.00	6.00E+08	9.17	5.50E+07	1.50	9.00E+06
Donor 3	100.00	2.00E+08	10.00	2.00E+07	0.14	2.70E+05

Figure 2. Two-step magnetic-activated cell sorting (MACS) strategy for enrichment of human T2NKT cells. (A) Two-step MACS strategy consisted first in a CD56 positive selection from human PBMC with CD56 REAlease microbeads. These beads were then detached from the cell surface after separation. In the second step, NKT cells were enriched using CD3 microbeads. The outcome of this procedure was a $CD3^+$ $CD56^+$ cell isolate enriched in NKT cells. (B) Summary table indicating the frequency of cells relative to preMACS values and absolute (Abs) cell numbers after each MACS step. (C) Gating of human leucocytes enriched for $CD56^+$ $CD3^+$ cells using the two-step MACS protocol. The sample was enriched for iNKT cells (2 % of total $CD3^+$ T cells) and T2NKT cells (5.3 % of total $CD3^+$ T cells). (D) Expression of the transcription regulator promyelocytic leukemia zinc finger (PLZF) in subsets of human lymphocytes. Differential expression of PLZF was observed between conventional T cells (blue line) and NK cells (black line). There was similar PLZF expression in T2NKT cells (red line) and NK cells, whereas iNKT cells (green line) showed higher expression. (E) A $CD4^+$ $FoxP3^+$ $CD25^+$ $CD127^{low}$ subpopulation of $CD3^+$ $CD56^+$ $CD161^+$ $TCR\gamma\delta^-$ $TCRV\alpha7.2^-$ $TCRV\alpha24^-$ T2NKT cells after the two-step enrichment process was identified in all 3 donors (one donor is shown as an example).

3.4.4 Expansion of T2NKT cells without losing NKT cell markers

To perform functional experiments with T2NKT cells, it was necessary to flow-sort them to purity. NKT cells were enriched from PBMC by magnetic bead selection then stained with CD3, CD4, CD56, CD161, TCR-Vα24, TCR-Vα7.2 and TCR-γδ for flow-sorting (Supplementary Figure 5). As illustrated, T2NKT cells were isolated as $CD3^+$ $CD4^+$ $CD56^+$ $CD161^+$ TCR-$Vα24^-$ TCR-$Vα7.2^-$ and TCR-$γδ^-$ living cells (Figure 3A). Following this strategy, 2 – 7 x 10^4 T2NKT cells could be isolated from a typical starting population of 4 – 6 x 10^8 unsorted PBMC.

Because the absolute number of T2NKT cells recovered with our optimized protocol was so limited, we next investigated whether they could be expanded *in vitro*. Purified T2NKT cells were stimulated with MACSiBeads, IL-2 and TGF-β1 for 3 weeks (Figure 3B). The cultured cells were then counted by flow cytometry (Figure 3C). After 21 days of *in vitro* stimulation, T2NKT cells maintained expression of $CD3^+$ $CD56^+$ $CD161^+$ and PLZF (Figure 3D). In addition, a subset of $CD3^+$ $CD56^+$ $CD161^+$ $CD4^+$ $CD25^+$ $CD127^{low}$ $PLZF^+$ $FoxP3^+$ T2NKT cells was still detectable, representing 16.9 ± 3.6 % of total T2NKT cells (Figure 3D & E). Hence, we were able to expand T2NKT cells by ≥15-fold without loss of key markers, meaning that we can obtain sensible numbers of phenotypically normal T2NKT cells for use in functional studies.

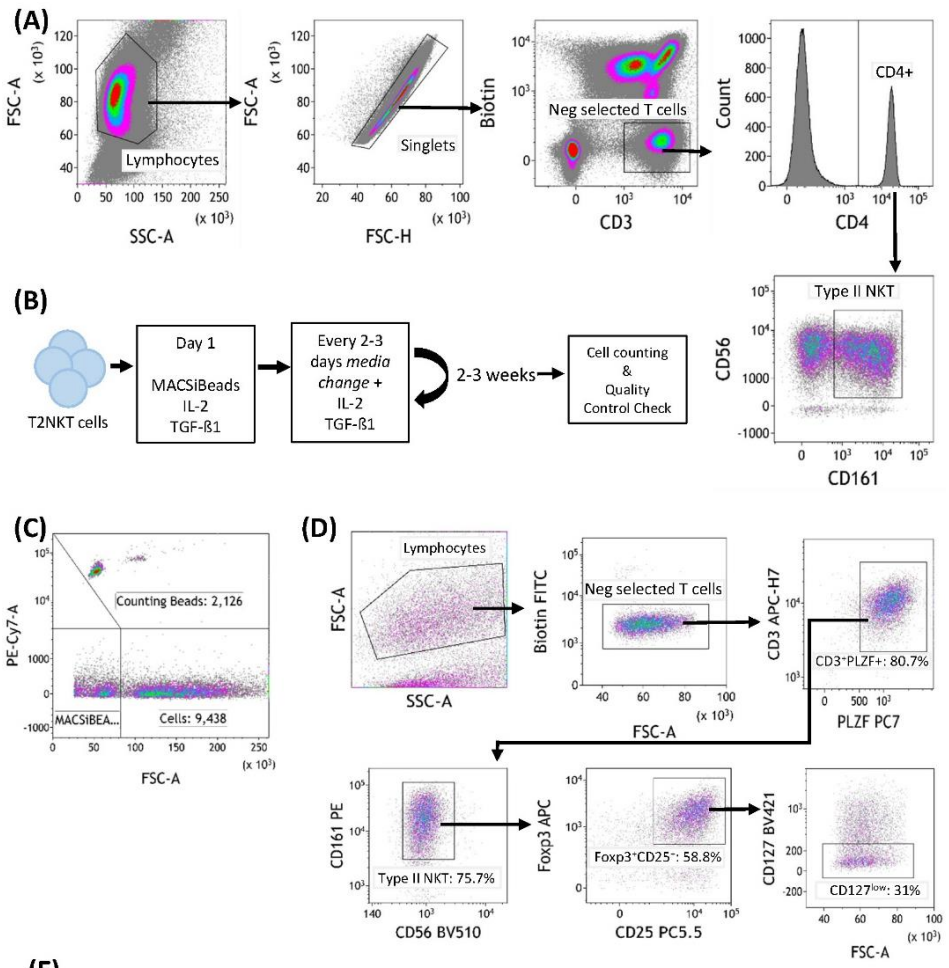

(E)

	Day 0	Day 21	
	Absolute number	Absolute number	%Foxp3+
Donor 1	6.80E+04	1.53E+06	19.61
Donor 2	4.38E+04	6.74E+05	12.81
Donor 3	2.50E+04	1.96E+06	18.34

Figure 3. In vitro expansion of FoxP3$^+$ T2NKT cells. (A) Gating strategy to flow-sort T2NKT cell after double-step MACS enrichment. From left to right, cells were gated for lymphocytes based on FSC/SSC and singlets. Biotin FITC excluded cells labeled with TCRVα7.2, TCRVα24 or TCRγδ antibody. Cells were then gated for CD3$^+$ CD4$^+$ CD56$^+$ CD161$^+$. (B) Schematic map depicting each step of the expansion protocol. (C) Cell counting after 3 weeks expansion using Flow Cytometry Counting Beads. Counting beads were positive for PE-Cy7, cells were separated from MACSiBeads based on FSC. (D) Quality control analysis of T2NKT cell expansion after 3 weeks. Lymphocytes were separated from MACSiBeads and dead cells by FSC/SSC. MAIT cells, γδ T cells and iNKT cells were excluded by staining with Biotin FITC. Within the CD3$^+$ T cell population, PLZF was highly expressed (80.7 % of the total lymphocyte population). These cells were mainly CD56$^+$ CD161$^+$ (75.7 % of the total lymphocyte population) and a subset expressed regulatory-like phenotype FoxP3$^+$ CD25$^+$ CD127^{low} (31 % of the total lymphocyte population). (E) Summary table indicating absolute number of cells before expansion (day 0) and after expansion (day 21). Percentage of FoxP3$^+$ cells after expansion is included.

3.5 Discussion

Here, we present a strategy for identifying and enriching human T2NKT cells from blood and liver tissue. Further, we describe a novel subset of T2NKT cells that stably expresses FoxP3, suggesting it may play a role in regulating innate-like lymphocyte responses in fatty livers.

We propose a working definition of T2NKT cells based upon CD3, CD56 and CD161 coexpression, and exclusion of iNKT cells, MAIT cells and γδ T cells. Practically speaking, our definition is superior to detection with lipid-loaded CD1d tetramers for several reasons - namely, lipid-loaded CD1d tetramers label only a subset of T2NKT cells at best, CD1d tetramer staining is variable and does not clearly resolve positive and negative populations , and we lack a positive-control cell. We corroborated our working definition of T2NKT cells by showing an intermediate level of PLZF expression in the population identified as T2NKT cells [249].

Our optimized sorting protocol achieves an overall recovery of 2.5 – 6.8 x 10^4 T2NKT cells from a starting number of 2 – 7 x 10^8 peripheral blood mononuclear cells, which is an acceptable yield for such a rare cell population. Although the absolute number of T2NKT cells recovered was very low, we were able to expand them in culture by more than 15-fold without detectable phenotypic changes. Therefore, we can reliably obtain sufficient T2NKT cells for *in vitro* functional experiments.

This short report provides a technical basis for future immune monitoring studies. In particular, our methods will allow us to investigate how the balance between “effector” FoxP3$^-$ T2NKT cells and putative “regulatory” FoxP3$^+$ T2NKT cells influence outcomes after transplantation of steatotic livers.

Author Contributions

JY conceived the project, designed and performed experiments, analyzed data and wrote the manuscript. JW analyzed data and approved the manuscript. GG provided statistical review. EG approved the manuscript. JH provided critical feedback and edited the manuscript. KK edited the manuscript and is corresponding author. All authors contributed to the article and approved the submitted version.

Acknowledgements

Flow-sorting was conducted at the Central FACS Facility of the Leibniz Institute for Immunotherapy. We are grateful to Rita Brunner-Ploss, Irina Fink and Jaqueline Dirmeier for technical support.

The Supplementary Material for this article can be found online at:

https://www.frontiersin.org/articles/10.3389/fimmu.2022.898473/full#supplementary-material

- UNPUBLISHED ARTICLE -

4. Identification of a Surrogate Marker for IL-4^{+} iNKT Cells as a Diagnostic Biomarker of Liver Steatosis

4.1 Abstract

Background: Invariant Natural Killer T cells (iNKT) play critical roles in liver homeostasis and pathogenesis. We have recently described the expansion of an IL-4$^+$ iNKT cell subpopulation in steatotic subjects compared to non-steatotic subjects. We sought to use IL-4$^+$ iNKT cells as a diagnosis biomarker of steatosis but due to its rare frequency in blood and technical variability, it is yet unfeasible. Here, we aim to identify an extracellular surrogate marker of IL-4$^+$ iNKT cells as an alternative approach for the diagnosis of steatosis. **Methods**: We analyzed the expression of 376 human surface markers in expanded iNKT cells by flow cytometry. The best candidates, defined by R and AUROC scores, were combined in 9 different panels and tested in expanded iNKT cells from 6 donors. **Results and conclusions**: We identified CD202b, also known as angiopoietin-1 receptor, as a strong surrogate marker of IL-4$^+$ iNKT cells that could discriminate IL-4$^-$ from IL-4$^+$ expanded iNKT cells. For the purpose of this experiment, we had to expand iNKT cells to get enough initial number of cells. Further studies should validate the expression of CD202b in fresh IL-4$^+$ iNKT cells and the biological relevance of the receptor.

4.2 Introduction

Noninvasive biomarkers are being investigated as alternatives to biopsy in steatosis. Particularly, inflammation is a major hallmark of NAFLD pathogenesis. Interestingly, the liver is enriched in subsets of unconventional T lymphocytes that play important roles in pathogen defense and homeostasis [250]. Invariant Natural Killer T cells (iNKT) express a semi-invariant T cell receptor (TCR) α chain that recognizes lipids presented by the MHC-class I-like CD1d molecule [43]. The frequency of iNKT cells in blood is very low, ranging between 0.01-0.1 % of circulating lymphocytes [251]. In contrast, ~0.5 % of intrahepatic T lymphocytes are iNKT cells [40, 252]. Based on mice models, many studies evidence the protective [121, 150] and pathogenic [174, 175, 253] role of iNKT cells in NAFLD. Some of the discrepancies found between studies can be explained by the mouse model used. None of the current murine models resemble the complete human NAFLD spectrum. Concanavalin A intravenous injection leads to severe acute hepatitis associated with the infiltration of $CD4^+$ T cells [254]. In contrast, injection of the iNKT agonist alpha-galactosylceramide (α-GalCer) induces mild hepatitis characterized by the activation of innate immunity [175, 255]. Hua et al. reported a rapid increase in IL-4^+ iNKT cells after α-GalCer injection associated with neutrophil infiltration [175]. In this context, TNF-α^+ iNKT cells also played a critical role in inducing hepatitis [174]. Recently, we have identified changes in the frequency of iNKT cells in peripheral blood and in the liver of steatotic patients compared to healthy subjects. In a cohort of 105 patients, steatotic patients showed a negative association with the frequency of iNKT cells relative to all $CD3^+$ T cells in peripheral blood (unpublished data). Intrahepatic iNKT cells were enriched in patients with steatosis grade 2-4 (n=15) compared with steatosis grade 0-1 patients (n=28), especially the IL-4^+ iNKT cell subpopulation (unpublished data). When evaluating changes in the frequency of IL-4^+ iNKT cells in circulation, the results showed a positive trend with steatosis grade but it was not significant. We hypothesize that the technical variability of the staining and the low frequency of iNKT cells are limiting steps. We propose to identify an

extracellular surrogate marker to omit the intracellular staining as a way to improve the measurement of IL-4^{+} iNKT cell alterations in blood and correlate it with the steatosis degree.

4.3 Methods

4.3.1 iNKT cell isolation and expansion

Peripheral blood mononuclear cells (PBMC) were isolated by Ficoll gradient centrifugation as previously described [40]. PBMCs were resuspended in 400 µl MACS buffer [PBS, 0.5 % Albunorm (00200331, Octapharma, Germany), 0.4 % UltraPure 0.5M EDTA (15575-038, Invitrogen, USA)] per 10^8 cells and iNKT cells were isolated by AutoMACS Pro Separator. Briefly, cells were incubated with 60 µl Anti-iNKT MicroBeads (130-094-842, Miltenyi, Germany) per 10^8 cells for 15 mins at 4 °C. Cells were washed with 2 ml MACS buffer, centrifuged at 300 x g for 10 mins and resuspended in 500 µl MACS buffer per 10^8 cells. iNKT cells were isolated using the Possel_S program. After recovery, cells were washed with 2 ml warm iNKT medium [500 ml RPMI (72400-021, Gibco), 50 ml FCS, 5 ml Pen/Strep, 5 ml sodium pyruvate, 15 ml 7.5 % NaHCO3 and 55 µl 2-Mercaptoethanol], and cultured in a T25 Flask (353109, Corning) with 10 ml Stimulation media 1 [iNKT medium, 100 ng/ml α-GalCer (AG-CN2-0013-C250, Biomol, Germany), 50 ng/ml IL-2 (AF-200-02, Peprotech), 10 ng/ml IL-15 (AF-200-15, Peprotech), 10 ng/ml IL-1β (130-093-897, Miltenyi), 20 ng/ml IL-23 (130-095-757, Miltenyi) and 5 ng/ml TGF-β1 (130-095-067, Miltenyi)]. On day 5, cell media was replaced with Stimulation media 2 (Stimulation media 1 without α-GalCer). On day 9, we replaced media with Stimulation media 3 (Stimulation media 2 with 25 ng/ml IL-2 and 5 ng/ml IL-15). On day 12, iNKT cells were harvested and frozen down in RPMI with 10 % DMSO at -80°C liquid nitrogen.

4.3.2 iNKT cell activation and screening

iNKT cells were thawn and remained in culture overnight in iNKT media. Cells were resuspended in 1 ml iNKT media supplemented with 50 ng/ml PMA (P1585, Merck) and 1 µg/ml Ionomycin (I0634, Merck) per 5 x 10^6 cells and incubated for 4 h in a cell incubator. To stop cell activation, cells were washed with 10 ml cold sterile PBS and proceeded to be stained with IL-4 Secretion Assay (130-054-102, Miltenyi) following the manufacturer's instructions. Subsequent extracellular marker staining was performed as we previously described [40] (Supplementary Figure 1). We used the MACS Marker Screen (130-127-043, Miltenyi) to evaluate the expression of 378 human surface markers in iNKT cells and detected by CytoFlex LX cytometer (Beckman Coulter).

4.4 Results

iNKT cells from 3 donors were expanded for 12 days in vitro and stimulated with Ionomycin/PMA for 4 h. Cells were barcoded with CD45 antibodies to identify the donors and pooled together. 378 human surface markers were evaluated as potential surrogate markers of IL-4^+ iNKT cells by flow cytometry (Figure 1).

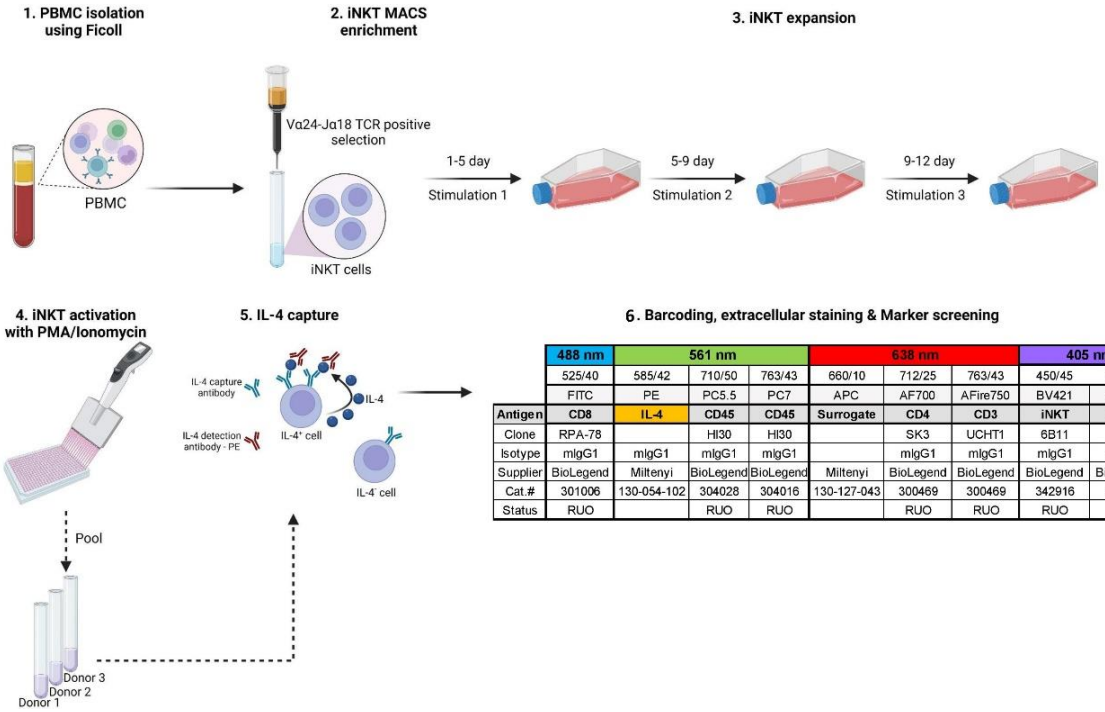

	488 nm	561 nm			638 nm			405 nm		808 nm
	525/40	585/42	710/50	763/43	660/10	712/25	763/43	450/45	525/40	885/40
	FITC	PE	PC5.5	PC7	APC	AF700	AFire750	BV421	BV510	Viability
Antigen	**CD8**	**IL-4**	**CD45**	**CD45**	**Surrogate**	**CD4**	**CD3**	**iNKT**	**CD45**	**ViaKr808**
Clone	RPA-T8		HI30	HI30		SK3	UCHT1	6B11	HI30	
Isotype	mIgG1	mIgG1	mIgG1	mIgG1		mIgG1	mIgG1	mIgG1	mIgG1	
Supplier	BioLegend	Miltenyi	BioLegend	BioLegend	Miltenyi	BioLegend	BioLegend	BioLegend	BioLegend	BC
Cat.#	301006	130-054-102	304028	304016	130-127-043	300469	300469	342916	304036	C36628
Status	RUO		RUO	RUO		RUO	RUO	RUO	RUO	RUO

Figure 1. Illustration depicting the experimental steps for the identification of IL-4$^+$ iNKT cell surrogate markers. Steps 1-3 include iNKT cell isolation and expansion. Activation of iNKT cells in step 4 is necessary to detect IL-4$^+$ cells in step 5. The flow cytometry panel used for the identification of IL-4$^+$ iNKT cell surrogate markers is shown in step 6.

We determined the performance of each marker in classifying IL-4$^+$ iNKT cells based on the area under the ROC curve (AUROC) and the relation between the marker expression and IL-4$^+$ according to the R-value. The median of the 3 donors was plotted in an AUROC-R graph (Figure 2A). Markers were ranked based on the AUROC-R vector distance and the top-12 candidates with the highest distance were considered for further evaluation (Figure 2B).

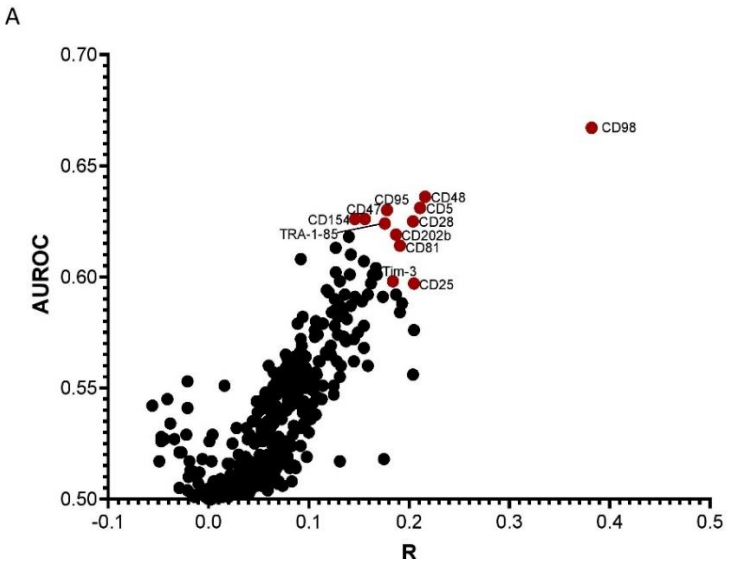

Marker	R	AUROC
CD5	0.211	0.631
CD25	0.205	0.597
CD28	0.204	0.625
CD47	0.156	0.626
CD48	0.216	0.636
CD81	0.191	0.614
CD95	0.178	0.63
CD98	0.382	0.667
CD154	0.146	0.626
CD202b	0.187	0.619
Tim-3	0.184	0.598
TRA-1-85	0.176	0.624

Figure 2. (A) Representation of the 378 markers' performance as IL-4$^+$ iNKT cell surrogates based on the R and the AUROC values. The top 12 surrogate markers with the highest vector distance are labeled in red. (B) List of the top 12 surrogate markers with their corresponding R and AUROC values arranged in alphabetical order.

Nine FACS panels were designed to identify the optimal marker combination (Supplementary Figure 2). We tested the nine-combinatory panels in expanded iNKT cells from 6 different donors. Surprisingly, CD202b alone returned as a strong surrogate marker of IL-4$^+$ iNKT cells (Figure 3). The results of the linear regression analysis showed that CD202b correlates positively with IL-4$^+$ iNKT cells.

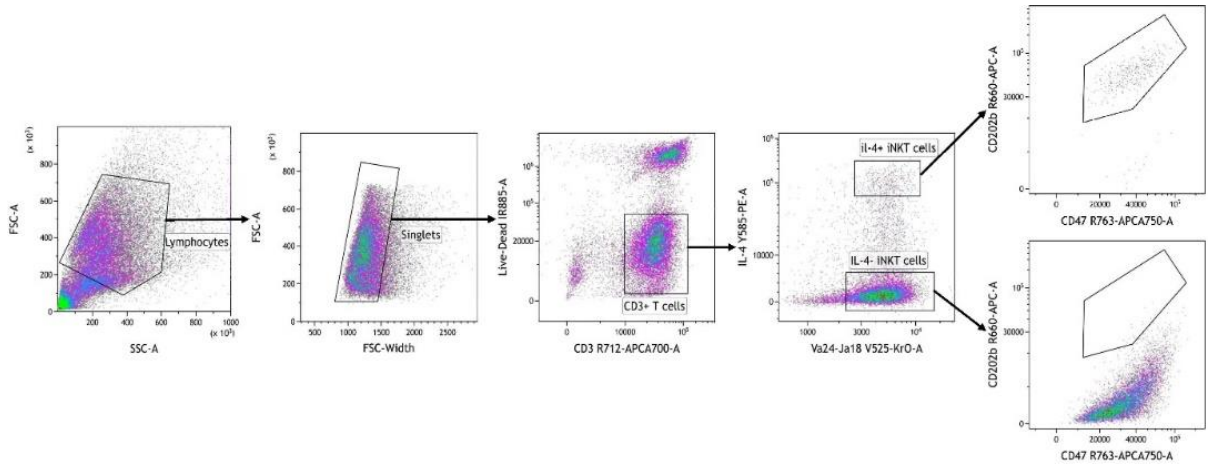

Figure 3. FACS gating of CD202b as a surrogate marker of IL-4$^+$ iNKT cells. Cells were gated as CD3$^+$ TCRVα24$^+$ iNKT cells and only the IL-4$^+$ subpopulation expresses CD202b.

4.5 Discussion

We have recently observed an increased frequency of intrahepatic IL-4$^+$ iNKT cells in steatotic patients. However, we could not find statistically significant alterations in peripheral blood mainly limited by the low frequency and the technical variability. We aimed to use an extracellular surrogate marker of IL-4$^+$ iNKT to reduce the technical variability by simplifying the staining procedure. Here we have identified CD202b, also known as angiopoietin-1 receptor, as a surrogate marker of IL-4$^+$ iNKT cells from a screening of 378 human surface markers. CD202b is a member of the receptor tyrosine kinase family of proteins and is expressed by endothelial cells and their progenitors, quiescent hematopoietic stem cells and in a subpopulation of monocytes [256, 257]. The latter are associated with tumor progression and metastasis [258]. The role of CD202b in IL-4$^+$ iNKT cells has not yet been studied. Interestingly, a prospective study involving 104 patients with obesity observed that serum angiopoietin-2 (Ang2), a ligand of CD202b, increased significantly with increasing histological grades of steatosis but not with fibrosis [257]. In different models of NAFLD mouse models, treatment with the Ang2 inhibitor L1-10 reduced liver ballooning and fibrosis, ameliorated leukocyte adhesion and inflammatory markers, and attenuated hepatocellular carcinoma progression [257]. Based on these findings, intrahepatic IL-4$^+$ iNKT cell expansion is likely to represent a pathogenic subpopulation. Th2 cytokines have been linked with hepatic fibrosis [45, 46]. IL-4 and IL-13 stimulate the synthesis of collagen in fibroblasts [47–49] and recruit inflammatory monocytes [50]. We will further investigate the role of CD202b in IL-4$^+$ iNKT cells and evaluate the diagnosis potential of CD202b$^+$ iNKT cells in steatosis.

4.6 Supplementary Material

	488 nm	561 nm			638 nm			405 nm		808 nm
	525/40	585/42	710/50	763/43	660/10	712/25	763/43	450/45	525/40	885/40
	FITC	PE	PC5.5	PC7	APC	AF700	AFire750	BV421	BV510	Viability
Antigen	**CD8**	**IL-4**	**CD45**	**CD45**	**Surrogate**	**CD4**	**CD3**	**iNKT**	**CD45**	**ViaKr808**
Clone	RPA-78		Hl30	Hl30		SK3	UCHT1	6B11	Hl30	
Isotype	mIgG1	mIgG1	mIgG1	mIgG1		mIgG1	mIgG1	mIgG1	mIgG1	
Supplier	BioLegend	Miltenyi	BioLegend	BioLegend	Miltenyi	BioLegend	BioLegend	BioLegend	BioLegend	BC
Cat.#	301006	130-054-102	304028	304016	130-127-043	300469	300469	342916	304036	C36628
Status	RUO		RUO	RUO		RUO	RUO	RUO	RUO	RUO

Supplementary Figure 1. Flow cytometry panel for the identification of potential IL-4^{+} iNKT cell surrogate markers.

		488 nm			561 nm			638 nm			405 nm		808 nm
		525/40	610/20	690/50	585/42	710/50	763/43	660/10	712/25	763/43	450/45	525/40	885/40
		VioBright B515	PE-Vio 615	PerCP-Vio700	PE	PE-Cy5.5	PE-Vio 770	APC	R720	APC-Vio 770	VBr V423	BV510	Viability
Panel_1	Antigen	CD98	CD8	CD4	IL-4	CD25	CD48	CD95	CD3	CD5	CD28	Vα24-Jα18	ViaKr808
	Clone	REA387	REA734	REA623		B1.49.9	REA426	REA738	REA613	REA782	REA612	6B11	
	Isotype	REA	REA	REA	mIgG1	mIgG2a	REA	REA	REA	REA	REA	mIgG1	
	Supplier	Miltenyi	Miltenyi	Miltenyi	Miltenyi	BC	Miltenyi	Miltenyi	Miltenyi	Miltenyi	Miltenyi	BioLegend	BC
	Cat.#	130-126-996	130-110-685	130-113-790	130-054-102	B92458	130-106-518	130-113-070	130-127-397	130-111-110	130-127-223	342918	C36628
	Status	RUO	RUO	RUO		IVD	RUO	RUO	RUO	RUO	RUO	RUO	RUO
Panel_2	Antigen	CD98	CD8	CD4	IL-4	CD25	CD154	Tim-3	CD3	CD47	CD28	Vα24-Jα18	ViaKr808
	Clone	REA387	REA734	REA623		B1.49.9	REA238	REA602	REA613	REA220	REA612	6B11	
	Isotype	REA	REA	REA	mIgG1	mIgG2a	REA	REA	REA	REA220	REA	mIgG1	
	Supplier	Miltenyi	Miltenyi	Miltenyi	Miltenyi	BC	Miltenyi	Miltenyi	Miltenyi	Miltenyi	Miltenyi	BioLegend	BC
	Cat.#	130-126-996	130-110-685	130-113-790	130-054-102	B92458	130-114-140	130-119-819	130-127-397	130-123-637	130-127-223	342918	C36628
	Status	RUO	RUO	RUO		IVD	RUO	RUO	RUO	RUO	RUO	RUO	RUO
Panel_3	Antigen	CD98	CD8	CD4	IL-4	CD25	TRA-1-85	CD202b	CD3	CD81	CD28	Vα24-Jα18	ViaKr808
	Clone	REA387	REA734	REA623		B1.49.9	REA476	REA198	REA613	REA513	REA612	6B11	
	Isotype	REA	REA	REA	mIgG1	mIgG2a	REA	REA	REA	REA	REA	mIgG1	
	Supplier	Miltenyi	Miltenyi	Miltenyi	Miltenyi	BC	Miltenyi	Miltenyi	Miltenyi	Miltenyi	Miltenyi	BioLegend	BC
	Cat.#	130-126-996	130-110-685	130-113-790	130-054-102	B92458	130-107-159	130-101-632	130-127-397	130-107-923	130-127-223	342918	C36628
	Status	RUO	RUO	RUO		IVD	RUO	RUO	RUO	RUO	RUO	RUO	RUO
Panel_4	Antigen	CD98	CD8	CD4	IL-4	CD25	CD48	Tim-3	CD3	CD81	CD28	Vα24-Jα18	ViaKr808
	Clone	REA387	REA734	REA623		B1.49.9	REA426	REA602	REA613	REA513	REA612	6B11	
	Isotype	REA	REA	REA	mIgG1	mIgG2a	REA	REA	REA	REA	REA	mIgG1	
	Supplier	Miltenyi	Miltenyi	Miltenyi	Miltenyi	BC	Miltenyi	Miltenyi	Miltenyi	Miltenyi	Miltenyi	BioLegend	BC
	Cat.#	130-126-996	130-110-685	130-113-790	130-054-102	B92458	130-106-518	130-119-819	130-127-397	130-107-923	130-127-223	342918	C36628
	Status	RUO	RUO	RUO		IVD	RUO	RUO	RUO	RUO	RUO	RUO	RUO
Panel_5	Antigen	CD98	CD8	CD4	IL-4	CD25	CD154	CD202b	CD3	CD5	CD28	Vα24-Jα18	ViaKr808
	Clone	REA387	REA734	REA623		B1.49.9	REA238	REA198	REA613	REA782	REA612	6B11	
	Isotype	REA	REA	REA	mIgG1	mIgG2a	REA	REA	REA	REA	REA	mIgG1	
	Supplier	Miltenyi	Miltenyi	Miltenyi	Miltenyi	BC	Miltenyi	Miltenyi	Miltenyi	Miltenyi	Miltenyi	BioLegend	BC
	Cat.#	130-126-996	130-110-685	130-113-790	130-054-102	B92458	130-114-140	130-101-632	130-127-397	130-111-110	130-127-223	342918	C36628
	Status	RUO	RUO	RUO		IVD	RUO	RUO	RUO	RUO	RUO	RUO	RUO
Panel_6	Antigen	CD98	CD8	CD4	IL-4	CD25	TRA-1-85	CD95	CD3	CD47	CD28	Vα24-Jα18	ViaKr808
	Clone	REA387	REA734	REA623		B1.49.9	REA476	REA738	REA613	REA220	REA612	6B11	
	Isotype	REA	REA	REA	mIgG1	mIgG2a	REA	REA738	REA	REA220	REA	mIgG1	
	Supplier	Miltenyi	Miltenyi	Miltenyi	Miltenyi	BC	Miltenyi	Miltenyi	Miltenyi	Miltenyi	Miltenyi	BioLegend	BC
	Cat.#	130-126-996	130-110-685	130-113-790	130-054-102	B92458	130-107-159	130-113-070	130-127-397	130-123-637	130-127-223	342918	C36628
	Status	RUO	RUO	RUO		IVD	RUO	RUO	RUO	RUO	RUO	RUO	RUO
Panel_7	Antigen	CD98	CD8	CD4	IL-4	CD25	CD48	CD202b	CD3	CD47	CD28	Vα24-Jα18	ViaKr808
	Clone	REA387	REA734	REA623		B1.49.9	REA426	REA198	REA613	REA220	REA612	6B11	
	Isotype	REA	REA	REA	mIgG1	mIgG2a	REA	REA	REA	REA220	REA	mIgG1	
	Supplier	Miltenyi	Miltenyi	Miltenyi	Miltenyi	BC	Miltenyi	Miltenyi	Miltenyi	Miltenyi	Miltenyi	BioLegend	BC
	Cat.#	130-126-996	130-110-685	130-113-790	130-054-102	B92458	130-106-518	130-101-632	130-127-397	130-123-637	130-127-223	342918	C36628
	Status	RUO	RUO	RUO		IVD	RUO	RUO	RUO	RUO	RUO	RUO	RUO
Panel_8	Antigen	CD98	CD8	CD4	IL-4	CD25	CD154	CD95	CD3	CD81	CD28	Vα24-Jα18	ViaKr808
	Clone	REA387	REA734	REA623		B1.49.9	REA238	REA738	REA613	REA513	REA612	6B11	
	Isotype	REA	REA	REA	mIgG1	mIgG2a	REA	REA738	REA	REA	REA	mIgG1	
	Supplier	Miltenyi	Miltenyi	Miltenyi	Miltenyi	BC	Miltenyi	Miltenyi	Miltenyi	Miltenyi	Miltenyi	BioLegend	BC
	Cat.#	130-126-996	130-110-685	130-113-790	130-054-102	B92458	130-114-140	130-113-070	130-127-397	130-107-923	130-127-223	342918	C36628
	Status	RUO	RUO	RUO		IVD	RUO	RUO	RUO	RUO	RUO	RUO	RUO
Panel_9	Antigen	CD98	CD8	CD4	IL-4	CD25	TRA-1-85	Tim-3	CD3	CD5	CD28	Vα24-Jα18	ViaKr808
	Clone	REA387	REA734	REA623		B1.49.9	REA476	REA602	REA613	REA782	REA612	6B11	
	Isotype	REA	REA	REA	mIgG1	mIgG2a	REA	REA	REA	REA	REA	mIgG1	
	Supplier	Miltenyi	Miltenyi	Miltenyi	Miltenyi	BC	Miltenyi	Miltenyi	Miltenyi	Miltenyi	Miltenyi	BioLegend	BC
	Cat.#	130-126-996	130-110-685	130-113-790	130-054-102	B92458	130-107-159	130-119-819	130-127-397	130-111-110	130-127-223	342918	C36628
	Status	RUO	RUO	RUO		IVD	RUO	RUO	RUO	RUO	RUO	RUO	RUO

Supplementary Figure 2. Combinatory flow cytometry panels designed to identify the best combination of markers as surrogates of IL-4^{+} iNKT cells.

- UNPUBLISHED ARTICLE -

5. Diagnosis Value of sCD46 in Early Liver Inflammation

5.1 Abstract

Background: Biomarkers of early liver inflammation could serve as a diagnosis approach for liver pathogenesis. Matrix metalloproteinases (MMPs) are activated by hepatocyte stress, leading to extracellular matrix remodeling and membrane receptor shedding. CD46 is a membrane-bound complement regulatory that can be post-translationally regulated via proteolytic cleavage, resulting in soluble (s)CD46. Here we investigate human sCD46 in serum as a potential biomarker of early liver injury and study the regulation of CD46 shedding. **Methods**: We developed and validated a sandwich enzyme linked immunosorbent assay (ELISA) that measures human sCD46. Fat-loaded HepaRG cells were used as an in vitro model of steatosis. MMPs and components of the prostaglandin synthesis pathway were measured using quantitative polymerase chain reaction (qPCR) and ELISA. **Results**: The in-house sCD46 ELISA passed accuracy and precision tests. A significant increase of sCD46 concentration in serum was observed in steatosis compared to healthy donors. Similarly, fat-loaded HepaRG cells also increased the shedding of CD46 compared to unloaded cells. The upregulation of PTGES2 upon fat-loading of HepaRG cells induced an increase of MMP-1 at the transcriptional and protein level. Knockdown of PTGES2 downregulated MMP-1 and reduced sCD46 concentrations in supernatant. In addition to fat stimuli, HepaRG cells exposed to different FDA-approved drugs responded with different degrees of CD46 shedding. We observed that the frequency of drugs with hepatotoxic risk or direct cytotoxicity increased with higher sCD46 concentrations. **Conclusions**: sCD46 is proposed as a biomarker to diagnose steatosis in humans. We identified an upregulation of the PGE_2-MMP1-sCD46 axis as a response to fat stimuli. sCD46 is not only induced upon fat but also under hepatotoxic and cytotoxic drugs. This brings the opportunity to use sCD46 ELISA assay as a non-invasive diagnostic method for steatosis and potentially a complementary data readout to identify hepatotoxic drugs.

5.2 Introduction

The human membrane cofactor protein CD46, also known as MCP, is a ubiquitously expressed receptor in humans [259]. CD46 protects host cells from complement damage [260] and modulates immune responses via costimulatory signals [261]. Sánchez et al. demonstrated that colligation of CD3 and CD46 potentiated the effector responses of $CD4^+$ T regulatory cell 1 (Tr1) in secreting IL-2, IFN-γ and IL-10 [262]. Similarly, co-stimulation with CD46 resulted in $CD8^+$ T cells expansion and IFN-γ secretion [263]. Interestingly, CD46 was also identified as a cellular receptor for opportunistic viruses such as group B adenoviruses [264], measle virus [265] and human herpesvirus 6 [266].

Dysregulation of CD46 is associated with a list of immune-related diseases such as multiple sclerosis [267], asthma [268], rheumatoid arthritis [269] or bullous pemphigoid [270]. The expression of CD46 is regulated at different stages including post-translational proteolytic cleavage. Soluble CD46 particles (sCD46) are active molecules and protect tumors from the complement system [271]. In autoimmune diseases, serum sCD46 levels were reported to be upregulated in systemic lupus erythematosus patients [272] and in bullous pemphigoid [270]. Recently, we have identified an increased level of sCD46 in serum of steatotic patients compared to healthy controls. The shedding of the receptor from the cell surface of HepaRG cells induced the expansion of $IL\text{-}4^+$ iNKT cells in vitro. Here, we developed and validated a sCD46 ELISA assay. Our results show that the in-house sCD46 ELISA assay is a reliable kit to measure sCD46 in sera, plasma and culture supernatants for routine analysis. We further investigated the regulation of CD46 shedding upon encounter with different FDA-approved drugs. The shedding of CD46 was triggered by anti-neoplastic agents and other hepatotoxic-associated drugs, but could also be downregulated for instance with the α2 adrenergic receptor agonist UK-14304. Interestingly, non-steroidal anti-inflammatory drugs (NSAIDs) were also associated with increased sCD46. RNA-seq data and qPCR analysis confirmed that fat-loaded (FL)-HepaRG cells

compared to unloaded (UL)-HepaRG cells display alterations in different enzymes from the prostaglandin pathway, with a significant upregulation of Prostaglandin E Synthase 2 (PTGES2). Particularly, we identified a dose-dependent effect of prostaglandin E2 (PGE_2) in CD46 shedding involving upregulation of matrix metalloproteinase-1 (MMP-1). This could not be prevented by using selective antagonists of EP receptors.

5.3 Methods

5.3.1 Study approval and patient cohort

This study involving human research participants was performed in accordance with the Declaration of Helsinki, as well as and all applicable German and European laws as well as all ethical standards. Samples were obtained from 158 oncological patients undergoing liver surgery at the Department of Surgery, University Hospital Regensburg. Routine biochemical and haematological investigations were performed by an in-house accredited diagnostic laboratory (Institute of Clinical Chemistry and Laboratory Medicine, UKR). No study patients received systemic chemotherapy before surgery. This study was authorised by the Ethics Committee of the University of Regensburg (approval number 13-257-101). All participants gave full, informed written consent.

5.3.2 HepaRG cell culture

The HepaRG cell line was obtained from Biopredic International, France. HepaRG cells were cultured in 96-well plates at 10^4 cells/well in HepaRG growth medium (William's E medium supplemented with 10 % HyClone FetalClone II serum, 1 % penicillin/streptomycin, 1 % L-glutamine, 0.023 IE/ml insulin, 4.7 µg/ml hydrocortisone and 80 µg/ml gentamycin) for 2 weeks. Hepatic differentiation was induced with HepaRG growth medium supplemented with 1.8 % DMSO for an additional 2 weeks. The FL process was carried out in differentiated HepaRG cells

first undergoing 24 h in 1 % bovine serum albumin (BSA) HepaRG growth medium (diet medium) and then treated with a mixture of 0.5 mM palmitic acid and oleic acid 1:2 ratio (PA/OA) for further 24 h. Unloaded (UL)-HepaRG control cells were generated using only the carrier isopropanol.

5.3.3 Drug testing

We used the Tocriscreen Library of FDA-Approved Compounds (5932, Biotechne, USA) to screen for drugs that can modulate sCD46 shedding in HepaRG cells. Differentiated HepaRG cells were starved for 24 h. We replaced the medium with diet medium supplemented with 0.5 mM OA/PA, 1.25 % DMSO and 10 µM drug, and incubated overnight (O/N). For drug titration, we followed the above-mentioned protocol but the medium was supplemented with 0.5 mM OA/PA and 2 % DMSO to allow a broader range of drug concentrations.

5.3.4 siRNA knockdown

Knockdown (KD) was performed with Lipofectamine 2000 Transfection Reagent (11668019, Invitrogen) and ON-TARGETplus SMARTpool siRNA PTGES2 (80142, Dharmacon). The ON-TARGETplus Non-targeting Pool (D-001810-10, Dharmacon) was used as negative control. Briefly, 0.3 µl/well Lipofectamine 2000 was mixed with 10 µl/well Opti-MEM (31985062, Gibco). Then, 0.125 µl/well siRNA (20 µM) was mixed in 10 µl/well Opti-MEM. We prepared the transfection media by transferring dropwise the diluted siRNA into Lipofectamine 2000 in a 1:1 ratio and incubate it for 10 mins at room temperature (RT). HepaRG cell media was replaced with 80 µl/well of antibiotic- and serum-free HepaRG media. 20 µl/well of transfection media was added dropwise, shaked gently and returned into the cell incubator for 48 h.

5.3.5 Quantitative reverse transcription-PCR

SuperScript-III (18080093, Invitrogen) was used for reverse transcription. Quantitative reverse transcription-PCR was performed with a LightCycler™ real-time PCR system using the QuantiNova Probe RT-PCR Kit (208352, Qiagen) and Quantitect primers (Qiagen) listed in Supplementary Table 1. Gene expression was normalised against expression of ACTB.

5.3.6 RNA-Sequencing

RNA isolation from UL and FL-HepaRG cells was done using the RNeasy Mini Kit (74106, Qiagen) and a DNA cleanup was performed using the RNase-Free DNase Set (79254, Qiagen). Equimolar amounts of each library were single-end sequenced (75bp) on a NextSeq 550 instrument (Illumina, bcl2fastq software v2.20.0.422) using the NextSeq Control Software (NCS v2.2.0) and Real Time Analysis Software (RTA, v2.4.11). Quality control and read mapping to the human reference genome (GRCh38, Gencode release 29) was performed using an adapted version of the SnakePipes18 analysis pipeline (v1.2.2 including rDNA removal by Bowtie2 (v2.3.5) [273] mediated mapping). Transcript counts from Salmon (v0.13.1) [274] were imported by tximport [274] and summarized to gene-level ("original counts and offset") and prefiltered with edgeR:filterByExpr [275]. Quality control of the count matrix and DE-Gene calling was performed with DESeq2 (fdr=0.1) [276].

5.3.7 sCD46 ELISA

The sandwich ELISA consists of a monoclonal mouse IgG2B CD46 antibody (344519, R&D Systems, USA) immobilized on a 96-well Clear Polystyrene Microplate (DY990, R&D Systems, USA). The detection antibody is an affinity-purified polyclonal goat IgGa antibody conjugated to Biotin (BAF2005, R&D Systems, USA). The assay includes 8 standards prepared with Recombinant Human CD46 His-tag Protein (rhCD46, 10256-CD, R&D Systems) (0 (STD1), 0.03

(STD2), 0.06 (STD3), 0.12 (STD4). 0.24 (STD5), 0.48 (STD6), 0.95 (STD7), 1.91 (STD8) ng/ml) diluted in Reagent Diluent Concentrate 2 (841380, R&D Systems, USA) or the appropriate cell media. Before establishing the ELISA assay, we determined the optimal capture and detection antibody pair concentrations and tested it in 2 different blocking buffers, namely, Reagent diluent 1 (DY997, R&D Systems, USA) and Reagent diluent 2 (Supplementary Table 2A).

Plates were coated with 100 µl/well monoclonal CD46 antibody (4 µg/ml) in phosphate-buffered saline (PBS) and incubated with an adhesive strip O/N and RT. Plates were washed 3 times by decanting and filling wells with washing buffer (WA126, R&D Systems, USA) using a squirt bottle. Wells were blocked with 300 µl/well Reagent Diluent Concentrate 2 for 1 h at RT. Plates were washed and incubated with 100 µl/well STD, serum, plasma or supernatant samples for 2 h at RT. After repeating washing steps, 100 µl/well detection antibody (50 ng/ml) in PBS were incubated for 2 h at RT. Plates were washed and incubated with 100 µl/well streptavidin-HRP (DY998, R&D Systems) for 20 mins at RT. Following washing steps, plates were incubated with 100 µl/well substrate reagent (DY999B, R&D Systems) for 30 mins at RT, then with 50 µl/well stop solution (DY994, R&D Systems). Plates were read with a Thermo Scientific Varioskan Flash ELISA reader at 450 nm. Titers of samples and controls were calculated based on the standard curve.

This ELISA assay was validated for range, sensitivity, linearity, accuracy, precision (repeatability, intermediate precision and reproducibility) and robustness. For range, we determined the upper and lower limit of quantification (ULOQ and LLOQ, respectively). We measured the OD_{450nm} of rhCD46 in a 2-fold serial dilution from 122.07 ng/ml to 0.007 ng/ml in triplicate. The highest and lowest standard curve points were the first and last concentrations that had a coefficient of variation (CV) <30 % (SD/average concentration x 100) and an 80 – 120 % backfit (measured/nominal titer x 100). Sensitivity was calculated as the mean of 12 blank readouts added to 3 times the standard deviation (SD) [277]. Linearity was determined by taking a known

concentration of stock serum sample and diluting it in a 2-fold serial dilution (1:80 to 1:640) in quadruplicates. The measured titers (pg/ml) were transformed into log values to obtain a normal distribution of data and plotted against the log nominal values. The steepness of the resulting linear regression indicates the linearity, being 1 the highest score. Accuracy was tested through spike recovery. 5 serum samples were spiked with different concentrations of rhCD46. The same samples were measured without spikes. Based on the unspiked titers plus the spike, we worked out the nominal titer. The obtained backfit (measured:nominal titer ratio) was used as a measure of accuracy. Repeatability was ascertained by measuring a serum sample five times and reporting the CV. For intermediate precision, we diluted the same serum sample 1:320 & 1:640 in Reagent concentrate 2. Samples were aliquoted in 4 cryotubes and stored at -80 °C. Each day, we measured for 5 times the titers of both dilutions and calculated the CV. Intermediate precision was reported as the CV of the 4 independent ELISAs. Reproducibility was tested by a second operator conducting the same experiment and comparing the obtained titers to the first operators. Robustness was assessed with different incubation times for detection antibody, blocking, analyte and capture antibody. Each condition was performed in duplicates and compared to the standard protocol. Any condition that performed CV >10 % was considered to significantly bias the readout.

5.3.8 Competitive FACS-based sCD46 assay

Anti-CD46 antibody (130-104-509, Miltenyi) binds to CD46 receptor in MOLT-4 cells. When restraining the antibody concentration and cell number to 0.25 µl and 3 x 10^5 cells/100 µl total staining volume, respectively, a reduction in the median fluorescent intensity (MFI) can be appreciated by adding a specific concentration of rhCD46. A titration curve can be performed by using different concentrations of rhCD46.

5.4 Results

5.4.1 Development of an ELISA for quantification of sCD46 levels

Following a cross titration experiment, we determined the optimal capture and detection antibodies in two different blocking buffers based on the signal/noise ratio (Supplementary Table 2 A & B). The established conditions (4 µg/ml CD46 capture antibody, 50 ng/ml detection antibody and Reagent diluent 2) were used for the subsequent validation experiments.

5.4.2 Calibration curve and limit of detection

To determine the range of the assay, we diluted rhCD46 in a 2-fold serial dilution in triplicates. The resulting calibration curve defined the linearity range of the assay between 30 – 954 ng/ml (Figure 1A). Retrieving the values from the calibration curve, we identified the ULOQ and LLOQ as the last values that had a CV <30 % and an 80 – 120 % backfit. The ULOQ and LLOQ of the assay were 954.37 pg/ml and 59.60 pg/ml, respectively (Table 1A). We reported a limit of detection (LOD) of 8.95 pg/ml (Table 1A).

5.4.3 Spike recovery

The complexity of the serum matrix can interfere with the accuracy of the assay. Spike recovery tests the specificity of the assay by introducing an exact spike (rhCD46) concentration into the matrix and then diluting it with the same matrix complex. We measured the concentration of sCD46 in unspiked and spiked samples and then determined the bias, which is the difference between the nominal and the measured values in percentage. The acceptance criteria were set at biases <25 %. From 5 serum samples tested with different spike concentrations, we obtained a mean bias of 5.5 % (Figure 1B), thus the matrix did not affect drastically the accuracy of the measurements.

5.4.4 Repeatability, intermediate precision and reproducibility

Precision was tested at 3 different levels (repeatability, intermediate precision and reproducibility). Repeatability is the variation across successive measurements of a specific analyte under the same conditions. The acceptance criteria were set at CV <10 %. We determined the concentration of sCD46 in a human serum sample in 2 different dilutions (1:320 and 1:640) 5 times. The resulting concentrations were 52.03 ± 0.57 ng/ml with a CV of 1.097 % for 1:320 dilution and 53.38 ± 1.83 ng/ml with a CV of 3.42 % for 1:640 dilution (Figure 1C). The intermediate precision accounts for the variability across independent experiments measuring a specific analyte under the same conditions. We repeated the above experiment a total of 4 times on consecutive days and obtained a titer of 49.57 ± 2.57 ng/ml with a CV of 5.18 % for 1:320 dilution and 48.95 ± 6.69 ng/ml with a CV of 13.67 % for 1:640 dilution (Figure 1C). The exact experiment with another sCD46 human serum sample was performed by two different operators and demonstrated with a CV of 4.53 % in 1:320 dilution and 13.68 % in 1:640 dilution that the assay could be reproduced (Figure 1C).

5.4.5 Linearity

Linearity tests the accuracy of measurements across a specific concentration range. To test linearity, we took a human serum sample and performed 4 serial dilutions in reagent diluent 2 (1:80, 1:160, 1:320 and 1:640) in quadruplicates. The test showed that serial dilutions across this range accurately matched its nominal values (Figure 1D) with an $R^2 = 0.99$ and a slope of 1.021, indicating strong linearity. To determine whether the matrix complex of reagent diluent 2 biased the assay across the dilution range, we plotted residues in a Bias-Nominal graph (Figure 1E). There was no strong linearity based on $R^2 = 0.05$, hence indicating that the accuracy of the measurements was not directly biased by the components of the diluent.

5.4.6 Robustness

The assay was challenged by altering different incubation times in the protocol and determining the variations associated with these changes, namely, the time of incubation of the capture antibody, blocking, analyte and detection antibody. We prepared a stock of 0.475 ng/ml rhCD46 and measured it in quadruplicates for each variable. A one-way ANOVA was performed to determine statistically significant changes from the standard method. The assay showed that within an interval of 1 h blocking time, there were not differences in the measurement, while the effect of different incubation times in the coating antibody, analyte or capture antibody resulted in significant changes (Figure 1F). Thus, strict compliance with the standard protocol is advised.

5.4.7 Performance compared to sCD46 commercial kits and the FACS-based competitive assay

We tested 4 commercial ready-to-use human CD46 ELISA kit from MyBioSource (MBS3802163), United States Biological (357260), Biorbyt (orb562879) and Aviva Systems Biology (OKEH00920). We tested the kits for sensitivity and repeatability. Following the manufacturer´s instructions, all the commercial kits failed to detect sCD46 in serum or showed unacceptable CV (Figure 1G). We took the CD46 standards from the kits and attempted to perform a standard curve using the in-house sCD46 ELISA. None of the standards was detectable in our assay (Supplementary Table 3). We previously reported a clinical correlation between steatotic patients and sera sCD46 levels using a competitive cell-based FACS assay. To compare it with the ELISA assay, we titrated the rhCD46 between 0-125 ng/ml in triplicates. Our results showed that the ELISA is more sensitive than the FACS-based assay under measurements of 15 ng/ml (Figure 1H).

5.4.8 sCD46 ELISA can discriminate non-steatotic patients from steatotic patients

When examining the correlation between steatosis and serum sCD46 in a cohort of healthy individuals with different clinically diagnosed hepatic steatosis degrees, we found that the in-house ELISA could discriminate steatotic from non-steatotic patients (Figure 1I). Although we could not statistically differentiate moderate from severe steatotic patients, patients with more severe steatosis grade had a tendency for higher sCD46 concentration (Figure 1I).

A

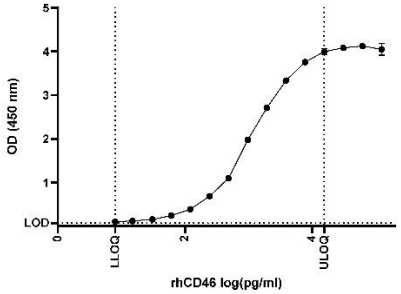

F

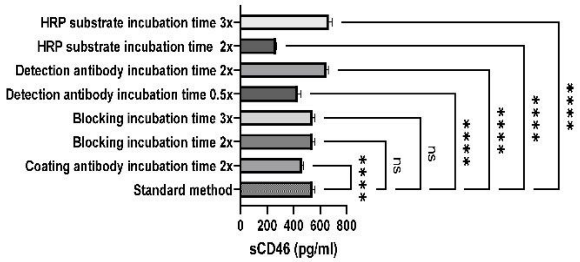

B

Sample	Average % Recovery	Range %
Serum (n=5)	105.5	101 – 112

G

	Aviva Systems Biology		Biorbyt		MyBioSource		United States Biological	
Dilution	1:320	1:640	1:320	1:640	1:19	1:38	1:320	1:640
N	4	4	4	4	4	4	4	4
Mean (ng/ml)	2.33	7.63	5.04	2.14	-10.99	-6.29	4.56	0.47
SD	1.53	2.09	0.93	1.26	12.00	33.14	2.12	0.68
CV %	65.42	27.36	18.49	59.18	NA	NA	46.42	144.49

C

	Intra-assay precision		Inter-assay precision		Reproducibility	
Dilution	1:320	1:640	1:320	1:640	1:320	1:640
N	5	5	20	20	10	10
Mean (ng/ml)	52.03	53.38	49.57	48.95	35.71	26.94
SD	0.57	1.83	2.57	6.69	1.62	3.69
CV %	1.10	3.42	5.18	13.67	4.53	13.68

H

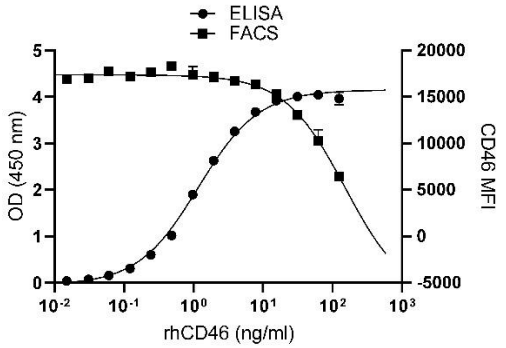

D

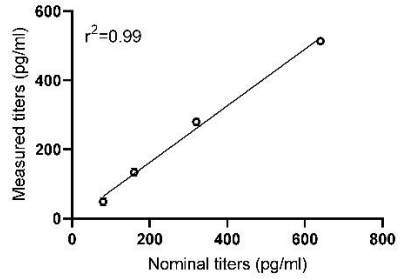

E

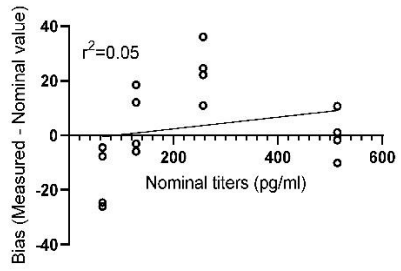

I

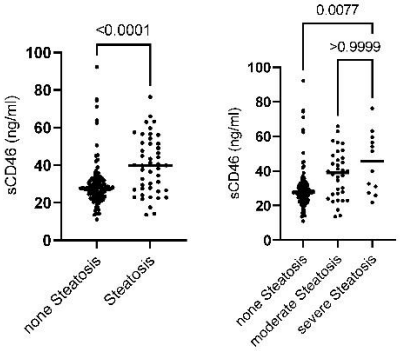

Figure 1. Validation of the in-house sCD46 ELISA. (A) Titration curve using recombinant human CD46 (rhCD46) as the analyte. Lower limit of quantification (LLOQ) and upper limit of quantification (ULOQ) are indicated in the X-Axis and the limit of detection (LOD) is indicated in the Y-Axis. (B) Accuracy (spike recovery) of human serum samples. (C) Intra-assay precision, inter-assay precision and reproducibility of human serum sample at two different dilution factors. (D) Analysis of linearity. (E) Linear regression of the bias plotted against nominal titers (F) Robustness based on incubation timing. (G) Performance of commercial CD46 ELISA kits in detecting serum sCD46. (H) rhCD46 titration in ELISA and competitive FACS-based assay. (I) Concentration of serum sCD46 measured by ELISA in healthy and steatotic patients.

5.4.9 The prostaglandin pathway mediates regulation of CD46 shedding

We previously showed that the process of fat-loading HepaRG cells induces cleavage of CD46 receptor. These results were confirmed with the in-house sCD46 ELISA in seven independent replicates (Figure 2A). To investigate the intrinsic mechanisms responsible for the cleavage of CD46, we performed an RNA sequencing in FL- and UL-HepaRG cells. We identified that several genes involved in the prostaglandin pathway were dysregulated in FL-HepaRG cells compared to UL-HepaRG cells (Figure 2B). We confirmed via qPCR an upregulation of Prostaglandin E Synthase 2 (PTGES2) in FL-HepaRG cells (Figure 2C). We tested the response of FL-HepaRG cells to different concentrations of PGE_2 and observed a sCD46 dose-dependent increase (Figure 2D). qPCR data showed that the expression of MMP-1 was upregulated in FL-HepaRG cells treated with 1 mM PGE_2 compared to control vehicle cells (Figure 2E). ELISA confirmed that MMP-1 concentration in supernatant was increased in FL-HepaRG cells exposed to 1mM PGE_2 (Figure 2F). Similarly, the shedding of CD46 could be prevented in a dose-dependent manner with the MMP inhibitor TAPI-1 (Figure 2G). However, blocking the prostanoid pathway with nonsteroidal anti-inflammatory drugs (NSAIDs), namely Aspiring, Celocoxib and Ibuprofen, showed an increased shedding of CD46 (Figure 2E).

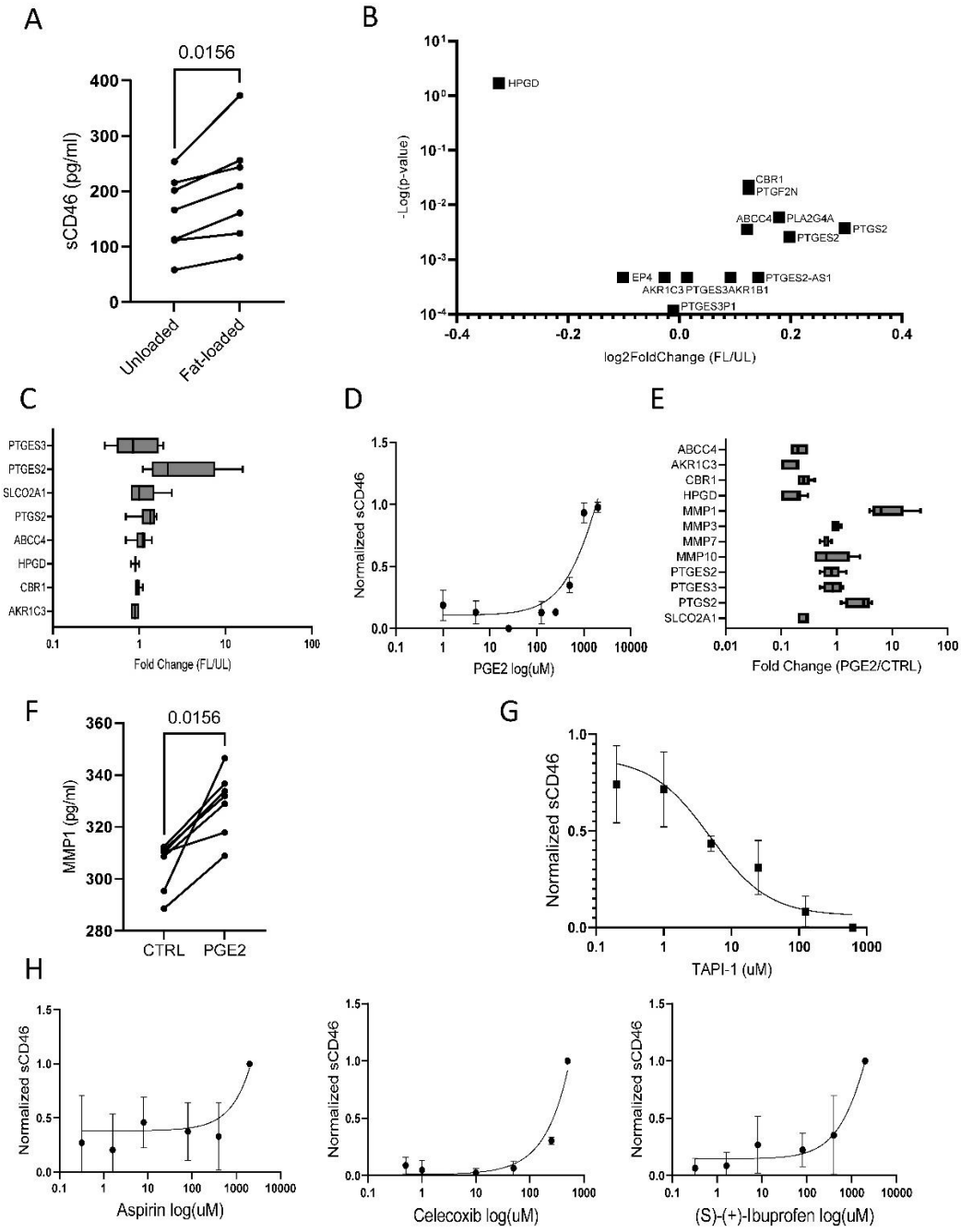

Figure 2. Fat-induced shedding of CD46 involves the prostaglandin E2 (PGE2) pathway and matrix metalloproteinases (MMPs). (A) Fat-loading (FL) of HepaRG cells increased the concentration of sCD46 in the supernatant compared to unloaded (UL). (B) RNA sequencing data indicates an upregulation of the PGE2 pathway in response to FL. (C) qPCR results expressed as fold-change of FL/UL HepaRG cells (n=6). (D) PGE2 treatment induces in a dose-dependent manner the shedding of CD46 in FL cells (n=3). (E) qPCR results expressed as fold-change of PGE2 treatment compared to control DMSO. (F) MMP1 ELISA measurements of FL-HepaRG cells treated with PGE2 or untreated control supernatants (n=7). (G) The effect of MMP inhibitor TAPI-1 in CD46 shedding measured via ELISA (n=3). (H) The effect of NSAIDs in CD46 shedding (n=3). All the data is represented as independent replicates and error bars indicate standard deviation.

Because NSAIDs not only block PGE_2, but also PGI_2, PGD_2, $PGF_{2\alpha}$ and TXA_2 production, we hypothesize that PGE_2 promotes shedding upon fat stimuli (Figure 3A) and other prostaglandins might contribute to some extend in the prevention of CD46 shedding. To corroborate this hypothesis, we used PTGES2-KD FL-HepaRG cells to evaluate its role in the shedding of CD46. Although the KD efficiency was low (~20 %), it was sufficient to observe a downregulation of MMP1 transcription levels in PTGES2-KD cells (Figure 3B). When measuring sCD46 supernatants in six independent replicates, we observed a reduction in sCD46 concentration compared to controls transfected with a scrambled siRNA (Figure 3C). We could not characterize a specific EP receptor that prevents the shedding of CD46 (Figure 3D). Instead, we found that there exists a fine balance of EP receptors and that dysregulations with selective antagonists induced increased shedding of CD46.

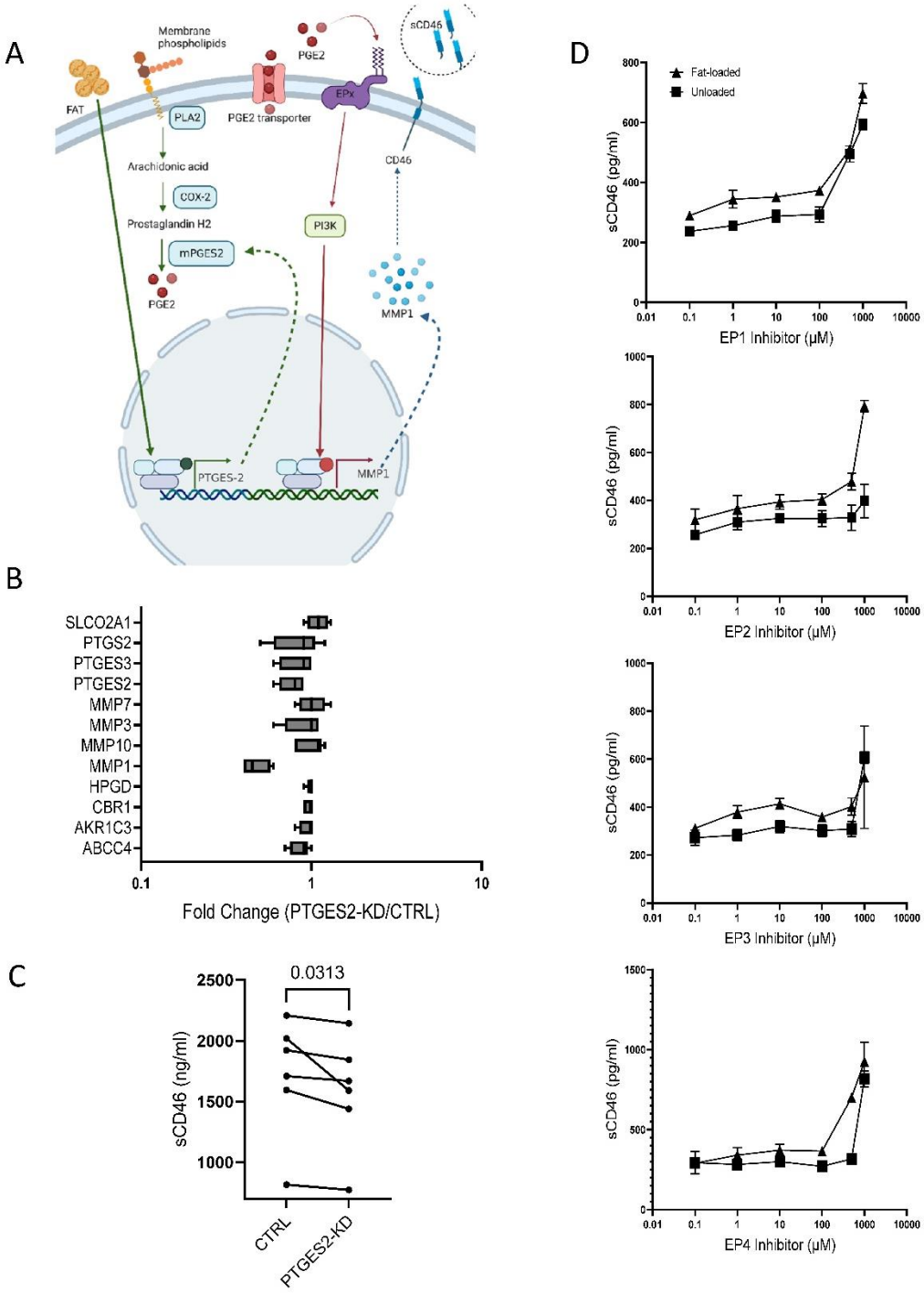

Figure 3. PGE2 modulates the shedding of CD46 via MMP-1 through the EP4 receptor. (A) Illustration of the interaction between fat-loading, PGE2 and MMPs in the shedding of CD46 receptor. FL-HepaRG cells have an upregulation of PTGES2 expression. PGE2 upregulates MMP-1 and COX-2 expression, acting as a positive feedback of the PGE2 pathway. MMP1 activity increases the shedding of CD46. (B) qPCR data expressed as fold change of PTGES-KD HepaRG cells and control cells transfected with scrambled siRNA. (C) sCD46 ELISA of supernatants in PTGES-KD HepaRG cells compared to controls. (D) sCD46 ELISA in HepaRG cells treated with selective prostaglandin receptor inhibitors.

5.4.10 sCD46 can be a potential data readout of hepatotoxic high-throughput drug screenings

HepaRG cells activate a shedding receptor mechanism upon fat-loading. We hypothesize that sCD46 could also be used as a datareadout of hepatotoxicity upon exposure of harmful drugs. We tested 159 FDA-approved drugs in FL-HepaRG cells and identified changes in sCD46 concentration compared to FL-HepaRG cells treated with vehicle DMSO alone. Doxorubicin hydrochloride and Vorinostat induced the highest CD46 shedding in three independent replicates compared to DMSO controls (Figure 4A). Doxorubicin is an antibiotic used to arrest cell growth in cancer cells by damaging DNA. According to clinical reports, doxorubicin is linked to hepatotoxicity in a dose-dependent manner and low doses can cause hepatic necrosis and acute liver failure (ALF) [278]. We labeled drug´s risk of DILI according to the DILIrank dataset publically accessible from the FDA [279]. We ranked drugs according to sCD46 levels and observed an association between DILI risk and CD46 shedding (Figure 4B). The top-30 drugs with higher CD46 shedding consisted of 40 % antineoplastic agents but only two of them were associated with DILI risk according to DILIrank database. Thus, these agents might directly induce HepaRG cell death leading to an increased shedding of CD46. This could also explain why the top-30 drugs disrupted the ascending trend of DILI-events upon higher sCD46 concentrations (Figure 4B). We labeled drugs according to the FDA drug labels and observed that 16 out of 24 antineoplastic agents induced higher sCD46 compared to DMSO control (Figure 4C). Thus, CD46 shedding in HepaRG cells also increases with drugs inhibiting cell growth independently of DILI case reports. We also observe that NSAIDs increased CD46 shedding as reported previously (Figure 4C). These results support the use of sCD46 ELISA assay as a complementary test to assess drug hepatotoxicity.

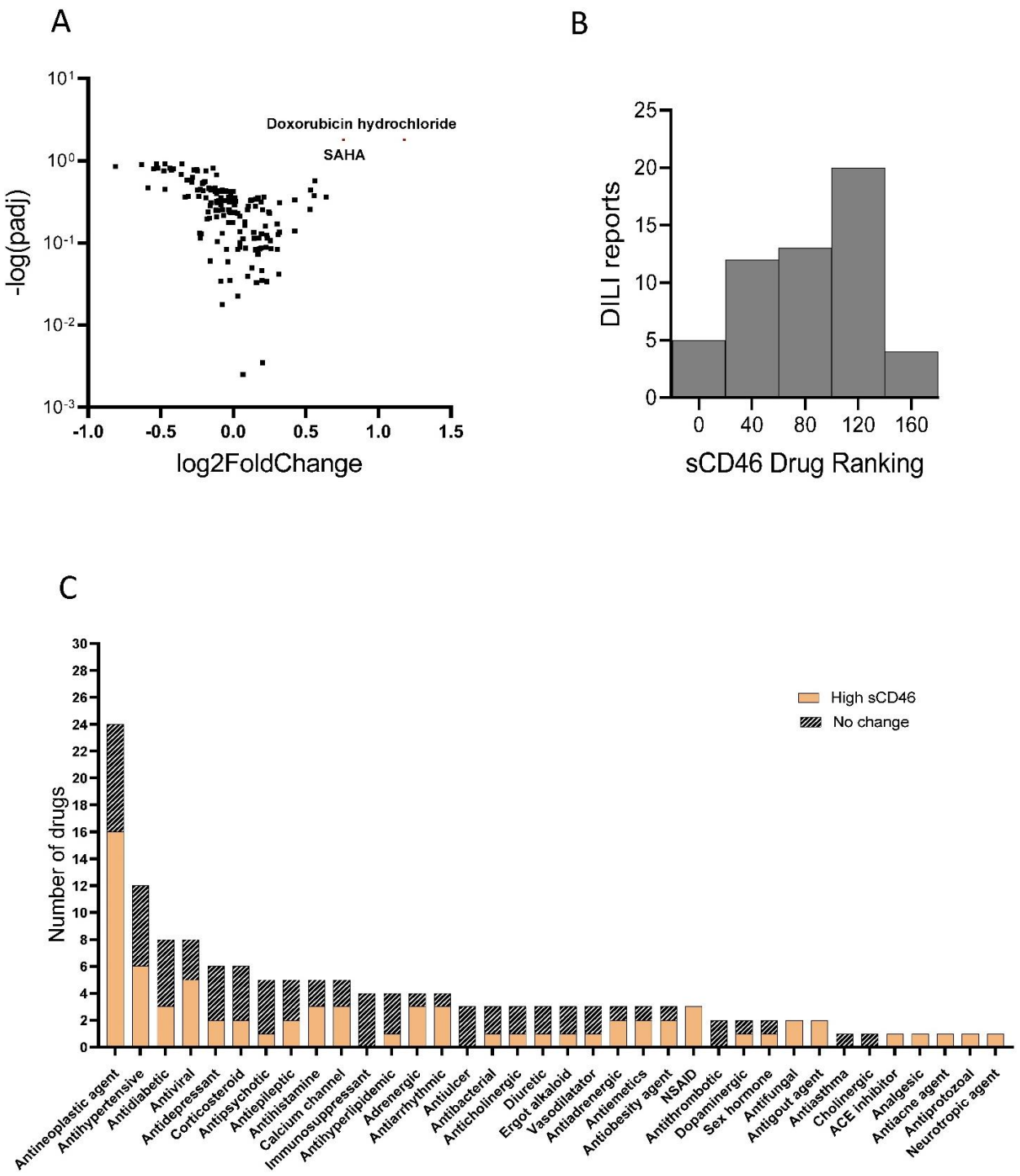

Figure 4. sCD46 as a biomarker for hepatotoxic drug screening. (A) Volcano plot showing the distribution of 159 FDA-approved drugs tested in FL-HepaRG cells according to their adjusted P-values (padj) and fold-change. Drugs labeled in red indicate statistically significant changes compared to control DMSO. (B) Histogram representing a ranking of the drugs tested according to the median expression of sCD46 (n=3) and their association with drug-induced liver injury reports extracted from the FDA DILIRank dataset. (C) Categorization of drugs according to the labels established by the FDA and representation of the proportion of drugs inducing higher sCD46 compared to control DMSO (brown).

5.5 Discussion

CD46 is a multifunctional receptor involved in many infectious and immunological diseases. Upon fat-loading, HepaRG cells cleave the receptor from the cell surface. We have shown that excessive shedding of membrane receptors is an alarming sign of early hepatocyte injury and that increased sCD46 was correlated with steatosis. Here, we describe and validate a specific and cost-sensitive sandwich ELISA for the detection of human sCD46 in serum, plasma and supernatants. When comparing it to five commercial CD46 ELISA kits, none of them could detect sCD46 in serum. Thus, we developed and validated the only available ELISA assay that can measure sCD46. We demonstrated that the sCD46 ELISA assay holds potential as a non-invasive diagnostic tool for steatosis. Although we could not discriminate between mild and severe steatosis, we require bigger sample cohorts to address this question. Since fat-loading increased sCD46 release, we sought to test our sCD46 ELISA as a general screening assay for drug hepatoxicity. Among the 159 FDA-approved drugs tested, we showed that as the concentration of sCD46 increases, so does the frequency of reported DILI events. However, the drugs that induced the highest sCD46 release were mainly antineoplastic agents without hepatotoxic reports. This suggests that general cytotoxic agents also induce shedding of CD46 independently of DILI reports and future studies should test the accuracy and advantages of using sCD46 ELISA for screening hepatotoxic drugs.

At the molecular level, this study identified that CD46 cleavage is mediated via MMPs, giving special attention to MMP-1 upregulation. The activation of MMPs upon cellular stress is recognized as an early inflammatory sign [280, 281]. Dyregulations in the cell surface of hepatocytes can trigger an innate immune response through cell-to-cell contact or damage-associated molecular patterns (DAMPs) signals coming from the cleaved receptors [108, 253]. Here we showed that PGE_2 pathway is activated in steatosis and that it mediates MMP-1 activation. These findings are in line with previous studies in mice where mPGES-2–deficient mice

fed with a high-fat or methionine-choline-deficient diet showed reduced hepatic lipid accumulation and reduced hepatic inflammation [282]. However, when we attempted to block the prostaglandin pathway via COX-1/2 inhibitors, we observed an increased shedding of CD46. This could be related to the complex balance of prostaglandins or to the cytotoxic nature of the drugs. Thus, we approached this issue by impairing the effect of PGE_2. There are four different G protein-coupled receptors that PGE_2 can bind to and activate, namely EP1-4 receptors. Each of them triggers a distinctive intracellular signaling pathway [283]. When blocking EP-specific receptors with antagonist drugs, we observed a dose-dependent increased shedding of CD46 in FL-HepaRG cells, suggesting that the four EP receptors control the shedding of CD46. Based on our RNA-seq data, we could identify a downregulation of EP4 in FL-HepaRG cells (Figure 2B). For future directions, the downregulation mechanisms of EP4 receptor in FL-HepaRG cells should be addressed.

5.6 Conclusions

This study proposes to use sCD46 biomarker as a novel approach to detect early signs of hepatic inflammation. We developed and validated a unique sCD46 ELISA assay that showed potential as a non-invasive diagnostic tool for steatosis and hepatotoxic drug screening. We further established a connection between the PGE_2 pathway, MMP-1 activity and CD46 shedding. Blocking selective EP receptors could not ameliorate CD46 shedding, hence indicating that the four EP receptors prevent the shedding of CD46. Overall, sCD46 ELISA assay served as a tool to diagnose steatosis in patients, test hepatotoxic compounds in vitro and identify novel targets for NAFLD treatment.

5.7 Supplementary material

Supplementary Table 1. List of qPCR primers.

Target	Catalogue number	Company
PTGDS	QT01006901	Qiagen
HPGDS	QT00022043	Qiagen
PTGES2	QT00246337	Qiagen
PTGES3	QT00241927	Qiagen
AKR1B10P2	QT01185835	Qiagen
AKR2C3	QT00013692	Qiagen
CBR1	QT00015260	Qiagen
PTGIS	QT00047747	Qiagen
SLCO2A1	QT00095375	Qiagen
ABCC4	QT00077266	Qiagen
HPGD	QT00013454	Qiagen
ACTB	QT01680476	Qiagen
MMP1	QT00014581	Qiagen
MMP3	QT00060025	Qiagen
MMP7	QT00001456	Qiagen
MMP10	QT00001470	Qiagen

Supplementary Table 2. ELISA grid experiment. Signal:noise average values from different concentrations of capture and detection CD46 antibodies in (A) Reagent diluent 2 and (B) in Reagent diluent 1.

A

	50 ng/ml detection						100 ng/ml detection					
	1 ug/ml capture		2 ug/ml capture		4 ug/ml capture		1 ug/ml capture		2 ug/ml capture		4 ug/ml capture	
	Signal:noise	CV	Signal:noise	CV	Signal:noise	CV	Signal:noise	CV	Signal:noise	CV	Signal:noise	CV
1 ng/ml rhCD46	7.744	0.547	27.541	2.659	33.606	3.759	7.829	0.590	23.263	4.437	27.190	2.391
2 ng/ml rhCD46	13.141	2.420	38.022	1.422	44.356	4.083	13.420	0.367	31.868	3.291	34.834	0.757
4 ng/ml rhCD46	19.096	0.070	46.883	1.951	52.854	2.947	18.960	2.854	37.370	4.763	40.064	0.952
	200 ng/ml detection						400 ng/ml detection					
	1 ug/ml capture		2 ug/ml capture		4 ug/ml capture		1 ug/ml capture		2 ug/ml capture		4 ug/ml capture	
	Signal:noise	CV	Signal:noise	CV	Signal:noise	CV	Signal:noise	CV	Signal:noise	CV	Signal:noise	CV
1 ng/ml rhCD46	6.176	8.279	16.640	0.435	21.292	1.721	4.462	1.382	10.748	5.319	13.436	0.148
2 ng/ml rhCD46	9.636	4.902	22.874	1.385	26.921	0.500	6.501	2.393	14.153	2.968	16.406	0.231
4 ng/ml rhCD46	14.056	5.044	27.314	0.755	28.406	4.696	9.121	1.711	14.737	21.216	16.389	12.013

B

	50 ng/ml detection						100 ng/ml detection					
	1 ug/ml capture		2 ug/ml capture		4 ug/ml capture		1 ug/ml capture		2 ug/ml capture		4 ug/ml capture	
	Signal:noise	CV	Signal:noise	CV	Signal:noise	CV	Signal:noise	CV	Signal:noise	CV	Signal:noise	CV
1 ng/ml rhCD46	3.299	8.360	9.541	3.222	11.532	5.233	3.527	2.647	8.701	4.916	11.004	2.484
2 ng/ml rhCD46	5.562	6.178	15.257	3.722	19.044	4.981	5.623	4.557	14.386	7.012	17.747	0.835
4 ng/ml rhCD46	9.098	9.195	24.724	3.086	29.713	2.456	9.705	4.658	24.148	5.988	29.775	1.979
	200 ng/ml detection						400 ng/ml detection					
	1 ug/ml capture		2 ug/ml capture		4 ug/ml capture		1 ug/ml capture		2 ug/ml capture		4 ug/ml capture	
	Signal:noise	CV	Signal:noise	CV	Signal:noise	CV	Signal:noise	CV	Signal:noise	CV	Signal:noise	CV
1 ng/ml rhCD46	3.152	1.745	7.299	0.307	9.343	0.210	2.414	4.714	5.085	1.034	6.226	1.309
2 ng/ml rhCD46	4.995	1.764	11.985	0.291	15.692	1.546	3.460	0.109	8.461	2.204	10.089	1.502
4 ng/ml rhCD46	7.701	5.556	19.531	0.874	24.896	1.346	5.791	7.899	13.618	1.207	15.529	3.769

- UNPUBLISHED ARTICLE –

6. Discussion: Innate Immune Biomarkers of Early Liver Inflammation

6.1 Abstract

In this discussion, I put the work of this thesis in a broader context and explain how my findings contribute to the field of biomarkers of early liver inflammation. Novel biomarkers are required to increase the sensitivity and specificity of in vitro diagnostic (IVD) tests for early liver disease. An inflammatory cascade is triggered when the liver´s innate immune system senses danger. Some insults induce an excessive inflammatory response, which disrupts the liver´s immunotolerance and promotes pathogenesis. Chapter 1 of this thesis is a review discussing the role of different liver-resident innate immune cells and their contribution to hepatic inflammation. Although inflammation is a hallmark of liver pathology, there are different models of inflammatory cascades typical of particular liver pathologies. In this thesis, I explore the possibility of detecting early liver pathology by measuring the soluble form of innate immune receptors and early changes in innate cell populations. The dysregulation of cell membrane receptors in stressed hepatocytes is a trigger of pathologic innate immune responses. Proteolytic release of membrane-bound receptors are a source of damage-associated molecular patterns (DAMPs) sensing and inflammation. In this discussion, I provide an overview of my findings, describe on-going work and present a strategy for future development of these results into IVD assays. Introduction If we could reliably identify early, asymptomatic liver disease, it might be possible to control its progression to late-stage pathologies, such as cirrhosis, which imports a higher risk of hepatocellular carcinoma (HCC) and liver failure [272, 273]. Routine liver function tests (LFTs) survey liver function, synthetic capacity or cell death, but are not sensitive or specific enough to detect early liver disease [274]. Components of the innate inflammatory cascade initiated by diverse liver injuries are proposed as alternative or complementary markers of early liver pathogenesis [275]. The human liver has a prominent innate immune compartment, which is enriched in Kupffer cells (KCs), Natural Killer cells (NK), Natural Killer T cells (NKT), γδ T cells and Mucosal-associated Invariant T cells (MAIT) [276]. We are slowly beginning to understand the contribution of these subsets to liver homeostasis and disease. Here, we evaluate the diagnostic potential of innate immune biomarkers in early liver diseases including non-alcoholic fatty liver disease (NAFLD), alcoholic liver disease (ALD), drug-induced liver injury (DILI) and after liver transplantation (LT).

6.2 Introduction

6.2.1 Evaluating liver disease markers

Any biomarker under investigation should be evaluated according to its diagnostic potential, which refers to either the discriminative property or the predictive ability of the assay. These features can generally be assessed using measures of diagnostic accuracy. Sensitivity indicates the accuracy of identifying a subject with disease and is calculated as the percentage of true positive subjects with disease classified in a total group of subjects. Specificity refers to the accuracy of excluding a subject without disease and is calculated as the percentage of true negative subjects without disease classified within the total. Predictive values define the probability of having the disease in a subject tested positive for disease (PPV) or the probability of not having a disease in a subject tested negative for disease (NPV). Attention should be paid when using predictive values since they depend on disease prevalence. This means that studies using populations with different disease prevalence should not be compared because PPV values increase with higher prevalence while NPV values decrease. Likelihood ratio (LR) determines the probability that a positive test result is to occur in subjects with disease compared to without disease. When a test is designed to diagnose disease, an LR > 10 is desired and is calculated as the ratio between sensitivity and false-positive rate (1-specificity). Receiver operating characteristic (ROC) curve plots the sensitivity against the false-positive rate at different cut-off values. Measuring the area under the curve (AUC) of a ROC curve is indicative of the discriminative power of a test. It does not tell us about the sensitivity nor the specificity of the test. Instead, it is a useful tool to compare the general assessment of two diagnostic tests. The ideal diagnostic test has an AUC of 1.0 and good diagnostic accuracy is generally accepted in AUC>0.7.

6.2.2 Liver Function Tests and their limitations

Alanine aminotransferase (ALT) is a widely used clinical hepatocellular marker. It is highly expressed in hepatocytes compared to other cell types and leakage of ALT after hepatocyte death is indicative of liver injury [284]. Aspartate aminotransferase (AST) is another liver enzyme usually used together with ALT. Although ALT is more specific for the liver, there are diseases where abnormal values are observed in AST but not in ALT, such as in alcohol liver disease ALD [285]. Nonetheless, ALT and AST levels are reported to increase after extreme exercise for up to 7 days [286] or in patients with polymyositis [287], and remain in circulation after resolved liver injury. Alkaline phosphatase (ALP) is an enzyme highly expressed in the liver, bones and kidneys that helps to break down proteins. Elevated levels in blood suggest blockage of flow in the biliary tract [288, 289]. The results should be read carefully because ALP is an early marker of osteogenesis and bone calcification, and abnormal levels are found in menopausal women [290]. Total bilirubin (TBIL) levels correlate with whole liver function and increased levels indicate that the liver is not clearing bilirubin properly [291]. Caution should be taken because hyperbilirubinemia can happen because of an excessive production of bilirubin, impaired liver uptake, conjugation defects or biliary excretion defects [292], thus it is not specific nor sensitive of liver function [293]. Gamma-glutamyl transferase (GGT) is highly expressed in the liver but also in kidneys, bile ducts and intestines [294]. GGT is involved in the synthesis and degradation of glutathione and drug detoxification [295]. A high GGT test is found in chronic viral hepatitis infection and bile duct injury [296]. Because GGT is not expressed in bones, it is helpful to rule out ALP elevations due to osteogenesis and predicts liver mortality [297, 298]. However, GGT elevations are also associated with cardiovascular risk factors and some cancers [299]. LFTs have limited clinical interpretation because they lack specificity to the liver and disease etiology, and are insensitive markers during early liver injury [300]. This opens the market for novel biomarkers that can complement or replace traditional LFTs, with special attention to innate immune biomarkers.

6.3 Innate immune biomarkers

6.3.1 Non-alcoholic fatty liver disease

The prevalence of NAFLD diagnosed through imaging is 25 % and its incidence is on the rise worldwide [301, 302]. The pathological condition ranges from simple steatosis to non-alcoholic steatohepatitis (NASH). The latter has an estimated prevalence of 3-4 % [301]. Undiagnosed NASH is a dangerous condition because it can rapidly progress toward fibrosis, cirrhosis, and finally, HCC [303]. Biopsy remains the gold standard to diagnose NAFLD, fibrosis stage and NASH but carries limitations including poor sample quality, sampling error, high cost and risk of complications [304, 305]. Additionally, biopsy cannot identify early signs of steatosis and, according to the American Association for the Study of Liver diseases (AASLD), it is not recommended as a general clinical practice. Routine LFTs are not sensitive. For example, ALT showed low diagnostic potential when discriminating simple steatosis, NASH and advanced NASH, with the best classification performance in steatosis patients (53 % correctly classified, AUROC = 0.68) [306]. Imaging methods can clinically discriminate moderate from severe steatosis but it is influenced by confounding factors like fibrosis and operator variability [307]. Additionally, similar to biopsy, imaging is a time-consuming technique, expensive and requires qualified personnel. During the early stages of liver steatosis, critical changes in the immune landscape of the liver reflect the progression of the disease [143, 308, 309]. NKT cells and γδ T cells respond to lipid antigens [42, 43, 310], thus making them interesting targets as biomarkers of early steatosis.

γδ T cells exacerbate the progression of NAFLD in mice via IL-17A secretion [160, 161]. In humans, an increased frequency of circulating $V\delta2^-$ γδ T cells was reported in steatotic patients compared to healthy controls [143]. Changes in $V\delta2^-$ γδ T cells can be measured via qPCR or flow cytometry. Additionally, in autoimmune hepatitis, changes in Vδ1/Vδ2 ratio are observed but

not in γδ T cells [178]. Thus, it is interesting to consider absolute numbers and peripheral immune cell ratios.

NKT cells can be classified according to their T Cell Receptor (TCR) as invariant (i)NKT cells and type II NKT cells (T2NKT). In mice, adoptive transfer of iNKT cells can regulate hepatic steatosis via IL-10 [150]. An increased frequency of intrahepatic iNKT cells is associated with steatotic patients [157]. Similarly, our group identified a dysregulation in the frequency of iNKT cells in blood and in liver of patients undergoing liver transplantation where liver biopsies were available (unpublished data). In a cohort of 105 patients, steatotic patients showed a negative association with the frequency of iNKT cells relative to all $CD3^+$ T cells in peripheral blood (unpublished data). Intrahepatic iNKT cells were enriched in patients with steatosis grade 2-4 (n=15) compared with steatosis grade 0-1 patients (n=28), especially the IL-4^+ iNKT cell subpopulation (unpublished data). Th2 cytokines promote hepatic fibrosis [168, 311]. IL-4 and IL-13 stimulate synthesis of collagen in fibroblasts [312–314] and recruit inflammatory monocytes [315]. However, IL-4 also plays a role in tissue regeneration. Mice with complete IL-4Rα-knockout have impaired M2-type macrophage polarization and present delayed resolution of spontaneous fibrosis [315]. Whether the IL-4^+ iNKT cell expansion represents a pathogenic or a compensatory mechanism against steatosis is unclear. In Chapter 4 of the thesis, we identified a surrogate marker of IL-4^+ iNKT cells from a screening of 378 human surface markers by flow cytometry. This biomarker has potential as a sensitive surrogate of IL-4^+ iNKT cell expansion in blood. We are currently studying the biological function of this marker. Assessment in a larger validation cohort is planned. The role of T2NKT cells in steatosis is unclear. In mice, T2NKT cells are reported to regulate iNKT cells by preventing inflammation [126]. Inflammation is a double-edged sword in the liver. Self-limited acute inflammation is a necessary process to eliminate pathogens and induce apoptosis of hepatic stellate cells (HSCs) to regulate fibrosis [62], but uncontrolled inflammation is harmful. In Chapter 3 of the thesis, we published a novel FACS-based method to isolate and characterize

T2NKT cells from blood and liver. Based on this methodology, we identified a FoxP3$^+$ T2NKT cell subset enriched in the liver. This subpopulation could potentially exert immunoregulatory functions in NAFLD and is likely to suffer alterations during pathogenesis [40]. Unfortunately, the research is still hampered by the limiting number of cells in blood.

Monocytes and neutrophil infiltration are early signs of liver inflammatory and fibrosis progression [18]. A systematic review identified increased concentration of CCL2 and CXCL8 in serum of NAFLD patients compared to controls [316]. Stressed hepatocytes, activated KCs and HSCs secrete CCL2 to recruit circulating CCR2$^+$ monocytes and neutrophils to the liver [317]. In a Chinese study involving more than 4000 patients diagnosed with NAFLD, the monocyte to high-density lipoprotein cholesterol ratio (MHR) combined with laboratory parameters (ALT, AST, total cholesterol, triglycerides, fasting blood glucose, creatinine, uric acid and body mass index) showed an AUC of 0.931 [318]. The study did not stratify patients according to the severity of NAFLD; hence, the value of MHR as an early diagnostic biomarker remains elusive. A recent study found a strong association between NLR and fibrosis stage ($r=0.892$, $p<0.001$), but the association with early signs of NAFLD were weaker, namely, hepatocyte ballooning degeneration ($r=0.426$, $p=0.024$), lobular inflammation ($r=0.694$, $p<0.001$) and steatosis ($r=0.498$, $p=0.007$) [319].

The complement system is a strong contributor of the liver innate system, mainly produced by the liver and positively associated with NAFLD [320–322]. Complement factors are predominantly detected in hepatocytes via immunohistochemistry (IHC) with macrovesicular steatosis while healthy liver biopsies showed undetectable complement binding [320]. The activation of the complement cascade is suggested to be caused by fat-induced apoptosis. C1q, mannose-binding lectin and CRP can then recognize apoptotic cells and recruit the complement system [323, 324]. An activated complement system leads to the formation of the complement Membrane Attack Complex (MAC) that generates pores in the cell membrane and induces osmolysis [325]. The

release of intracellular components can induce further activation of the innate system. Some products of the complement cascade, namely C3a and C5a, are strong chemoattractants of neutrophils, thus promoting local inflammation and tissue damage [325]. Serum C5a levels measured via enzyme-linked immunosorbent assay (ELISA) were higher in obese children with NAFLD compared with lean controls [326]. Mild liver steatosis represents a confounding factor in many studies and results should be interpreted with caution. It is yet to be assessed the specificity of these biomarkers in distinguishing obese subjects from NAFLD patients [320].

Matrix metalloproteases (MMPs) participate in the shedding of various receptors as an immunoregulatory mechanism [327]. Its soluble counterparts can be potentially measured in serum via ELISA. Based on proteomics data performed in our group, we identified dysregulations of cellular receptors in fat-loaded HepaRG cells compared to controls. Among the list of candidates, CD46 was confirmed to play a role in preventing the expansion of IL-4^{+} iNKT cells in a cell-to-cell manner. The complement regulatory protein CD46 is ubiquitously expressed and protects the host cell from the complement system by proteolytic cleavage of C3b and C4b [328]. Additional roles of CD46 in humans have been reported such as in reproduction or T-cell co-stimulation [328, 329]. As previously discussed, steatotic hepatocytes present high depositions of activated C3, which could be contributed partly by the dysregulation of CD46 receptor in steatotic hepatocytes [328]. However, the overall contribution of CD46 downregulation in the activation of the complement system in steatosis has not been elucidated yet. The downregulation of CD46 receptor is mediated via MMP leading to the release of soluble CD46 (sCD46). Because steatosis is a process prior to inflammation, we hypothesize that sCD46 could be a useful biomarker for steatosis and early inflammation. In Chapter 5 of this thesis, we developed a sCD46 ELISA that passed all the corresponding validation tests to show precision, accuracy and robustness. When evaluating the predictability power of serum sCD46 as a non-invasive biomarker to discriminate steatosis from non-steatosis, we reported an AUC of 0.831. The accuracy in a 3-way

discrimination between no steatosis, moderate steatosis and severe steatosis was 69.6 %. Our investigations focus on understanding the MMP-CD46-iNKT axis both as diagnostic and therapeutic approach. In this thesis, the microsomal prostaglandin E synthase-2 (mPGES-2) transcription levels was observed to be increased in HepaRG cells modelling steatosis. Addition of prostaglandin E2 (PGE_2) in cell culture upregulated the transcription levels of MMP-1 by ~10-fold and led to a significant increase in sCD46. However, inhibition of PGE_2 receptors could not prevent the shedding of sCD46. Instead, we observed an increased shedding in a dose-dependent manner. This suggests that EP receptors control the shedding of CD46 and dysregulations of the receptors can increase MMP expression. Our RNA-seq data points out a potential downregulation of EP4 in HepaRG cells loaded with fat.

6.3.2 Alcohol-related liver disease

ALD refers to liver damage caused by alcohol misuse – that is 20-50 g/day of alcohol use in women and 60-80 g/day in men [330]. The phenotypic manifestation is similar to NAFLD ranging from fatty liver, alcoholic hepatitis, alcoholic cirrhosis and HCC [331]. The current diagnosis of ALD is based on a standard assessment of liver damage including physical examination and laboratory analysis of AST, ALT and GGT levels combined with the history of alcohol consumption or detection of ethanol in serum, urine, breath or body fluids. Data from a study of 8700 adults in the US indicated that LFTs alone or in combination are weak in identifying alcohol misuse with a sensitivity below 50 % [332]. The biomarkers included in the study were ALT, AST, GGT, Mean Corpuscular Volume (MCV), and apolipoprotein A1 and B. A group analysed the proteomic changes in ALD patients from plasma samples.

Alcohol disrupts the cellular membrane and induces necrosis. As a response, hepatocytes produce tissue repair proteins like Augmenter of Liver Regeneration (ALR). ALR is ubiquitously expressed and is known to promote liver regeneration [333, 334]. Its expression is much greater

in liver parenchymal tissue and testis [333]. It is recognized as a damage responsive protein and potentially an indicator of hepatocyte stress [335]. In vitro, rat hepatoytes treated with hepatotoxic agents such as lipopolisaccharides (LPS) showed increased secretion of ALR measured in ELISA [335]. ALR can also activate the innate immune system. Rat KCs are sensitive to ALR and respond by expressing the pro-inflammatory cytokines IL-6, TNF-α, and nitric oxide (NO) [336]. In alcohol-fed mice with liver steatosis, ALR is reduced in liver tissues suggesting its release in blood [337]. Liver tissues from advanced ALD and NASH but not HCV-infected patients showed lower levels of ALR compared to controls by immunoblot analysis [337]. In patients with acute and fulminant hepatitis, ALR levels were also increased in serum measured by ELISA [338]. Interestingly, serum ALR elevated before ALT in a rat model injected with LPS and remained significantly higher compared to basal levels at 24 hours [335]. Mice with ALR-knockout presented with increased steatosis, mitochondrial dysfunction and ROS generation [337]. This suggests that ALR is a biomarker of early liver injury and inflammation, and future studies should address its specificity and sensitivity as a useful biomarker for early signs of ALD pathogenesis.

Alcohol breaks down into free radicals such as acetaldehyde, ROS and specific metabolites of alcohol catabolism (ethyl-glucuronide or ethyl sulfate) which result in the activation and proliferation of KCs [339]. CD163 is a receptor protein expressed on KCs and is sensitive to cleavage upon KC activation, resulting in soluble CD163 (sCD163) release [340]. The role of sCD163 in inflammation consists in controlling hyperactivation of monocytes by reducing TNF-α, IL-1β, IL-6 and IL-8 secretion [341]. However, the levels of sCD163 correlate with IL-6, IL-8 and IL-10 secretion, suggesting that CD163 shedding is a consequence of the inflammatory environment [342–344]. In patients, sCD163 is elevated in ALD compared to healthy controls and an association is found between disease severity and sCD163 levels via ELISA detection [345]. TNF-related apoptosis-inducing ligand (TRAIL) is expressed in KCs and NK cells upon activation. Stressed hepatocytes and profibrogenic HSCs are eliminated via TRAIL-induced apoptosis to

resolve inflammation [346, 347]. In mice, serum ALT showed to be statistically higher in alcohol-fed mice with TNF-α receptor 1 (TNF-R1) knockout compared to wild-type [348]. The addition of PEGylated TRAIL treatment improved elimination of HSCs in a rat model of ALD [347]. Serum TRAIL levels in alcoholic hepatitis patients, determined by western blot, inversely correlated with the severity of the disease [349]. Similarly, NK cells are downregulated in human ALD [117, 118]. These results encourage the study of $TRAIL^+$ NK cell and KCs alterations as early diagnostic biomarkers of liver injury caused by alcohol misuse. Based on the results of Chapter 5 of this thesis, we could integrate the sCD46 ELISA assay as a diagnosis tool for steatosis to identify early ALD progression. This is relevant to provide an appropriate clinical management of ALD patients and prevent the development of a more serious form of pathology.

6.3.3 Drug-induced liver injury

DILI is a leading cause of complications in drug development, black box warnings and post-marketing withdrawals [350–352]. More than a thousand medications are reported to have hepatotoxic effects [353, 354]. The incidence of DILI is less than 0.02 % in western patients making it hard to establish a causal relationship between drugs and hepatotoxicity [355, 356]. The current diagnosis of DILI pathogenesis relies on the exclusion of other causes of liver damage and the evidence of liver damage based on traditional LFTs [357]. It is complicated to identify drug hepatotoxicity from clinical trials data with a degree of confidence because small alterations in LFT values are likely to be caused by other disorders [358]. We still rely upon reports from pharmacovigilance studies to establish causality [359]. DILI is induced by the metabolic exhaustion of hepatocytes, conversion to the active form of drugs during detoxification, and hepatocyte necrosis [360, 361]. Damaged hepatocytes release DAMPs signals such as high mobility group box-1 (HMGB1) and osteopontin (OPN) [108, 253].

HMGB1, released by necrotic hepatocytes, is not fully oxidized compared to its apoptotic counterpart [362] and act as a pro-inflammatory mediator of innate immunity via toll-like receptor-4 (TLR4) and Receptor for Advanced Glycation Endproducts (RAGE) [363]. Elevations of total HMGB1 are reported in patients with acetaminophen (APAP) overdose [364]. The elevation of HMGB1 appears faster than ALT elevations [365] and has a better prediction score when combined with microRNA (miR)-122 and K18 [364].

OPN promotes liver regeneration and its concentrations are elevated in serum of DILI patients with poor outcomes [366]. OPN measured via ELISA had a greater prognostic value for predicting liver transplantation in DILI patients compared to K18 [366]. iNKT are reported to produce OPN [367]. In mice, OPN can activate iNKT cells and exacerbate the disease [253, 367]. The pathogenic role of iNKT cells in exacerbating liver damage was further confirmed in halothane-DILI and APAP-DILI (Cheng L 2010 & Mizrahi 2018). γδ T cells are known to produce rapid and large amounts of pro-inflammatory IL-17 [39]. In an APAP-DILI mouse model, the depletion of γδ T cells attenuated liver damage and was associated with decreased neutrophil infiltration [368]. These results encourage the study of iNKT and IL-17^{+} γδ T cells as early biomarkers of DILI.

A study showed that the frequency of human circulating monocytes is depleted in APAP-induced acute liver failure [369]. Increased levels of CCL2 in serum of these patients measured via ELISA suggest infiltration of monocytes in the liver [369]. The same study reported increased levels of CCL2, CCL3, IL-6, IL-10 and transforming growth factor-beta 1 (TGF-β1) in the liver determined by IHC [369]. The severity of APAP-DILI positively correlates with CCL2 levels in human serum and negatively correlates with the number of circulating monocytes [369]. KCs are enriched in the necrotic areas of human liver biopsies and are suggested to be a primary source of CCL2 secretion [369]. Thus, circulating CCR2^{+} monocytes might be a useful biomarker to detect early APAP-induced injury.

Biomarkers for identifying idiosyncratic drug hepatotoxicity is mainly limited by the low prevalence and the interference with other liver pathologies [370]. Immune checkpoint inhibitors (ICI) also present idiosyncratic patterns of hepatitis [371]. In this thesis, we evaluated the performance of 59 biomarkers previously reported to predict immune-related adverse events risk after ICI therapy in melanoma patients. Our work shows that current LFTs and flow cytometry biomarkers perform poorly in predicting risk for drug-induced hepatitis and that new biomarkers are required [207]. Thus, early detection of idiosyncratic hepatitis is uncommon and studies are preferentially focused on identifying biomarkers that can predict high-DILI risk.

A section in Chapter 5 describes the establishment of an in vitro assay for hepatotoxic drug testing using sCD46 measured by ELISA as a data readout. As we previously discussed, CD46 shedding represents an early sign of liver damage upon fat-loading and might also be applicable upon exposure to other drugs. We found that the shedding of CD46 is increased in response to several anti-neoplastic drugs with reported cases of ALT/AST elevations. Among the 159 tested drugs, doxorubicin hydrochloride showed the highest shedding of CD46 response. Doxorubicin is an antineoplastic medication linked to hepatotoxicity and a major cause of DILI [278]. We also reported that three common non-steroidal anti-inflammatory drugs (NSAIDs), namely Celecoxib, Ibuprofen and Aspirin, also increased the shedding of CD46. NSAIDs target the prostaglandin-endoperoxide synthase COX-1 and COX-2, and block the prostaglandin pathway. Based on our studies, blocking PGE_2 pathway prevents increased shedding response but complete blockage of the prostaglandin pathway, thus preventing the synthesis of other prostaglandins as well, might induce opposite signals [372]. Another drug that induced high sCD46 concentrations was APAP, which targets COX-2 and is a major cause of DILI. Overall, we propose that the sCD46 ELISA assay could assist as a hepatotoxic parameter in the drug development field. The analytical validation shows that sCD46 can be measured in an accurate, precise and robust way. The clinical validation shows that sCD46 is sensitive, specific, with good positive predictive value and AUC

score. As point-of-care testing, it has clinical value because it can measure serum and plasma, and is assayed relatively rapidly via a low-cost ELISA.

6.3.4 Liver transplantation

Liver transplantation (LT) is the only treatment for advanced cirrhosis with liver failure [373]. Transplantation is also becoming more frequent in NASH patients [374]. In 2022, LT involving living donors increased to 603 transplants, approximately 6 % compared to the previous year (OPTN data). A critical step in the management of graft tolerance is the appropriate use of immunosuppressive drugs (IS), which has remarkably improved the risk of rejection. The use of IS is associated with complications such as *de novo* malignancies and infections, among others [375]. Some patients develop spontaneous acceptance of the graft without the requirement of IS, suggesting the need to stratify patients to spare unnecessary immunosuppression [376, 377]. Unfortunately, traditional blood tests are unable to discriminate rejection from other etiologies such as ischemia or infection [378]. Liver biopsy remains the gold standard for assessing graft injury and is complemented with blood routine analysis for liver function [379]. In Chapter 2 of this thesis, we have presented a clinical case of an HCC patient under an off-label compassionate therapy with immune-checkpoint inhibitor atezolizumab plus bevazicumab (Atezo/Bev). In line with previous reports, we discussed the applicability of different immune biomarkers in monitoring early LT rejection in this particular context. CD28 expression levels by $CD4^+$ T cells and peripheral blood $CD4^+$ T cell numbers returned as potential biomarkers of early warning of LT rejection following ICI therapy [380]. However, this clinical study highlights the need for innovative biomarkers. We currently lack biomarkers that confirm ICI therapy response. HCC patients with PD-L1-negative tumors also benefit from Nivolumab (anti-PD-1 antibody). With the approval of new ICI therapies, the limitations of the current LFTs are more noticeable. New biomarkers with higher sensitivity and specificity are needed to monitor the risk of liver rejection or therapeutic

response. Although in this thesis we have not investigated the potential of sCD46 as a biomarker in liver rejection and therapy response, it might be worth considering it. Many cancers overexpress CD46 [381]. Particularly, in HCC, CD46 is overexpressed compared to cirrhosis and chronic hepatitis [382]. Furthermore, there are many early-phase clinical studies studying anti-CD46 therapy in many cancers [382].

Innate immune cells are investigated as potential biomarkers in LT settings. A prospective open-label non-controlled IS withdrawal trial in HCV-infected stable LT recipients reported that the high blood Vδ1/Vδ2 T cell ratio is a favorable biomarker for LT patient IS withdrawal with a 82 % sensitivity, 53 % specificity, 67 % positive predictive value and 73 % negative predictive value [383]. Vδ1 T cells are enriched in epithelia and regulate immune responses [384]. Biopsies from grafts of IS-free recipients showed an increased Vδ1/Vδ2 T cell ratio, measured via qPCR, compared to recipients under IS [385]. The same study reported that there is an expansion of a unique Vδ1-bearing T-cell clone which was not identified in recipients under IS [385].

From a retrospective study of 300 peripheral blood samples, 13 unique genes were found to correlate with pediatric and adult liver tolerance compared to stable patients on chronic IS [386]. Interestingly, these genes are highly expressed in NK cells, suggesting a possible role of NK cells in operational tolerance [386]. The combination of 3 of these genes, namely *SENP6, ERBB2* and *FEM1C*, showed promising prediction scores by qPCR with 100 % sensitivity, 83 % specificity and AUC of 0.988 [386]. Similarly, in a prospective multicenter trial of IS withdrawal, the expansion of NK cells and decreased Vδ2-TCR γδ T cells in blood samples was reported in operationally tolerant recipients before IS withdrawal as compared to non-tolerant patients [387]. These promising results support the investigation of γδ T cells and NK cells as routine biomarkers of early liver rejection.

6.4 Regulatory aspect of biomarker approval

sCD46 ELISA and other biomarkers holding potential as diagnosis tools ideally will be translated into the clinical settings. In this section, I would like to discuss the critical points before and during the submission of an application to the corresponding regulatory entity in order to achieve an approved biomarker. This also serves as an outlook of the future steps that need to be pursuit for sCD46 ELISA development.

Diagnostic biomarkers with good discriminatory or predictive accuracy are encouraged to identify a potential manufacturer that can produce kits under good manufacturing practices (GMP). The kit should be revaluated in different laboratories with retrospective samples and larger cohorts. The applicants should test the kit in multicentre clinical studies to define the limitations and fitness of the biomarker in the real clinical setting. If the biomarker achieves encouraging results, an application may be submitted to the corresponding regulatory agency for qualification. According to the FDA framework, the Biomarker Qualification Program assesses biomarkers in seven different categories: susceptibility/risk, diagnostic, monitoring, prognostic, predictive, pharmacodynamic/response and safety. The applicant submits a letter of intent addressing the biomarker´s potential value, information about the current scientific understanding, context of use and the measuring approach. If the FDA accepts the application, a qualification plan should be followed. Detailed information about the current advances including the analytical method and performance characteristics should be attached. The knowledge gaps and a defined plan to address them is also necessary. If the FDA accepts it, a full qualification package (FQP) compiling all the supporting evidences will be requested. The FDA will make a final decision based on the FQP and if positive, the biomarker is qualified to be used in the context of use in any of the Center for Drug Evaluation and Research (CDER) drug development program. It is worth to note that a qualified biomarker indicates that we can rely on the biomarker´s output within the stated context of use such as point-of-care, clinical trials primary end-point, commercial laboratories testing,

among others. However, the biomarker measurement method is not recognized as such by the agency.

6.5 Conclusions

LFTs are routinely conducted, widely available and cost-effective. However, there are still critical unmet needs in assessing liver pathologies. The missing gaps discussed in this review reflect the need for more sensitive biomarkers to identify early signs of liver injury. We contemplate innate immune biomarkers as promising non-invasive and early-inflammation sensors that could serve as complementary tests to LFTs or alternatives to current inflammatory tests such as CRP or IL-6 test. Immune cells, complement proteins, shed receptors, cytokines and chemokines can be routinely screened via qPCR, ELISA or flow cytometry. Of interest, the release of receptors and proteins can influence the innate immunity of the liver. For instance, HMGB1 and OPN act as DAMP signals triggering pro-inflammatory responses even in the absence of pathogens. MMPs are the main enzymes involved in extracellular matrix (ECM) remodelling, which is necessary for tissue regeneration. MMPs can also contribute to liver inflammation by increasing vascular permeability for leukocyte infiltration [388], shedding of cytokines to its mature form in the case of TNF-α [389], TGF-β [390] or IL-1β [391], and immune-related receptors such as CD163 [392] or CD46 [259]. MMP alterations can be detected in early stages of fibrogenesis [393] and our data suggest that they can even be detected during steatosis. However, MMPs have a complex biology playing different roles based on cell or tissue type [393]. Thus, detecting MMPs as early liver injury biomarkers is neither specific nor reliable, but the cleaved products might be. The work related to this thesis supports the use of early inflammatory signs originating from the innate immune system or stressed hepatocytes as a way to identify pathogenesis and liver disease progression.

Overall, this thesis contributed to the liver immunology field with the following achievements:

- Developing a sorting method to isolate T2NKT cells from human blood and liver.
- Identifying a novel FoxP3^{+} T2NKT cell subset present in human liver biposies.
- Identifying CD202b as a surrogate marker of IL-4^{+} iNKT cells.
- Developing the only validated ELISA assay to measure the cleaved form of human CD46 receptor.
- Demonstrating the superiority of the sCD46 ELISA assay in the diagnosis of steatosis compared to the sCD46 FACS-based competitive assay.
- Demonstrating the applicability of the sCD46 ELISA assay as a drug-screening assay.
- Identifying and describing the activation of PGE_2-MMP1-sCD46 axis during steatosis.

7. References

1. Wisse E, Braet F, Luo D, Zanger R de, Jans D, Crabbé E, Vermoesen A. Structure and function of sinusoidal lining cells in the liver. Toxicol Pathol. 1996;24:100–11. doi:10.1177/019262339602400114.

2. Wake K, Sato T. "The sinusoid" in the liver: lessons learned from the original definition by Charles Sedgwick Minot (1900). Anat Rec (Hoboken). 2015;298:2071–80. doi:10.1002/ar.23263

3. Ben-Moshe S, Itzkovitz S. Spatial heterogeneity in the mammalian liver. Nat Rev Gastroenterol Hepatol. 2019;16:395–410. doi:10.1038/s41575-019-0134-x.

4. McEnerney L, Duncan K, Bang B-R, Elmasry S, Li M, Miki T, et al. Dual modulation of human hepatic zonation via canonical and non-canonical Wnt pathways. Exp Mol Med. 2017;49:e413. doi:10.1038/emm.2017.226.

5. Cheng ML, Nakib D, Perciani CT, MacParland SA. The immune niche of the liver. Clin Sci (Lond). 2021;135:2445–66. doi:10.1042/CS20190654.

6. Dusseaux M, Martin E, Serriari N, Péguillet I, Premel V, Louis D, et al. Human MAIT cells are xenobiotic-resistant, tissue-targeted, CD161hi IL-17-secreting T cells. Blood. 2011;117:1250–9. doi:10.1182/blood-2010-08-303339.

7. Tang X-Z, Jo J, Tan AT, Sandalova E, Chia A, Tan KC, et al. IL-7 licenses activation of human liver intrasinusoidal mucosal-associated invariant T cells. J Immunol. 2013;190:3142–52. doi:10.4049/jimmunol.1203218.

8. Doherty DG. Immunity, tolerance and autoimmunity in the liver: A comprehensive review. J Autoimmun. 2016;66:60–75. doi:10.1016/j.jaut.2015.08.020.

9. Freitas-Lopes MA, Mafra K, David BA, Carvalho-Gontijo R, Menezes GB. Differential Location and Distribution of Hepatic Immune Cells. Cells 2017. doi:10.3390/cells6040048.

10. Wehr A, Baeck C, Heymann F, Niemietz PM, Hammerich L, Martin C, et al. Chemokine receptor CXCR6-dependent hepatic NK T Cell accumulation promotes inflammation and liver fibrosis. J Immunol. 2013;190:5226–36. doi:10.4049/jimmunol.1202909.

11. Hammerich L, Tacke F. Role of gamma-delta T cells in liver inflammation and fibrosis. World J Gastrointest Pathophysiol. 2014;5:107–13. doi:10.4291/wjgp.v5.i2.107.

12. Jeffery HC, van Wilgenburg B, Kurioka A, Parekh K, Stirling K, Roberts S, et al. Biliary epithelium and liver B cells exposed to bacteria activate intrahepatic MAIT cells through MR1. J Hepatol. 2016;64:1118–27. doi:10.1016/j.jhep.2015.12.017.

13. Sitia G, Iannacone M, Aiolfi R, Isogawa M, van Rooijen N, Scozzesi C, et al. Kupffer cells hasten resolution of liver immunopathology in mouse models of viral hepatitis. PLoS Pathog. 2011;7:e1002061. doi:10.1371/journal.ppat.1002061.

14. Dou L, Shi X, He X, Gao Y. Macrophage Phenotype and Function in Liver Disorder. Front Immunol. 2019;10:3112. doi:10.3389/fimmu.2019.03112.

15. Ju C, Tacke F. Hepatic macrophages in homeostasis and liver diseases: from pathogenesis to novel therapeutic strategies. Cell Mol Immunol. 2016;13:316–27. doi:10.1038/cmi.2015.104.

16. Tran S, Baba I, Poupel L, Dussaud S, Moreau M, Gélineau A, et al. Impaired Kupffer Cell Self-Renewal Alters the Liver Response to Lipid Overload during Non-alcoholic Steatohepatitis. Immunity. 2020;53:627-640.e5. doi:10.1016/j.immuni.2020.06.003.

17. Heymann F, Hammerich L, Storch D, Bartneck M, Huss S, Rüsseler V, et al. Hepatic macrophage migration and differentiation critical for liver fibrosis is mediated by the chemokine receptor C-C motif chemokine receptor 8 in mice. Hepatology. 2012;55:898–909. doi:10.1002/hep.24764.

18. Karlmark KR, Weiskirchen R, Zimmermann HW, Gassler N, Ginhoux F, Weber C, et al. Hepatic recruitment of the inflammatory Gr1+ monocyte subset upon liver injury promotes hepatic fibrosis. Hepatology. 2009;50:261–74. doi:10.1002/hep.22950.

19. Mossanen JC, Krenkel O, Ergen C, Govaere O, Liepelt A, Puengel T, et al. Chemokine (C-C motif) receptor 2-positive monocytes aggravate the early phase of acetaminophen-induced acute liver injury. Hepatology. 2016;64:1667–82. doi:10.1002/hep.28682.

20. Krenkel O, Tacke F. Liver macrophages in tissue homeostasis and disease. Nat Rev Immunol. 2017;17:306–21. doi:10.1038/nri.2017.11.

21. Dixon LJ, Barnes M, Tang H, Pritchard MT, Nagy LE. Kupffer cells in the liver. Compr Physiol. 2013;3:785–97. doi:10.1002/cphy.c120026.

22. Cowley SC. MAIT cells and pathogen defense. Cell Mol Life Sci. 2014;71:4831–40. doi:10.1007/s00018-014-1708-y.

23. Gao B, Ma J, Xiang X. MAIT cells: a novel therapeutic target for alcoholic liver disease? Gut. 2018;67:784–6. doi:10.1136/gutjnl-2017-315284.

24. Lamichhane R, Munro F, Harrop TWR, La Harpe SM de, Dearden PK, Vernall AJ, et al. Human liver-derived MAIT cells differ from blood MAIT cells in their metabolism and response to TCR-independent activation. Eur J Immunol. 2021;51:879–92. doi:10.1002/eji.202048830.

25. Gracey E, Qaiyum Z, Almaghlouth I, Lawson D, Karki S, Avvaru N, et al. IL-7 primes IL-17 in mucosal-associated invariant T (MAIT) cells, which contribute to the Th17-axis in ankylosing spondylitis. Ann Rheum Dis. 2016;75:2124–32. doi:10.1136/annrheumdis-2015-208902.

26. Mehta H, Lett MJ, Klenerman P, Filipowicz Sinnreich M. MAIT cells in liver inflammation and fibrosis. Semin Immunopathol. 2022;44:429–44. doi:10.1007/s00281-022-00949-1.

27. Lett MJ, Mehta H, Keogh A, Jaeger T, Jacquet M, Powell K, et al. Stimulatory MAIT cell antigens reach the circulation and are efficiently metabolised and presented by human liver cells. Gut. 2022;71:2526–38. doi:10.1136/gutjnl-2021-324478.

28. Shiromizu CM, Jancic CC. γδ T Lymphocytes: An Effector Cell in Autoimmunity and Infection. Front Immunol. 2018;9:2389. doi:10.3389/fimmu.2018.02389.

29. Toulon A, Breton L, Taylor KR, Tenenhaus M, Bhavsar D, Lanigan C, et al. A role for human skin-resident T cells in wound healing. J Exp Med. 2009;206:743–50. doi:10.1084/jem.20081787.

30. Deusch K, Moebius U, zum Meyer Büschenfelde KH, Meuer SC. T lymphocyte control of autoreactivity: analysis with human T cell clones and limiting dilution culture. Eur J Immunol. 1986;16:1433–8. doi:10.1002/eji.1830161119.

31. Luoma AM, Castro CD, Adams EJ. γδ T cell surveillance via CD1 molecules. Trends Immunol. 2014;35:613–21. doi:10.1016/j.it.2014.09.003.

32. Davey MS, Willcox CR, Hunter S, Kasatskaya SA, Remmerswaal EBM, Salim M, et al. The human Vδ2+ T-cell compartment comprises distinct innate-like Vγ9+ and adaptive Vγ9- subsets. Nat Commun. 2018;9:1760. doi:10.1038/s41467-018-04076-0.

33. Park JH, Lee HK. Function of γδ T cells in tumor immunology and their application to cancer therapy. Exp Mol Med. 2021;53:318–27. doi:10.1038/s12276-021-00576-0.

34. Feurle J, Espinosa E, Eckstein S, Pont F, Kunzmann V, Fournié J-J, et al. Escherichia coli produces phosphoantigens activating human gamma delta T cells. J Biol Chem. 2002;277:148–54. doi:10.1074/jbc.M106443200.

35. Blazquez J-L, Benyamine A, Pasero C, Olive D. New Insights Into the Regulation of γδ T Cells by BTN3A and Other BTN/BTNL in Tumor Immunity. Front Immunol. 2018;9:1601. doi:10.3389/fimmu.2018.01601.

36. Harly C, Guillaume Y, Nedellec S, Peigné C-M, Mönkkönen H, Mönkkönen J, et al. Key implication of CD277/butyrophilin-3 (BTN3A) in cellular stress sensing by a major human γδ T-cell subset. Blood. 2012;120:2269–79. doi:10.1182/blood-2012-05-430470.

37. Riquelme P, Haarer J, Kammler A, Walter L, Tomiuk S, Ahrens N, et al. TIGIT+ iTregs elicited by human regulatory macrophages control T cell immunity. Nat Commun. 2018;9:2858. doi:10.1038/s41467-018-05167-8.

38. Mangan BA, Dunne MR, O'Reilly VP, Dunne PJ, Exley MA, O'Shea D, et al. Cutting edge: CD1d restriction and Th1/Th2/Th17 cytokine secretion by human Vδ3 T cells. J Immunol. 2013;191:30–4. doi:10.4049/jimmunol.1300121.

39. Papotto PH, Ribot JC, Silva-Santos B. IL-17+ γδ T cells as kick-starters of inflammation. Nat Immunol. 2017;18:604–11. doi:10.1038/ni.3726.

40. Yang Zhou J, Werner JM, Glehr G, Geissler EK, Hutchinson JA, Kronenberg K. Identification and Isolation of Type II NKT Cell Subsets in Human Blood and Liver. Front Immunol. 2022;13:898473. doi:10.3389/fimmu.2022.898473.

41. Bayatipoor H, Mehdizadeh S, Jafarpour R, Shojaei Z, Pashangzadeh S, Motallebnezhad M. Role of NKT cells in cancer immunotherapy-from bench to bed. Med Oncol. 2022;40:29. doi:10.1007/s12032-022-01888-5.

42. Dasgupta S, Kumar V. Type II NKT cells: a distinct CD1d-restricted immune regulatory NKT cell subset. Immunogenetics. 2016;68:665–76. doi:10.1007/s00251-016-0930-1.

43. Borg NA, Wun KS, Kjer-Nielsen L, Wilce MCJ, Pellicci DG, Koh R, et al. CD1d-lipid-antigen recognition by the semi-invariant NKT T-cell receptor. Nature. 2007;448:44–9. doi:10.1038/nature05907.

44. Bricard G, Venkataswamy MM, Yu KOA, Im JS, Ndonye RM, Howell AR, et al. A-galactosylceramide analogs with weak agonist activity for human iNKT cells define new candidate anti-inflammatory agents. PLoS One. 2010;5:e14374. doi:10.1371/journal.pone.0014374.

45. Takahashi T, Suzuki T. Role of sulfatide in normal and pathological cells and tissues. J Lipid Res. 2012;53:1437–50. doi:10.1194/jlr.R026682.

46. Renukaradhya GJ, Khan MA, Vieira M, Du W, Gervay-Hague J, Brutkiewicz RR. Type I NKT cells protect (and type II NKT cells suppress) the host's innate antitumor immune response to a B-cell lymphoma. Blood. 2008;111:5637–45. doi:10.1182/blood-2007-05-092866.

47. Terabe M, Berzofsky JA. The immunoregulatory role of type I and type II NKT cells in cancer and other diseases. Cancer Immunol Immunother. 2014;63:199–213. doi:10.1007/s00262-013-1509-4.

48. Rhost S, Sedimbi S, Kadri N, Cardell SL. Immunomodulatory type II natural killer T lymphocytes in health and disease. Scand J Immunol. 2012;76:246–55. doi:10.1111/j.1365-3083.2012.02750.x.

49. Sedimbi SK, Hägglöf T, Garimella MG, Wang S, Duhlin A, Coelho A, et al. Combined proinflammatory cytokine and cognate activation of invariant natural killer T cells enhances anti-DNA antibody responses. Proc Natl Acad Sci U S A. 2020;117:9054–63. doi:10.1073/pnas.1920463117.

50. Mikulak J, Bruni E, Oriolo F, Di Vito C, Mavilio D. Hepatic Natural Killer Cells: Organ-Specific Sentinels of Liver Immune Homeostasis and Physiopathology. Front Immunol. 2019;10:946. doi:10.3389/fimmu.2019.00946.

51. Cai L, Zhang Z, Zhou L, Wang H, Fu J, Zhang S, et al. Functional impairment in circulating and intrahepatic NK cells and relative mechanism in hepatocellular carcinoma patients. Clin Immunol. 2008;129:428–37. doi:10.1016/j.clim.2008.08.012.

52. Marquardt N, Béziat V, Nyström S, Hengst J, Ivarsson MA, Kekäläinen E, et al. Cutting edge: identification and characterization of human intrahepatic CD49a+ NK cells. J Immunol. 2015;194:2467–71. doi:10.4049/jimmunol.1402756.

53. Hudspeth K, Donadon M, Cimino M, Pontarini E, Tentorio P, Preti M, et al. Human liver-resident CD56(bright)/CD16(neg) NK cells are retained within hepatic sinusoids via the engagement of CCR5 and CXCR6 pathways. J Autoimmun. 2016;66:40–50. doi:10.1016/j.jaut.2015.08.011.

54. Stegmann KA, Robertson F, Hansi N, Gill U, Pallant C, Christophides T, et al. CXCR6 marks a novel subset of T-bet(lo)Eomes(hi) natural killer cells residing in human liver. Sci Rep. 2016;6:26157. doi:10.1038/srep26157.

55. Cuff AO, Robertson FP, Stegmann KA, Pallett LJ, Maini MK, Davidson BR, Male V. Eomeshi NK Cells in Human Liver Are Long-Lived and Do Not Recirculate but Can Be Replenished from the Circulation. J Immunol. 2016;197:4283–91. doi:10.4049/jimmunol.1601424.

56. Peng H, Wisse E, Tian Z. Liver natural killer cells: subsets and roles in liver immunity. Cell Mol Immunol. 2016;13:328–36. doi:10.1038/cmi.2015.96.

57. Tang L, Peng H, Zhou J, Chen Y, Wei H, Sun R, et al. Differential phenotypic and functional properties of liver-resident NK cells and mucosal ILC1s. J Autoimmun. 2016;67:29–35. doi:10.1016/j.jaut.2015.09.004.

58. Daussy C, Faure F, Mayol K, Viel S, Gasteiger G, Charrier E, et al. T-bet and Eomes instruct the development of two distinct natural killer cell lineages in the liver and in the bone marrow. J Exp Med. 2014;211:563–77. doi:10.1084/jem.20131560.

59. Sojka DK, Plougastel-Douglas B, Yang L, Pak-Wittel MA, Artyomov MN, Ivanova Y, et al. Tissue-resident natural killer (NK) cells are cell lineages distinct from thymic and conventional splenic NK cells. Elife. 2014;3:e01659. doi:10.7554/eLife.01659.

60. Kumar S. Natural killer cell cytotoxicity and its regulation by inhibitory receptors. Immunology. 2018;154:383–93. doi:10.1111/imm.12921.

61. Backes CS, Friedmann KS, Mang S, Knörck A, Hoth M, Kummerow C. Natural killer cells induce distinct modes of cancer cell death: Discrimination, quantification, and modulation of apoptosis, necrosis, and mixed forms. J Biol Chem. 2018;293:16348–63. doi:10.1074/jbc.RA118.004549.

62. Zhang Y, Wu Y, Shen W, Wang B, Yuan X. Crosstalk between NK cells and hepatic stellate cells in liver fibrosis (Review). Mol Med Rep 2022. doi:10.3892/mmr.2022.12724.

63. Shi J, Zhao J, Zhang X, Cheng Y, Hu J, Li Y, et al. Activated hepatic stellate cells impair NK cell anti-fibrosis capacity through a TGF-β-dependent emperipolesis in HBV cirrhotic patients. Sci Rep. 2017;7:44544. doi:10.1038/srep44544.

64. Subedi N, Verhagen LP, Bosman EM, van Roessel I, Tel J. Understanding natural killer cell biology from a single cell perspective. Cell Immunol. 2022;373:104497. doi:10.1016/j.cellimm.2022.104497.

65. Guillot A, Tacke F. Liver Macrophages: Old Dogmas and New Insights. Hepatol Commun. 2019;3:730–43. doi:10.1002/hep4.1356.

66. Zhang H, Zahid A, Ismail H, Tang Y, Jin T, Tao J. An overview of disease models for NLRP3 inflammasome over-activation. Expert Opin Drug Discov. 2021;16:429–46. doi:10.1080/17460441.2021.1844179.

67. Zheng D, Liwinski T, Elinav E. Inflammasome activation and regulation: toward a better understanding of complex mechanisms. Cell Discov. 2020;6:36. doi:10.1038/s41421-020-0167-x.

68. Kimura K, Sekiguchi S, Hayashi S, Hayashi Y, Hishima T, Nagaki M, Kohara M. Role of interleukin-18 in intrahepatic inflammatory cell recruitment in acute liver injury. J Leukoc Biol. 2011;89:433–42. doi:10.1189/jlb.0710412.

69. Barbier L, Ferhat M, Salamé E, Robin A, Herbelin A, Gombert J-M, et al. Interleukin-1 Family Cytokines: Keystones in Liver Inflammatory Diseases. Front Immunol. 2019;10:2014. doi:10.3389/fimmu.2019.02014.

70. Diaz O, Vidalain P-O, Ramière C, Lotteau V, Perrin-Cocon L. What role for cellular metabolism in the control of hepatitis viruses? Front Immunol. 2022;13:1033314. doi:10.3389/fimmu.2022.1033314.

71. Platt L, Easterbrook P, Gower E, McDonald B, Sabin K, McGowan C, et al. Prevalence and burden of HCV co-infection in people living with HIV: a global systematic review and meta-analysis. Lancet Infect Dis. 2016;16:797–808. doi:10.1016/S1473-3099(15)00485-5.

72. McGlynn KA, Petrick JL, El-Serag HB. Epidemiology of Hepatocellular Carcinoma. Hepatology. 2021;73 Suppl 1:4–13. doi:10.1002/hep.31288.

73. Zaki MYW, Fathi AM, Samir S, Eldafashi N, William KY, Nazmy MH, et al. Innate and Adaptive Immunopathogeneses in Viral Hepatitis; Crucial Determinants of Hepatocellular Carcinoma. Cancers (Basel) 2022. doi:10.3390/cancers14051255.

74. Hösel M, Quasdorff M, Ringelhan M, Kashkar H, Debey-Pascher S, Sprinzl MF, et al. Hepatitis B Virus Activates Signal Transducer and Activator of Transcription 3 Supporting Hepatocyte Survival and Virus Replication. Cell Mol Gastroenterol Hepatol. 2017;4:339–63. doi:10.1016/j.jcmgh.2017.07.003.

75. Kakimi K, Guidotti LG, Koezuka Y, Chisari FV. Natural killer T cell activation inhibits hepatitis B virus replication in vivo. J Exp Med. 2000;192:921–30. doi:10.1084/jem.192.7.921.

76. Li F, Wei H, Wei H, Gao Y, Xu L, Yin W, et al. Blocking the natural killer cell inhibitory receptor NKG2A increases activity of human natural killer cells and clears hepatitis B virus infection in mice. Gastroenterology. 2013;144:392–401. doi:10.1053/j.gastro.2012.10.039.

77. Arababadi MK, Pourfathollah AA, Jafarzadeh A, Hassanshahi G, Mohit M, Hajghani M, et al. Evaluation of CCR5 Expression on NK Cells in Iranian Patients With Occult Hepatitis B Infection. Lab Med. 2010;41:735–8. doi:10.1309/LMAUISL84Q4SRSBT.

78. Lunemann S, Malone DFG, Hengst J, Port K, Grabowski J, Deterding K, et al. Compromised function of natural killer cells in acute and chronic viral hepatitis. J Infect Dis. 2014;209:1362–73. doi:10.1093/infdis/jit561.

79. Zhao J, Li Y, Jin L, Zhang S, Fan R, Sun Y, et al. Natural killer cells are characterized by the concomitantly increased interferon-γ and cytotoxicity in acute resolved hepatitis B patients. PLoS One. 2012;7:e49135. doi:10.1371/journal.pone.0049135.

80. Li J, Han Y, Jin K, Wan Y, Wang S, Liu B, et al. Dynamic changes of cytotoxic T lymphocytes (CTLs), natural killer (NK) cells, and natural killer T (NKT) cells in patients with acute hepatitis B infection. Virol J. 2011;8:199. doi:10.1186/1743-422X-8-199.

81. Zheng Q, Zhu YY, Chen J, Ye YB, Li JY, Liu YR, et al. Activated natural killer cells accelerate liver damage in patients with chronic hepatitis B virus infection. Clin Exp Immunol. 2015;180:499–508. doi:10.1111/cei.12597.

82. Dunn C, Brunetto M, Reynolds G, Christophides T, Kennedy PT, Lampertico P, et al. Cytokines induced during chronic hepatitis B virus infection promote a pathway for

NK cell-mediated liver damage. J Exp Med. 2007;204:667–80. doi:10.1084/jem.20061287.

83. Zou Y, Chen T, Han M, Wang H, Yan W, Song G, et al. Increased killing of liver NK cells by Fas/Fas ligand and NKG2D/NKG2D ligand contributes to hepatocyte necrosis in virus-induced liver failure. J Immunol. 2010;184:466–75. doi:10.4049/jimmunol.0900687.

84. Wang Y, Wang W, Shen C, Wang Y, Jiao M, Yu W, et al. NKG2D modulates aggravation of liver inflammation by activating NK cells in HBV infection. Sci Rep. 2017;7:88. doi:10.1038/s41598-017-00221-9.

85. Guidotti LG, McClary H, Loudis JM, Chisari FV. Nitric oxide inhibits hepatitis B virus replication in the livers of transgenic mice. J Exp Med. 2000;191:1247–52. doi:10.1084/jem.191.7.1247.

86. Duwaerts CC, Sun EP, Cheng C-W, van Rooijen N, Gregory SH. Cross-activating invariant NKT cells and kupffer cells suppress cholestatic liver injury in a mouse model of biliary obstruction. PLoS One. 2013;8:e79702. doi:10.1371/journal.pone.0079702.

87. Xue H, Li H, Ju L-L, Han X-D, Cheng T-C, Luo X, et al. Mucosal-associated invariant T cells in hepatitis B virus-related liver failure. World J Gastroenterol. 2020;26:4703–17. doi:10.3748/wjg.v26.i31.4703.

88. Chen M, Zhang D, Zhen W, Shi Q, Liu Y, Ling N, et al. Characteristics of circulating T cell receptor gamma-delta T cells from individuals chronically infected with hepatitis B virus (HBV): an association between V(delta)2 subtype and chronic HBV infection. J Infect Dis. 2008;198:1643–50. doi:10.1086/593065.

89. Chen M, Hu P, Ling N, Peng H, Lei Y, Hu H, et al. Enhanced functions of peripheral γδ T cells in chronic hepatitis B infection during interferon α treatment in vivo and in vitro. PLoS One. 2015;10:e0120086. doi:10.1371/journal.pone.0120086.

90. Wu X, Zhang J-Y, Huang A, Li Y-Y, Zhang S, Wei J, et al. Decreased Vδ2 γδ T cells associated with liver damage by regulation of Th17 response in patients with chronic hepatitis B. J Infect Dis. 2013;208:1294–304. doi:10.1093/infdis/jit312.

91. Brunetto MR, Bonino F. Interferon therapy of chronic hepatitis B. Intervirology. 2014;57:163–70. doi:10.1159/000360941.

92. Fisicaro P, Rossi M, Vecchi A, Acerbi G, Barili V, Laccabue D, et al. The Good and the Bad of Natural Killer Cells in Virus Control: Perspective for Anti-HBV Therapy. Int J Mol Sci 2019. doi:10.3390/ijms20205080.

93. Núñez O, Fernández-Martínez A, Majano PL, Apolinario A, Gómez-Gonzalo M, Benedicto I, et al. Increased intrahepatic cyclooxygenase 2, matrix metalloproteinase 2, and matrix metalloproteinase 9 expression is associated with

progressive liver disease in chronic hepatitis C virus infection: role of viral core and NS5A proteins. Gut. 2004;53:1665–72. doi:10.1136/gut.2003.038364.

94. Nishitsuji H, Funami K, Shimizu Y, Ujino S, Sugiyama K, Seya T, et al. Hepatitis C virus infection induces inflammatory cytokines and chemokines mediated by the cross talk between hepatocytes and stellate cells. J Virol. 2013;87:8169–78. doi:10.1128/JVI.00974-13.

95. Hosomura N, Kono H, Tsuchiya M, Ishii K, Ogiku M, Matsuda M, Fujii H. HCV-related proteins activate Kupffer cells isolated from human liver tissues. Dig Dis Sci. 2011;56:1057–64. doi:10.1007/s10620-010-1395-y.

96. van Wilgenburg B, Scherwitzl I, Hutchinson EC, Leng T, Kurioka A, Kulicke C, et al. MAIT cells are activated during human viral infections. Nat Commun. 2016;7:11653. doi:10.1038/ncomms11653.

97. Hengst J, Strunz B, Deterding K, Ljunggren H-G, Leeansyah E, Manns MP, et al. Nonreversible MAIT cell-dysfunction in chronic hepatitis C virus infection despite successful interferon-free therapy. Eur J Immunol. 2016;46:2204–10. doi:10.1002/eji.201646447.

98. Bolte FJ, Rehermann B. Mucosal-Associated Invariant T Cells in Chronic Inflammatory Liver Disease. Semin Liver Dis. 2018;38:60–5. doi:10.1055/s-0037-1621709.

99. Tseng CT, Miskovsky E, Houghton M, Klimpel GR. Characterization of liver T-cell receptor gammadelta T cells obtained from individuals chronically infected with hepatitis C virus (HCV): evidence for these T cells playing a role in the liver pathology associated with HCV infections. Hepatology. 2001;33:1312–20. doi:10.1053/jhep.2001.24269.

100. Nattermann J, Feldmann G, Ahlenstiel G, Langhans B, Sauerbruch T, Spengler U. Surface expression and cytolytic function of natural killer cell receptors is altered in chronic hepatitis C. Gut. 2006;55:869–77. doi:10.1136/gut.2005.076463.

101. Stegmann KA, Björkström NK, Ciesek S, Lunemann S, Jaroszewicz J, Wiegand J, et al. Interferon α-stimulated natural killer cells from patients with acute hepatitis C virus (HCV) infection recognize HCV-infected and uninfected hepatoma cells via DNAX accessory molecule-1. J Infect Dis. 2012;205:1351–62. doi:10.1093/infdis/jis210.

102. Senff T, Menne C, Cosmovici C, Lewis-Ximenez LL, Aneja J, Broering R, et al. Peripheral blood iNKT cell activation correlates with liver damage during acute hepatitis C. JCI Insight 2022. doi:10.1172/jci.insight.155432.

103. Grant DM. Detoxification pathways in the liver. J Inherit Metab Dis. 1991;14:421–30. doi:10.1007/BF01797915.

104. Francis P, Navarro VJ. StatPearls: Drug Induced Hepatotoxicity. Treasure Island (FL); 2022.

105. Kinashi Y, Hase K. Partners in Leaky Gut Syndrome: Intestinal Dysbiosis and Autoimmunity. Front Immunol. 2021;12:673708. doi:10.3389/fimmu.2021.673708.

106. Twardowska A, Makaro A, Binienda A, Fichna J, Salaga M. Preventing Bacterial Translocation in Patients with Leaky Gut Syndrome: Nutrition and Pharmacological Treatment Options. Int J Mol Sci 2022. doi:10.3390/ijms23063204.

107. Szabo G, Bala S. Alcoholic liver disease and the gut-liver axis. World J Gastroenterol. 2010;16:1321–9. doi:10.3748/wjg.v16.i11.1321.

108. Mihm S. Danger-Associated Molecular Patterns (DAMPs): Molecular Triggers for Sterile Inflammation in the Liver. Int J Mol Sci 2018. doi:10.3390/ijms19103104.

109. Kubes P, Mehal WZ. Sterile inflammation in the liver. Gastroenterology. 2012;143:1158–72. doi:10.1053/j.gastro.2012.09.008.

110. Schlechte J, Skalosky I, Geuking MB, McDonald B. Long-distance relationships - regulation of systemic host defense against infections by the gut microbiota. Mucosal Immunol. 2022;15:809–18. doi:10.1038/s41385-022-00539-2.

111. Choi SE, Jeong W-I. Innate Lymphoid Cells: New Culprits of Alcohol-Associated Steatohepatitis. Cell Mol Gastroenterol Hepatol. 2023;15:279–80. doi:10.1016/j.jcmgh.2022.10.012.

112. Enomoto N, Ikejima K, Bradford BU, Rivera CA, Kono H, Goto M, et al. Role of Kupffer cells and gut-derived endotoxins in alcoholic liver injury. J Gastroenterol Hepatol. 2000;15 Suppl:D20-5. doi:10.1046/j.1440-1746.2000.02179.x.

113. Kono H, Rusyn I, Yin M, Gäbele E, Yamashina S, Dikalova A, et al. NADPH oxidase-derived free radicals are key oxidants in alcohol-induced liver disease. J Clin Invest. 2000;106:867–72. doi:10.1172/JCI9020.

114. Nagy LE, Ding W-X, Cresci G, Saikia P, Shah VH. Linking Pathogenic Mechanisms of Alcoholic Liver Disease With Clinical Phenotypes. Gastroenterology. 2016;150:1756–68. doi:10.1053/j.gastro.2016.02.035.

115. Zhang L, Bansal MB. Role of Kupffer Cells in Driving Hepatic Inflammation and Fibrosis in HIV Infection. Front Immunol. 2020;11:1086. doi:10.3389/fimmu.2020.01086.

116. Koop DR, Klopfenstein B, Iimuro Y, Thurman RG. Gadolinium chloride blocks alcohol-dependent liver toxicity in rats treated chronically with intragastric alcohol despite the induction of CYP2E1. Mol Pharmacol. 1997;51:944–50. doi:10.1124/mol.51.6.944.

117. Pan H, Sun R, Jaruga B, Hong F, Kim W-H, Gao B. Chronic ethanol consumption inhibits hepatic natural killer cell activity and accelerates murine cytomegalovirus-induced hepatitis. Alcohol Clin Exp Res. 2006;30:1615–23. doi:10.1111/j.1530-0277.2006.00194.x.

118. Perney P, Portalès P, Corbeau P, Roques V, Blanc F, Clot J. Specific alteration of peripheral cytotoxic cell perforin expression in alcoholic patients: a possible role in alcohol-related diseases. Alcohol Clin Exp Res. 2003;27:1825–30. doi:10.1097/01.ALC.0000093742.22787.30.

119. Jeong W-I, Park O, Radaeva S, Gao B. STAT1 inhibits liver fibrosis in mice by inhibiting stellate cell proliferation and stimulating NK cell cytotoxicity. Hepatology. 2006;44:1441–51. doi:10.1002/hep.21419.

120. Lee K-C, Chen P, Maricic I, Inamine T, Hu J, Gong S, et al. Intestinal iNKT cells migrate to liver and contribute to hepatocyte apoptosis during alcoholic liver disease. Am J Physiol Gastrointest Liver Physiol. 2019;316:G585-G597. doi:10.1152/ajpgi.00269.2018.

121. Buschard K, Hansen AK, Jensen K, Lindenbergh-Kortleve DJ, Ruiter LF de, Krohn TC, et al. Alcohol facilitates CD1d loading, subsequent activation of NKT cells, and reduces the incidence of diabetes in NOD mice. PLoS One. 2011;6:e17931. doi:10.1371/journal.pone.0017931.

122. Cui K, Yan G, Xu C, Chen Y, Wang J, Zhou R, et al. Invariant NKT cells promote alcohol-induced steatohepatitis through interleukin-1β in mice. J Hepatol. 2015;62:1311–8. doi:10.1016/j.jhep.2014.12.027.

123. Mathews S, Feng D, Maricic I, Ju C, Kumar V, Gao B. Invariant natural killer T cells contribute to chronic-plus-binge ethanol-mediated liver injury by promoting hepatic neutrophil infiltration. Cell Mol Immunol. 2016;13:206–16. doi:10.1038/cmi.2015.06.

124. Maricic I, Sheng H, Marrero I, Seki E, Kisseleva T, Chaturvedi S, et al. Inhibition of type I natural killer T cells by retinoids or following sulfatide-mediated activation of type II natural killer T cells attenuates alcoholic liver disease in mice. Hepatology. 2015;61:1357–69. doi:10.1002/hep.27632.

125. Maricic I, Girardi E, Zajonc DM, Kumar V. Recognition of lysophosphatidylcholine by type II NKT cells and protection from an inflammatory liver disease. J Immunol. 2014;193:4580–9. doi:10.4049/jimmunol.1400699.

126. Halder RC, Aguilera C, Maricic I, Kumar V. Type II NKT cell-mediated anergy induction in type I NKT cells prevents inflammatory liver disease. J Clin Invest. 2007;117:2302–12. doi:10.1172/JCI31602.

127. Riva A, Patel V, Kurioka A, Jeffery HC, Wright G, Tarff S, et al. Mucosa-associated invariant T cells link intestinal immunity with antibacterial immune defects in alcoholic liver disease. Gut. 2018;67:918–30. doi:10.1136/gutjnl-2017-314458.

128. Zhang Y, Fan Y, He W, Han Y, Bao H, Yang R, et al. Persistent deficiency of mucosa-associated invariant T (MAIT) cells during alcohol-related liver disease. Cell Biosci. 2021;11:148. doi:10.1186/s13578-021-00664-8.

129. Li W, Lin EL, Liangpunsakul S, Lan J, Chalasani S, Rane S, et al. Alcohol Abstinence Does Not Fully Reverse Abnormalities of Mucosal-Associated Invariant T Cells in the Blood of Patients With Alcoholic Hepatitis. Clin Transl Gastroenterol. 2019;10:e00052. doi:10.14309/ctg.0000000000000052.

130. Lee J-H, Shim Y-R, Seo W, Kim M-H, Choi W-M, Kim H-H, et al. Mitochondrial Double-Stranded RNA in Exosome Promotes Interleukin-17 Production Through Toll-Like Receptor 3 in Alcohol-associated Liver Injury. Hepatology. 2020;72:609–25. doi:10.1002/hep.31041.

131. Marcellin P, Kutala BK. Liver diseases: A major, neglected global public health problem requiring urgent actions and large-scale screening. Liver Int. 2018;38 Suppl 1:2–6. doi:10.1111/liv.13682.

132. Noureddin M, Vipani A, Bresee C, Todo T, Kim IK, Alkhouri N, et al. NASH Leading Cause of Liver Transplant in Women: Updated Analysis of Indications For Liver Transplant and Ethnic and Gender Variances. Am J Gastroenterol. 2018;113:1649–59. doi:10.1038/s41395-018-0088-6.

133. Lazarus JV, Mark HE, Villota-Rivas M, Palayew A, Carrieri P, Colombo M, et al. The global NAFLD policy review and preparedness index: Are countries ready to address this silent public health challenge? J Hepatol. 2022;76:771–80. doi:10.1016/j.jhep.2021.10.025.

134. Nati M, Chung K-J, Chavakis T. The Role of Innate Immune Cells in Nonalcoholic Fatty Liver Disease. J Innate Immun. 2022;14:31–41. doi:10.1159/000518407.

135. Rodrigues RM, Guan Y, Gao B. Targeting adipose tissue to tackle NASH: SPARCL1 as an emerging player. J Clin Invest 2021. doi:10.1172/JCI153640.

136. Neuschwander-Tetri BA. Therapeutic Landscape for NAFLD in 2020. Gastroenterology. 2020;158:1984-1998.e3. doi:10.1053/j.gastro.2020.01.051.

137. Park J-W, Jeong G, Kim SJ, Kim MK, Park SM. Predictors reflecting the pathological severity of non-alcoholic fatty liver disease: comprehensive study of clinical and immunohistochemical findings in younger Asian patients. J Gastroenterol Hepatol. 2007;22:491–7. doi:10.1111/j.1440-1746.2006.04758.x.

138. Huang W, Metlakunta A, Dedousis N, Zhang P, Sipula I, Dube JJ, et al. Depletion of liver Kupffer cells prevents the development of diet-induced hepatic steatosis and insulin resistance. Diabetes. 2010;59:347–57. doi:10.2337/db09-0016.

139. Diehl KL, Vorac J, Hofmann K, Meiser P, Unterweger I, Kuerschner L, et al. Kupffer Cells Sense Free Fatty Acids and Regulate Hepatic Lipid Metabolism in High-Fat Diet and Inflammation. Cells 2020. doi:10.3390/cells9102258.

140. Ioannou GN, Landis CS, Jin G-Y, Haigh WG, Farrell GC, Kuver R, et al. Cholesterol Crystals in Hepatocyte Lipid Droplets Are Strongly Associated With Human Nonalcoholic Steatohepatitis. Hepatol Commun. 2019;3:776–91. doi:10.1002/hep4.1348.

141. Leroux A, Ferrere G, Godie V, Cailleux F, Renoud M-L, Gaudin F, et al. Toxic lipids stored by Kupffer cells correlates with their pro-inflammatory phenotype at an early stage of steatohepatitis. J Hepatol. 2012;57:141–9. doi:10.1016/j.jhep.2012.02.028.

142. Tercan H, Riksen NP, Joosten LAB, Netea MG, Bekkering S. Trained Immunity: Long-Term Adaptation in Innate Immune Responses. Arterioscler Thromb Vasc Biol. 2021;41:55–61. doi:10.1161/ATVBAHA.120.314212.

143. Diedrich T, Kummer S, Galante A, Drolz A, Schlicker V, Lohse AW, et al. Characterization of the immune cell landscape of patients with NAFLD. PLoS One. 2020;15:e0230307. doi:10.1371/journal.pone.0230307.

144. O'Shea D, Hogan AE. Dysregulation of Natural Killer Cells in Obesity. Cancers (Basel) 2019. doi:10.3390/cancers11040573.

145. Michelet X, Dyck L, Hogan A, Loftus RM, Duquette D, Wei K, et al. Metabolic reprogramming of natural killer cells in obesity limits antitumor responses. Nat Immunol. 2018;19:1330–40. doi:10.1038/s41590-018-0251-7.

146. Stiglund N, Strand K, Cornillet M, Stål P, Thorell A, Zimmer CL, et al. Retained NK Cell Phenotype and Functionality in Non-alcoholic Fatty Liver Disease. Front Immunol. 2019;10:1255. doi:10.3389/fimmu.2019.01255.

147. Li Z, Soloski MJ, Diehl AM. Dietary factors alter hepatic innate immune system in mice with nonalcoholic fatty liver disease. Hepatology. 2005;42:880–5. doi:10.1002/hep.20826.

148. Kremer M, Thomas E, Milton RJ, Perry AW, van Rooijen N, Wheeler MD, et al. Kupffer cell and interleukin-12-dependent loss of natural killer T cells in hepatosteatosis. Hepatology. 2010;51:130–41. doi:10.1002/hep.23292.

149. Guebre-Xabier M, Yang S, Lin HZ, Schwenk R, Krzych U, Diehl AM. Altered hepatic lymphocyte subpopulations in obesity-related murine fatty livers: potential

mechanism for sensitization to liver damage. Hepatology. 2000;31:633–40. doi:10.1002/hep.510310313.

150. Kim HM, Lee BR, Lee ES, Kwon MH, Huh JH, Kwon B-E, et al. iNKT cells prevent obesity-induced hepatic steatosis in mice in a C-C chemokine receptor 7-dependent manner. Int J Obes (Lond). 2018;42:270–9. doi:10.1038/ijo.2017.200.

151. Ohmura K, Ishimori N, Ohmura Y, Tokuhara S, Nozawa A, Horii S, et al. Natural killer T cells are involved in adipose tissues inflammation and glucose intolerance in diet-induced obese mice. Arterioscler Thromb Vasc Biol. 2010;30:193–9. doi:10.1161/ATVBAHA.109.198614.

152. Wu L, Parekh VV, Gabriel CL, Bracy DP, Marks-Shulman PA, Tamboli RA, et al. Activation of invariant natural killer T cells by lipid excess promotes tissue inflammation, insulin resistance, and hepatic steatosis in obese mice. Proc Natl Acad Sci U S A. 2012;109:E1143-52. doi:10.1073/pnas.1200498109.

153. Satoh M, Andoh Y, Clingan CS, Ogura H, Fujii S, Eshima K, et al. Type II NKT cells stimulate diet-induced obesity by mediating adipose tissue inflammation, steatohepatitis and insulin resistance. PLoS One. 2012;7:e30568. doi:10.1371/journal.pone.0030568.

154. Hams E, Locksley RM, McKenzie ANJ, Fallon PG. Cutting edge: IL-25 elicits innate lymphoid type 2 and type II NKT cells that regulate obesity in mice. J Immunol. 2013;191:5349–53. doi:10.4049/jimmunol.1301176.

155. Xu C-F, Yu C-H, Li Y-M, Xu L, Du J, Shen Z. Association of the frequency of peripheral natural killer T cells with nonalcoholic fatty liver disease. World J Gastroenterol. 2007;13:4504–8. doi:10.3748/wjg.v13.i33.4504.

156. Tajiri K, Shimizu Y, Tsuneyama K, Sugiyama T. Role of liver-infiltrating CD3+CD56+ natural killer T cells in the pathogenesis of nonalcoholic fatty liver disease. Eur J Gastroenterol Hepatol. 2009;21:673–80. doi:10.1097/MEG.0b013e32831bc3d6.

157. Adler M, Taylor S, Okebugwu K, Yee H, Fielding C, Fielding G, Poles M. Intrahepatic natural killer T cell populations are increased in human hepatic steatosis. World J Gastroenterol. 2011;17:1725–31. doi:10.3748/wjg.v17.i13.1725.

158. Syn W-K, Oo YH, Pereira TA, Karaca GF, Jung Y, Omenetti A, et al. Accumulation of natural killer T cells in progressive nonalcoholic fatty liver disease. Hepatology. 2010;51:1998–2007. doi:10.1002/hep.23599.

159. Li Y, Huang B, Jiang X, Chen W, Zhang J, Wei Y, et al. Mucosal-Associated Invariant T Cells Improve Nonalcoholic Fatty Liver Disease Through Regulating

Macrophage Polarization. Front Immunol. 2018;9:1994. doi:10.3389/fimmu.2018.01994.

160. Li F, Hao X, Chen Y, Bai L, Gao X, Lian Z, et al. The microbiota maintain homeostasis of liver-resident γδT-17 cells in a lipid antigen/CD1d-dependent manner. Nat Commun. 2017;7:13839. doi:10.1038/ncomms13839.

161. Torres-Hernandez A, Wang W, Nikiforov Y, Tejada K, Torres L, Kalabin A, et al. γδ T Cells Promote Steatohepatitis by Orchestrating Innate and Adaptive Immune Programming. Hepatology. 2020;71:477–94. doi:10.1002/hep.30952.

162. Xu X, Zhang S, Song X, Hu Q, Pan W. IL-17 enhances oxidative stress in hepatocytes through Nrf2/keap1 signal pathway activation. Int J Clin Exp Pathol. 2018;11:3318–23. doi:None.

163. Tan Z, Jiang R, Wang X, Wang Y, Lu L, Liu Q, et al. RORγt+IL-17+ neutrophils play a critical role in hepatic ischemia-reperfusion injury. J Mol Cell Biol. 2013;5:143–6. doi:10.1093/jmcb/mjs065.

164. Mehta P, Nuotio-Antar AM, Smith CW. γδ T cells promote inflammation and insulin resistance during high fat diet-induced obesity in mice. J Leukoc Biol. 2015;97:121–34. doi:10.1189/jlb.3A0414-211RR.

165. Kumar S, Duan Q, Wu R, Harris EN, Su Q. Pathophysiological communication between hepatocytes and non-parenchymal cells in liver injury from NAFLD to liver fibrosis. Adv Drug Deliv Rev. 2021;176:113869. doi:10.1016/j.addr.2021.113869.

166. Morgan MJ, Liu Z. Reactive oxygen species in TNFalpha-induced signaling and cell death. Mol Cells. 2010;30:1–12. doi:10.1007/s10059-010-0105-0.

167. Whiteside TL. NK cells in the tumor microenvironment and thioredoxin activity. J Clin Invest. 2020;130:5115–7. doi:10.1172/JCI141460.

168. Barron L, Wynn TA. Fibrosis is regulated by Th2 and Th17 responses and by dynamic interactions between fibroblasts and macrophages. Am J Physiol Gastrointest Liver Physiol. 2011;300:G723-8. doi:10.1152/ajpgi.00414.2010.

169. Oo YH, Adams DH. Regulatory T cells and autoimmune hepatitis: what happens in the liver stays in the liver. J Hepatol. 2014;61:973–5. doi:10.1016/j.jhep.2014.08.005.

170. Taylor SA, Assis DN, Mack CL. The Contribution of B Cells in Autoimmune Liver Diseases. Semin Liver Dis. 2019;39:422–31. doi:10.1055/s-0039-1688751.

171. Xiao F, Ai G, Yan W, Wan X, Luo X, Ning Q. Intrahepatic recruitment of cytotoxic NK cells contributes to autoimmune hepatitis progression. Cell Immunol. 2018;327:13–20. doi:10.1016/j.cellimm.2017.12.008.

172. Jeffery HC, Braitch MK, Bagnall C, Hodson J, Jeffery LE, Wawman RE, et al. Changes in natural killer cells and exhausted memory regulatory T Cells with corticosteroid therapy in acute autoimmune hepatitis. Hepatol Commun. 2018;2:421–36. doi:10.1002/hep4.1163.

173. Guan J, Wang G, Yang Q, Chen C, Deng J, Gu X, Zhu H. Natural Killer T Cells in Various Mouse Models of Hepatitis. Biomed Res Int. 2021;2021:1782765. doi:10.1155/2021/1782765.

174. Biburger M, Tiegs G. Activation-induced NKT cell hyporesponsiveness protects from alpha-galactosylceramide hepatitis and is independent of active transregulatory factors. J Leukoc Biol. 2008;84:264–79. doi:10.1189/jlb.0607352.

175. Wang H, Feng D, Park O, Yin S, Gao B. Invariant NKT cell activation induces neutrophil accumulation and hepatitis: opposite regulation by IL-4 and IFN-γ. Hepatology. 2013;58:1474–85. doi:10.1002/hep.26471.

176. Santodomingo-Garzon T, Swain MG. Role of NKT cells in autoimmune liver disease. Autoimmun Rev. 2011;10:793–800. doi:10.1016/j.autrev.2011.06.003.

177. Böttcher K, Rombouts K, Saffioti F, Roccarina D, Rosselli M, Hall A, et al. MAIT cells are chronically activated in patients with autoimmune liver disease and promote profibrogenic hepatic stellate cell activation. Hepatology. 2018;68:172–86. doi:10.1002/hep.29782.

178. Ferri S, Longhi MS, Molo C de, Lalanne C, Muratori P, Granito A, et al. A multifaceted imbalance of T cells with regulatory function characterizes type 1 autoimmune hepatitis. Hepatology. 2010;52:999–1007. doi:10.1002/hep.23792.

179. He Q, Lu Y, Tian W, Jiang R, Yu W, Liu Y, et al. TOX deficiency facilitates the differentiation of IL-17A-producing γδ T cells to drive autoimmune hepatitis. Cell Mol Immunol. 2022;19:1102–16. doi:10.1038/s41423-022-00912-y.

180. Panasiuk A, Prokopowicz D, Zak J, Panasiuk B, Wysocka J. Lymphocyte subpopulations in peripheral blood in primary sclerosing cholangitis. Hepatogastroenterology. 2004;51:1289–91.

181. Chang C-H, Chen Y-C, Yu Y-H, Tao M-H, Leung PSC, Ansari AA, et al. Innate immunity drives xenobiotic-induced murine autoimmune cholangitis. Clin Exp Immunol. 2014;177:373–80. doi:10.1111/cei.12298.

182. Liu H, Man K. New Insights in Mechanisms and Therapeutics for Short- and Long-Term Impacts of Hepatic Ischemia Reperfusion Injury Post Liver Transplantation. Int J Mol Sci 2021. doi:10.3390/ijms22158210.

183. Lu L, Zhou H, Ni M, Wang X, Busuttil R, Kupiec-Weglinski J, Zhai Y. Innate Immune Regulations and Liver Ischemia-Reperfusion Injury. Transplantation. 2016;100:2601–10. doi:10.1097/TP.0000000000001411.

184. Ito T, Naini BV, Markovic D, Aziz A, Younan S, Lu M, et al. Ischemia-reperfusion injury and its relationship with early allograft dysfunction in liver transplant patients. Am J Transplant. 2021;21:614–25. doi:10.1111/ajt.16219.

185. Zhai Y, Petrowsky H, Hong JC, Busuttil RW, Kupiec-Weglinski JW. Ischaemia-reperfusion injury in liver transplantation--from bench to bedside. Nat Rev Gastroenterol Hepatol. 2013;10:79–89. doi:10.1038/nrgastro.2012.225.

186. Francis Robertson, Victoria Male, Graham Wright, Barry Fuller, Brian Davidson. Recruitment of inflammatory monocytes after liver transplantation and correlation with clinical outcome. The Lancet. 2017;389:S84. doi:10.1016/S0140-6736(17)30480-4.

187. Kim H-Y, Kim S-J, Lee S-M. Activation of NLRP3 and AIM2 inflammasomes in Kupffer cells in hepatic ischemia/reperfusion. FEBS J. 2015;282:259–70. doi:10.1111/febs.13123.

188. Wu T, Zhang C, Shao T, Chen J, Chen D. The Role of NLRP3 Inflammasome Activation Pathway of Hepatic Macrophages in Liver Ischemia-Reperfusion Injury. Front Immunol. 2022;13:905423. doi:10.3389/fimmu.2022.905423.

189. Tsutsui H, Matsui K, Kawada N, Hyodo Y, Hayashi N, Okamura H, et al. IL-18 accounts for both TNF-alpha- and Fas ligand-mediated hepatotoxic pathways in endotoxin-induced liver injury in mice. J Immunol. 1997;159:3961–7.

190. Okamura H, Kashiwamura S, Tsutsui H, Yoshimoto T, Nakanishi K. Regulation of interferon-gamma production by IL-12 and IL-18. Curr Opin Immunol. 1998;10:259–64. doi:10.1016/s0952-7915(98)80163-5.

191. Beldi G, Banz Y, Kroemer A, Sun X, Wu Y, Graubardt N, et al. Deletion of CD39 on natural killer cells attenuates hepatic ischemia/reperfusion injury in mice. Hepatology. 2010;51:1702–11. doi:10.1002/hep.23510.

192. Linares I, Hamar M, Selzner N, Selzner M. Steatosis in Liver Transplantation: Current Limitations and Future Strategies. Transplantation. 2019;103:78–90. doi:10.1097/TP.0000000000002466.

193. Eggenhofer E, Groell A, Junger H, Kasi A, Kroemer A, Geissler EK, et al. Steatotic Livers Are More Susceptible to Ischemia Reperfusion Damage after Transplantation and Show Increased γδ T Cell Infiltration. Int J Mol Sci 2021. doi:10.3390/ijms22042036.

194. Shimamura K, Kawamura H, Nagura T, Kato T, Naito T, Kameyama H, et al. Association of NKT cells and granulocytes with liver injury after reperfusion of the portal vein. Cell Immunol. 2005;234:31–8. doi:10.1016/j.cellimm.2005.04.022.

195. Lappas CM, Day Y-J, Marshall MA, Engelhard VH, Linden J. Adenosine A2A receptor activation reduces hepatic ischemia reperfusion injury by inhibiting CD1d-

dependent NKT cell activation. J Exp Med. 2006;203:2639–48. doi:10.1084/jem.20061097.

196. Kuboki S, Sakai N, Tschöp J, Edwards MJ, Lentsch AB, Caldwell CC. Distinct contributions of CD4+ T cell subsets in hepatic ischemia/reperfusion injury. Am J Physiol Gastrointest Liver Physiol. 2009;296:G1054-9. doi:10.1152/ajpgi.90464.2008.

197. Nakajima S, Tanaka R, Yamashiro K, Chiba A, Noto D, Inaba T, et al. Mucosal-Associated Invariant T Cells Are Involved in Acute Ischemic Stroke by Regulating Neuroinflammation. J Am Heart Assoc. 2021;10:e018803. doi:10.1161/JAHA.120.018803.

198. Llewellyn HP, Arat S, Gao J, Wen J, Xia S, Kalabat D, et al. T cells and monocyte-derived myeloid cells mediate immunotherapy-related hepatitis in a mouse model. J Hepatol. 2021;75:1083–95. doi:10.1016/j.jhep.2021.06.037.

199. Sansom DM. CD28, CTLA-4 and their ligands: who does what and to whom? Immunology. 2000;101:169–77. doi:10.1046/j.1365-2567.2000.00121.x.

200. Triantafyllou E, Gudd CL, Mawhin M-A, Husbyn HC, Trovato FM, Siggins MK, et al. PD-1 blockade improves Kupffer cell bacterial clearance in acute liver injury. J Clin Invest 2021. doi:10.1172/JCI140196.

201. Hakanen H, Hernberg M, Mäkelä S, Yadav B, Brück O, Juteau S, et al. Anti-PD1 therapy increases peripheral blood NKT cells and chemokines in metastatic melanoma patients. Annals of Oncology. 2018;29:x3. doi:10.1093/annonc/mdy493.007.

202. Jarvis E-M, Collings S, Authier-Hall A, Dasyam N, Luey B, Nacey J, et al. Mucosal-Associated Invariant T (MAIT) Cell Dysfunction and PD-1 Expression in Prostate Cancer: Implications for Immunotherapy. Front Immunol. 2021;12:748741. doi:10.3389/fimmu.2021.748741.

203. Tomogane M, Sano Y, Shimizu D, Shimizu T, Miyashita M, Toda Y, et al. Human Vγ9Vδ2 T cells exert anti-tumor activity independently of PD-L1 expression in tumor cells. Biochem Biophys Res Commun. 2021;573:132–9. doi:10.1016/j.bbrc.2021.08.005.

204. Gubin MM, Esaulova E, Ward JP, Malkova ON, Runci D, Wong P, et al. High-Dimensional Analysis Delineates Myeloid and Lymphoid Compartment Remodeling during Successful Immune-Checkpoint Cancer Therapy. Cell. 2018;175:1014-1030.e19. doi:10.1016/j.cell.2018.09.030.

205. Jovanovic M, Gajovic N, Jurisevic M, Sekulic S, Arsenijevic N, Jocic M, et al. Anti-PD-1 therapy activates tumoricidic properties of NKT cells and contributes to the

overall deceleration of tumor progression in a model of murine mammary carcinoma. VSP. 2022;79:764–73. doi:10.2298/VSP210126039J.

206. Nallagangula KS, Nagaraj SK, Venkataswamy L, Chandrappa M. Liver fibrosis: a compilation on the biomarkers status and their significance during disease progression. Future Sci OA. 2018;4:FSO250. doi:10.4155/fsoa-2017-0083.

207. Glehr G, Riquelme P, Yang Zhou J, Cordero L, Schilling H-L, Kapinsky M, et al. External validation of biomarkers for immune-related adverse events after immune checkpoint inhibition. Front Immunol. 2022;13:1011040. doi:10.3389/fimmu.2022.1011040.

208. Vogel A, Meyer T, Sapisochin G, Salem R, Saborowski A. Hepatocellular carcinoma. Lancet. 2022;400:1345–62. doi:10.1016/S0140-6736(22)01200-4.

209. Haber PK, Puigvehí M, Castet F, Lourdusamy V, Montal R, Tabrizian P, et al. Evidence-Based Management of Hepatocellular Carcinoma: Systematic Review and Meta-analysis of Randomized Controlled Trials (2002-2020). Gastroenterology. 2021;161:879–98. doi:10.1053/j.gastro.2021.06.008.

210. El-Khoueiry AB, Sangro B, Yau T, Crocenzi TS, Kudo M, Hsu C, et al. Nivolumab in patients with advanced hepatocellular carcinoma (CheckMate 040): an open-label, non-comparative, phase 1/2 dose escalation and expansion trial. Lancet. 2017;389:2492–502. doi:10.1016/S0140-6736(17)31046-2.

211. Kudo M, Matilla A, Santoro A, Melero I, Gracián AC, Acosta-Rivera M, et al. CheckMate 040 cohort 5: A phase I/II study of nivolumab in patients with advanced hepatocellular carcinoma and Child-Pugh B cirrhosis. J Hepatol. 2021;75:600–9. doi:10.1016/j.jhep.2021.04.047.

212. Finn RS, Ryoo B-Y, Merle P, Kudo M, Bouattour M, Lim HY, et al. Pembrolizumab As Second-Line Therapy in Patients With Advanced Hepatocellular Carcinoma in KEYNOTE-240: A Randomized, Double-Blind, Phase III Trial. J Clin Oncol. 2020;38:193–202. doi:10.1200/JCO.19.01307.

213. Verset G, Borbath I, Karwal M, Verslype C, van Vlierberghe H, Kardosh A, et al. Pembrolizumab Monotherapy for Previously Untreated Advanced Hepatocellular Carcinoma: Data from the Open-Label, Phase II KEYNOTE-224 Trial. Clin Cancer Res. 2022;28:2547–54. doi:10.1158/1078-0432.CCR-21-3807.

214. Roy A. Updated Efficacy and Safety Data from IMbrave150: Atezolizumab Plus Bevacizumab vs. Sorafenib for Unresectable Hepatocellular Carcinoma. J Clin Exp Hepatol. 2022;12:1575–6. doi:10.1016/j.jceh.2022.07.003.

215. Lee C-K, Chan SL, Chon HJ. Could We Predict the Response of Immune Checkpoint Inhibitor Treatment in Hepatocellular Carcinoma? Cancers (Basel) 2022. doi:10.3390/cancers14133213.

216. Pallozzi M, Di Tommaso N, Maccauro V, Santopaolo F, Gasbarrini A, Ponziani FR, Pompili M. Non-Invasive Biomarkers for Immunotherapy in Patients with Hepatocellular Carcinoma: Current Knowledge and Future Perspectives. Cancers (Basel) 2022. doi:10.3390/cancers14194631.

217. Hutchinson JA, Kronenberg K, Riquelme P, Wenzel JJ, Glehr G, Schilling H-L, et al. Virus-specific memory T cell responses unmasked by immune checkpoint blockade cause hepatitis. Nat Commun. 2021;12:1439. doi:10.1038/s41467-021-21572-y.

218. Yin C, Baba T, He AR, Smith C. Immune checkpoint inhibitors in liver transplant recipients - a review of current literature. HR 2021. doi:10.20517/2394-5079.2021.11.

219. Vogel A, Sterneck M, Vondran F, Waidmann O, Klein I, Lindig U, et al. The use of immuno-oncologic therapy in hepatocellular carcinoma in the context of liver transplantation. An interdisciplinary benefit/risk assessment. [Der Einsatz der immunonkologischen Therapie beim hepatozellulären Karzinom im Kontext der Lebertransplantation Eine interdisziplinäre Risiko-Nutzen-Abwägung]. Z Gastroenterol. 2022;60:184–91. doi:10.1055/a-1649-8643.

220. Gaucher L, Adda L, Séjourné A, Joachim C, Chaby G, Poulet C, et al. Impact of the corticosteroid indication and administration route on overall survival and the tumor response after immune checkpoint inhibitor initiation. Ther Adv Med Oncol. 2021;13:1758835921996656. doi:10.1177/1758835921996656.

221. Gao Q, Wang X-Y, Qiu S-J, Yamato I, Sho M, Nakajima Y, et al. Overexpression of PD-L1 significantly associates with tumor aggressiveness and postoperative recurrence in human hepatocellular carcinoma. Clin Cancer Res. 2009;15:971–9. doi:10.1158/1078-0432.CCR-08-1608.

222. Zhu AX, Guan Y, Abbas AR, Koeppen H, Lu S, Hsu C-H, et al. Abstract CT044: Genomic correlates of clinical benefits from atezolizumab combined with bevacizumab vs. atezolizumab alone in patients with advanced hepatocellular carcinoma (HCC). Cancer Res. 2020;80:CT044-CT044. doi:10.1158/1538-7445.AM2020-CT044.

223. Miller ML, Daniels MD, Wang T, Wang Y, Xu J, Yin D, et al. Tracking of TCR-Transgenic T Cells Reveals That Multiple Mechanisms Maintain Cardiac Transplant Tolerance in Mice. Am J Transplant. 2016;16:2854–64. doi:10.1111/ajt.13814.

224. Hai Nam N, Taura K, Koyama Y, Nishio T, Yamamoto G, Uemoto Y, et al. Increased Expressions of Programmed Death Ligand 1 and Galectin 9 in Transplant Recipients Who Achieved Tolerance After Immunosuppression Withdrawal. Liver Transpl. 2022;28:647–58. doi:10.1002/lt.26336.

225. Munker S, Toni EN de. Use of checkpoint inhibitors in liver transplant recipients. United European Gastroenterol J. 2018;6:970–3. doi:10.1177/2050640618774631.

226. Shi X-L, Mancham S, Hansen BE, Knegt RJ de, Jonge J de, van der Laan, Luc J W, et al. Counter-regulation of rejection activity against human liver grafts by donor PD-L1 and recipient PD-1 interaction. J Hepatol. 2016;64:1274–82. doi:10.1016/j.jhep.2016.02.034.

227. D'Alessio A, Rimassa L, Cortellini A, Pinato DJ. PD-1 Blockade for Hepatocellular Carcinoma: Current Research and Future Prospects. J Hepatocell Carcinoma. 2021;8:887–97. doi:10.2147/JHC.S284440.

228. Myojin Y, Kodama T, Sakamori R, Maesaka K, Matsumae T, Sawai Y, et al. Interleukin-6 Is a Circulating Prognostic Biomarker for Hepatocellular Carcinoma Patients Treated with Combined Immunotherapy. Cancers (Basel) 2022. doi:10.3390/cancers14040883.

229. Zhu AX, Dayyani F, Yen C-J, Ren Z, Bai Y, Meng Z, et al. Alpha-Fetoprotein as a Potential Surrogate Biomarker for Atezolizumab + Bevacizumab Treatment of Hepatocellular Carcinoma. Clin Cancer Res. 2022;28:3537–45. doi:10.1158/1078-0432.CCR-21-3275.

230. Hatanaka T, Kakizaki S, Hiraoka A, Tada T, Hirooka M, Kariyama K, et al. Prognostic impact of C-reactive protein and alpha-fetoprotein in immunotherapy score in hepatocellular carcinoma patients treated with atezolizumab plus bevacizumab: a multicenter retrospective study. Hepatol Int. 2022;16:1150–60. doi:10.1007/s12072-022-10358-z.

231. Scheiner B, Pomej K, Kirstein MM, Hucke F, Finkelmeier F, Waidmann O, et al. Prognosis of patients with hepatocellular carcinoma treated with immunotherapy - development and validation of the CRAFITY score. J Hepatol. 2022;76:353–63. doi:10.1016/j.jhep.2021.09.035.

232. Mrzljak A, Vilibic-Cavlek T. Torque teno virus in liver diseases and after liver transplantation. World J Transplant. 2020;10:291–6. doi:10.5500/wjt.v10.i11.291.

233. Minguela A, García-Alonso AM, Marín L, Torio A, Sánchez-Bueno F, Bermejo J, et al. Evidence of CD28 upregulation in peripheral T cells before liver transplant acute rejection. Transplant Proc. 1997;29:499–500. doi:10.1016/s0041-1345(96)00226-6.

234. Kronenberg K, Riquelme P, Hutchinson JA. Standard protocols for immune profiling of peripheral blood leucocyte subsets by flow cytometry using DuraClone IM reagents; 2021.

235. Abou-Alfa GK, Lau G, Kudo M, Chan SL, Kelley RK, Furuse J, et al. Tremelimumab plus Durvalumab in Unresectable Hepatocellular Carcinoma. NEJM Evidence 2022. doi:10.1056/EVIDoa2100070.

236. Wu C-J, Lee P-C, Hung Y-W, Lee C-J, Chi C-T, Lee I-C, et al. Lenvatinib plus pembrolizumab for systemic therapy-naïve and -experienced unresectable hepatocellular carcinoma. Cancer Immunol Immunother. 2022;71:2631–43. doi:10.1007/s00262-022-03185-6.

237. Finn RS, Kudo M, Merle P, Meyer T, Qin S, Ikeda M, et al. LBA34 Primary results from the phase III LEAP-002 study: Lenvatinib plus pembrolizumab versus lenvatinib as first-line (1L) therapy for advanced hepatocellular carcinoma (aHCC). Annals of Oncology. 2022;33:S1401. doi:10.1016/j.annonc.2022.08.031.

238. Linares I, Hamar M, Selzner N, Selzner M. Steatosis in Liver Transplantation: Current Limitations and Future Strategies. Transplantation. 2019;103:78–90. doi:10.1097/TP.0000000000002466.

239. McCormack L, Petrowsky H, Jochum W, Mullhaupt B, Weber M, Clavien P-A. Use of severely steatotic grafts in liver transplantation: a matched case-control study. Annals of Surgery. 2007;246:940-6; discussion 946-8. doi:10.1097/SLA.0b013e31815c2a3f.

240. Jackson KR, Long J, Philosophe B, Garonzik-Wang J. Liver Transplantation Using Steatotic Grafts. Clin Liver Dis (Hoboken). 2019;14:191–5. doi:10.1002/cld.847.

241. Savage AK, Constantinides MG, Han J, Picard D, Martin E, Li B, et al. The transcription factor PLZF directs the effector program of the NKT cell lineage. Immunity. 2008;29:391–403. doi:10.1016/j.immuni.2008.07.011.

242. Chaudhry MS, Karadimitris A. Role and regulation of CD1d in normal and pathological B cells. The Journal of Immunology. 2014;193:4761–8. doi:10.4049/jimmunol.1401805.

243. Dhodapkar MV, Kumar V. Type II NKT Cells and Their Emerging Role in Health and Disease. The Journal of Immunology. 2017;198:1015–21. doi:10.4049/jimmunol.1601399.

244. Bai L, Picard D, Anderson B, Chaudhary V, Luoma A, Jabri B, et al. The majority of CD1d-sulfatide-specific T cells in human blood use a semiinvariant Vδ1 TCR. Eur J Immunol. 2012;42:2505–10. doi:10.1002/eji.201242531.

245. Singh AK, Rhost S, Löfbom L, Cardell SL. Defining a novel subset of CD1d-dependent type II natural killer T cells using natural killer cell-associated markers. Scand J Immunol. 2019;90:e12794. doi:10.1111/sji.12794.

246. Singh AK, Tripathi P, Cardell SL. Type II NKT Cells: An Elusive Population With Immunoregulatory Properties. Front Immunol. 2018;9:1969. doi:10.3389/fimmu.2018.01969.

247. Kuylenstierna C, Björkström NK, Andersson SK, Sahlström P, Bosnjak L, Paquin-Proulx D, et al. NKG2D performs two functions in invariant NKT cells: direct TCR-independent activation of NK-like cytolysis and co-stimulation of activation by CD1d. Eur J Immunol. 2011;41:1913–23. doi:10.1002/eji.200940278.

248. Cossarizza A, Chang H-D, Radbruch A, Acs A, Adam D, Adam-Klages S, et al. Guidelines for the use of flow cytometry and cell sorting in immunological studies (second edition). Eur J Immunol. 2019;49:1457–973. doi:10.1002/eji.201970107.

249. Nair S, Boddupalli CS, Verma R, Liu J, Yang R, Pastores GM, et al. Type II NKT-TFH cells against Gaucher lipids regulate B-cell immunity and inflammation. Blood. 2015;125:1256–71. doi:10.1182/blood-2014-09-600270.

250. Yang Zhou J. Innate immunity and early liver inflammation. Front. Immunol. 2023. doi:10.3389/fimmu.2023.1175147.

251. Montoya CJ, Pollard D, Martinson J, Kumari K, Wasserfall C, Mulder CB, et al. Characterization of human invariant natural killer T subsets in health and disease using a novel invariant natural killer T cell-clonotypic monoclonal antibody, 6B11. Immunology. 2007;122:1–14. doi:10.1111/j.1365-2567.2007.02647.x.

252. Slauenwhite D, Johnston B. Regulation of NKT Cell Localization in Homeostasis and Infection. Front Immunol. 2015;6:255. doi:10.3389/fimmu.2015.00255.

253. Diao H, Kon S, Iwabuchi K, Kimura C, Morimoto J, Ito D, et al. Osteopontin as a mediator of NKT cell function in T cell-mediated liver diseases. Immunity. 2004;21:539–50. doi:10.1016/j.immuni.2004.08.012.

254. Liu Y, Hao H, Hou T. Concanavalin A-induced autoimmune hepatitis model in mice: Mechanisms and future outlook. Open Life Sci. 2022;17:91–101. doi:10.1515/biol-2022-0013.

255. Biburger M, Tiegs G. Alpha-galactosylceramide-induced liver injury in mice is mediated by TNF-alpha but independent of Kupffer cells. J Immunol. 2005;175:1540–50. doi:10.4049/jimmunol.175.3.1540.

256. Arai F, Hirao A, Ohmura M, Sato H, Matsuoka S, Takubo K, et al. Tie2/angiopoietin-1 signaling regulates hematopoietic stem cell quiescence in the bone marrow niche. Cell. 2004;118:149–61. doi:10.1016/j.cell.2004.07.004.

257. Lefere S, van de Velde F, Hoorens A, Raevens S, van Campenhout S, Vandierendonck A, et al. Angiopoietin-2 Promotes Pathological Angiogenesis and Is a Therapeutic Target in Murine Nonalcoholic Fatty Liver Disease. Hepatology. 2019;69:1087–104. doi:10.1002/hep.30294.

258. Atanasov G, Pötner C, Aust G, Schierle K, Dietel C, Benzing C, et al. TIE2-expressing monocytes and M2-polarized macrophages impact survival and correlate with angiogenesis in adenocarcinoma of the pancreas. Oncotarget. 2018;9:29715–26. doi:10.18632/oncotarget.25690.

259. Ni Choileain S, Astier AL. CD46 processing: a means of expression. Immunobiology. 2012;217:169–75. doi:10.1016/j.imbio.2011.06.003.

260. Geller A, Yan J. The Role of Membrane Bound Complement Regulatory Proteins in Tumor Development and Cancer Immunotherapy. Front Immunol. 2019;10:1074. doi:10.3389/fimmu.2019.01074.

261. Arbore G, West EE, Rahman J, Le Friec G, Niyonzima N, Pirooznia M, et al. Complement receptor CD46 co-stimulates optimal human CD8+ T cell effector function via fatty acid metabolism. Nat Commun. 2018;9:4186. doi:10.1038/s41467-018-06706-z.

262. Sánchez A, Feito MJ, Rojo JM. CD46-mediated costimulation induces a Th1-biased response and enhances early TCR/CD3 signaling in human CD4+ T lymphocytes. Eur J Immunol. 2004;34:2439–48. doi:10.1002/eji.200324259.

263. Hansen AS, Slater J, Biltoft M, Bundgaard BB, Møller BK, Höllsberg P. CD46 is a potent co-stimulatory receptor for expansion of human IFN-γ-producing CD8+ T cells. Immunol Lett. 2018;200:26–32. doi:10.1016/j.imlet.2018.06.003.

264. Gaggar A, Shayakhmetov DM, Lieber A. CD46 is a cellular receptor for group B adenoviruses. Nature Medicine. 2003;9:1408–12. doi:10.1038/nm952.

265. Dörig RE, Marcil A, Chopra A, Richardson CD. The human CD46 molecule is a receptor for measles virus (Edmonston strain). Cell. 1993;75:295–305. doi:10.1016/0092-8674(93)80071-l.

266. Santoro F, Kennedy PE, Locatelli G, Malnati MS, Berger EA, Lusso P. CD46 is a cellular receptor for human herpesvirus 6. Cell. 1999;99:817–27. doi:10.1016/s0092-8674(00)81678-5.

267. Astier AL, Meiffren G, Freeman S, Hafler DA. Alterations in CD46-mediated Tr1 regulatory T cells in patients with multiple sclerosis. J Clin Invest. 2006;116:3252–7. doi:10.1172/JCI29251.

268. Xu Y-Q, Gao Y-D, Yang J, Guo W. A defect of CD4+CD25+ regulatory T cells in inducing interleukin-10 production from CD4+ T cells under CD46 costimulation in asthma patients. J Asthma. 2010;47:367–73. doi:10.3109/02770903.2010.481340.

269. Cardone J, Le Friec G, Vantourout P, Roberts A, Fuchs A, Jackson I, et al. Complement regulator CD46 temporally regulates cytokine production by

conventional and unconventional T cells. Nat Immunol. 2010;11:862–71. doi:10.1038/ni.1917.

270. Qiao P, Dang E, Cao T, Fang H, Zhang J, Qiao H, Wang G. Dysregulation of mCD46 and sCD46 contribute to the pathogenesis of bullous pemphigoid. Sci Rep. 2017;7:145. doi:10.1038/s41598-017-00235-3.

271. Hakulinen J, Junnikkala S, Sorsa T, Meri S. Complement inhibitor membrane cofactor protein (MCP; CD46) is constitutively shed from cancer cell membranes in vesicles and converted by a metalloproteinase to a functionally active soluble form. Eur J Immunol. 2004;34:2620–9. doi:10.1002/eji.200424969.

272. Kawano M, Seya T, Koni I, Mabuchi H. Elevated serum levels of soluble membrane cofactor protein (CD46, MCP) in patients with systemic lupus erythematosus (SLE). Clin Exp Immunol. 1999;116:542–6. doi:10.1046/j.1365-2249.1999.00917.x.

273. Langmead B, Salzberg SL. Fast gapped-read alignment with Bowtie 2. Nat Methods. 2012;9:357–9. doi:10.1038/nmeth.1923.

274. Love MI, Soneson C, Patro R. Swimming downstream: statistical analysis of differential transcript usage following Salmon quantification. F1000Res. 2018;7:952. doi:10.12688/f1000research.15398.3.

275. Robinson MD, McCarthy DJ, Smyth GK. edgeR: a Bioconductor package for differential expression analysis of digital gene expression data. Bioinformatics. 2010;26:139–40. doi:10.1093/bioinformatics/btp616.

276. Love MI, Huber W, Anders S. Moderated estimation of fold change and dispersion for RNA-seq data with DESeq2. Genome Biol. 2014;15:550. doi:10.1186/s13059-014-0550-8.

277. Armbruster DA, Pry T. Limit of blank, limit of detection and limit of quantitation. Clin Biochem Rev. 2008;29 Suppl 1:S49-52.

278. Hegazy Y, Turner M, Fettig D. S2674 A Subtle Case of Doxorubicin-induced Hepatotoxicity. Am J Gastroenterol. 2021;116:S1121-S1121. doi:10.14309/01.ajg.0000784228.17250.65.

279. Chen M, Suzuki A, Thakkar S, Yu K, Hu C, Tong W. DILIrank: the largest reference drug list ranked by the risk for developing drug-induced liver injury in humans. Drug Discov Today. 2016;21:648–53. doi:10.1016/j.drudis.2016.02.015.

280. Robert S, Gicquel T, Victoni T, Valença S, Barreto E, Bailly-Maître B, et al. Involvement of matrix metalloproteinases (MMPs) and inflammasome pathway in molecular mechanisms of fibrosis. Biosci Rep 2016. doi:10.1042/BSR20160107.

281. Manicone AM, McGuire JK. Matrix metalloproteinases as modulators of inflammation. Semin Cell Dev Biol. 2008;19:34–41. doi:10.1016/j.semcdb.2007.07.003.

282. Zhong D, Cai J, Hu C, Chen J, Zhang R, Fan C, et al. Inhibition of mPGES-2 ameliorates NASH by activating NR1D1 via heme. Hepatology 2022. doi:10.1002/hep.32671.

283. Markovič T, Jakopin Ž, Dolenc MS, Mlinarič-Raščan I. Structural features of subtype-selective EP receptor modulators. Drug Discov Today. 2017;22:57–71. doi:10.1016/j.drudis.2016.08.003.

284. Woreta TA, Alqahtani SA. Evaluation of abnormal liver tests. Med Clin North Am. 2014;98:1–16. doi:10.1016/j.mcna.2013.09.005.

285. Giannini EG, Testa R, Savarino V. Liver enzyme alteration: a guide for clinicians. CMAJ. 2005;172:367–79. doi:10.1503/cmaj.1040752.

286. Pettersson J, Hindorf U, Persson P, Bengtsson T, Malmqvist U, Werkström V, Ekelund M. Muscular exercise can cause highly pathological liver function tests in healthy men. Br J Clin Pharmacol. 2008;65:253–9. doi:10.1111/j.1365-2125.2007.03001.x.

287. Volochayev R, Csako G, Wesley R, Rider LG, Miller FW. Laboratory Test Abnormalities are Common in Polymyositis and Dermatomyositis and Differ Among Clinical and Demographic Groups. Open Rheumatol J. 2012;6:54–63. doi:10.2174/1874312901206010054.

288. Xu H, Yu X, Hu J. The Risk Assessment and Clinical Research of Bile Duct Injury After Transcatheter Arterial Chemoembolization for Hepatocellular Carcinoma. Cancer Manag Res. 2021;13:5039–52. doi:10.2147/CMAR.S303172.

289. Yang X, Schnackenberg LK, Shi Q, Salminen WF. Chapter 13 - Hepatic toxicity biomarkers. In: Gupta RC, editor. Biomarkers in Toxicology. Boston: Academic Press; 2014. p. 241–259. doi:10.1016/B978-0-12-404630-6.00013-0.

290. BHATTARAI T, BHATTACHARYA K, CHAUDHURI P, SENGUPTA P. Correlation of common biochemical markers for bone turnover, serum calcium, and alkaline phosphatase in post-menopausal women. Malays J Med Sci. 2014;21:58–61.

291. Méndez-Sánchez N, Vítek L, Aguilar-Olivos NE, Uribe M. Bilirubin as a Biomarker in Liver Disease. In: Preedy VR, editor. Biomarkers in Liver Disease. Dordrecht: Springer Netherlands; 2016. p. 1–25. doi:10.1007/978-94-007-7742-2_25-1.

292. Fevery J. Bilirubin in clinical practice: a review. Liver Int. 2008;28:592–605. doi:10.1111/j.1478-3231.2008.01716.x.

293. Guerra Ruiz AR, Crespo J, López Martínez RM, Iruzubieta P, Casals Mercadal G, Lalana Garcés M, et al. Measurement and clinical usefulness of bilirubin in liver disease. Advances in Laboratory Medicine / Avances en Medicina de Laboratorio. 2021;2:352–61. doi:10.1515/almed-2021-0047.

294. Cho Y-H, Lee Y, Choi J in, Lee SR, Lee SY. Chapter Three - Biomarkers in metabolic syndrome. In: Makowski GS, editor. Advances in Clinical Chemistry: Elsevier; 2022. p. 101–156. doi:10.1016/bs.acc.2022.07.003.

295. Hanigan MH. Gamma-glutamyl transpeptidase: redox regulation and drug resistance. Adv Cancer Res. 2014;122:103–41. doi:10.1016/B978-0-12-420117-0.00003-7.

296. Koenig G, Seneff S. Gamma-Glutamyltransferase: A Predictive Biomarker of Cellular Antioxidant Inadequacy and Disease Risk. Dis Markers. 2015;2015:818570. doi:10.1155/2015/818570.

297. Whitfield JB, Pounder RE, Neale G, Moss DW. Serum -glytamyl transpeptidase activity in liver disease. Gut. 1972;13:702–8. doi:10.1136/gut.13.9.702.

298. Donnan PT, McLernon D, Dillon JF, Ryder S, Roderick P, Sullivan F, Rosenberg W. Development of a decision support tool for primary care management of patients with abnormal liver function tests without clinically apparent liver disease: a record-linkage population cohort study and decision analysis (ALFIE). Health Technol Assess. 2009;13:iii-iv, ix-xi, 1-134. doi:10.3310/hta13250.

299. Alkozai EM, Lisman T, Porte RJ, Nijsten MW. Early elevated serum gamma glutamyl transpeptidase after liver transplantation is associated with better survival. F1000Res. 2014;3:85. doi:10.12688/f1000research.3316.1.

300. Bosch J, Berzigotti A, Garcia-Pagan JC, Abraldes JG. The management of portal hypertension: rational basis, available treatments and future options. J Hepatol. 2008;48 Suppl 1:S68-92. doi:10.1016/j.jhep.2008.01.021.

301. Younossi ZM, Koenig AB, Abdelatif D, Fazel Y, Henry L, Wymer M. Global epidemiology of nonalcoholic fatty liver disease-Meta-analytic assessment of prevalence, incidence, and outcomes. Hepatology. 2016;64:73–84. doi:10.1002/hep.28431.

302. Teng ML, Ng CH, Huang DQ, Chan KE, Tan DJ, Lim WH, et al. Global incidence and prevalence of nonalcoholic fatty liver disease. Clin Mol Hepatol. 2023;29:S32-S42. doi:10.3350/cmh.2022.0365.

303. Calzadilla Bertot L, Adams LA. The Natural Course of Non-Alcoholic Fatty Liver Disease. Int J Mol Sci 2016. doi:10.3390/ijms17050774.

304. Pouwels S, Sakran N, Graham Y, Leal A, Pintar T, Yang W, et al. Non-alcoholic fatty liver disease (NAFLD): a review of pathophysiology, clinical management and

effects of weight loss. BMC Endocr Disord. 2022;22:63. doi:10.1186/s12902-022-00980-1.

305. Sharma S, Khalili K, Nguyen GC. Non-invasive diagnosis of advanced fibrosis and cirrhosis. World J Gastroenterol. 2014;20:16820–30. doi:10.3748/wjg.v20.i45.16820.

306. Bell LN, Theodorakis JL, Vuppalanchi R, Saxena R, Bemis KG, Wang M, Chalasani N. Serum proteomics and biomarker discovery across the spectrum of nonalcoholic fatty liver disease. Hepatology. 2010;51:111–20. doi:10.1002/hep.23271.

307. Fedchuk L, Nascimbeni F, Pais R, Charlotte F, Housset C, Ratziu V. Performance and limitations of steatosis biomarkers in patients with nonalcoholic fatty liver disease. Aliment Pharmacol Ther. 2014;40:1209–22. doi:10.1111/apt.12963.

308. Narayanan S, Surette FA, Hahn YS. The Immune Landscape in Nonalcoholic Steatohepatitis. Immune Netw. 2016;16:147–58. doi:10.4110/in.2016.16.3.147.

309. Huby T, Gautier EL. Immune cell-mediated features of non-alcoholic steatohepatitis. Nat Rev Immunol. 2022;22:429–43. doi:10.1038/s41577-021-00639-3.

310. Uldrich AP, Le Nours J, Pellicci DG, Gherardin NA, McPherson KG, Lim RT, et al. CD1d-lipid antigen recognition by the γδ TCR. Nat Immunol. 2013;14:1137–45. doi:10.1038/ni.2713.

311. Wang M, Shen G, Xu L, Liu X, Brown JM, Feng D, et al. IL-1 receptor like 1 protects against alcoholic liver injury by limiting NF-κB activation in hepatic macrophages. J Hepatol. 2018;68:109–17. doi:10.1016/j.jhep.2017.08.023.

312. Chiaramonte MG, Donaldson DD, Cheever AW, Wynn TA. An IL-13 inhibitor blocks the development of hepatic fibrosis during a T-helper type 2-dominated inflammatory response. J Clin Invest. 1999;104:777–85. doi:10.1172/JCI7325.

313. Weng H-L, Liu Y, Chen J-L, Huang T, Xu L-J, Godoy P, et al. The etiology of liver damage imparts cytokines transforming growth factor beta1 or interleukin-13 as driving forces in fibrogenesis. Hepatology. 2009;50:230–43. doi:10.1002/hep.22934.

314. Wynn TA. Cellular and molecular mechanisms of fibrosis. J Pathol. 2008;214:199–210. doi:10.1002/path.2277.

315. Weng S-Y, Wang X, Vijayan S, Tang Y, Kim YO, Padberg K, et al. IL-4 Receptor Alpha Signaling through Macrophages Differentially Regulates Liver Fibrosis Progression and Reversal. EBioMedicine. 2018;29:92–103. doi:10.1016/j.ebiom.2018.01.028.

316. Pan X, Chiwanda Kaminga A, Liu A, Wen SW, Chen J, Luo J. Chemokines in Non-alcoholic Fatty Liver Disease: A Systematic Review and Network Meta-Analysis. Front Immunol. 2020;11:1802. doi:10.3389/fimmu.2020.01802.

317. She S, Ren L, Chen P, Wang M, Chen D, Wang Y, Chen H. Functional Roles of Chemokine Receptor CCR2 and Its Ligands in Liver Disease. Front Immunol. 2022;13:812431. doi:10.3389/fimmu.2022.812431.

318. Zhao Y, Xia J, He H, Liang S, Zhang H, Gan W. Diagnostic performance of novel inflammatory biomarkers based on ratios of laboratory indicators for nonalcoholic fatty liver disease. Front Endocrinol (Lausanne). 2022;13:981196. doi:10.3389/fendo.2022.981196.

319. Yilmaz H, Yalcin KS, Namuslu M, Celik HT, Sozen M, Inan O, et al. Neutrophil-Lymphocyte Ratio (NLR) Could Be Better Predictor than C-reactive Protein (CRP) for Liver Fibrosis in Non-alcoholic Steatohepatitis(NASH). Ann Clin Lab Sci. 2015;45:278–86.

320. Rensen SS, Slaats Y, Driessen A, Peutz-Kootstra CJ, Nijhuis J, Steffensen R, et al. Activation of the complement system in human nonalcoholic fatty liver disease. Hepatology. 2009;50:1809–17. doi:10.1002/hep.23228.

321. Xu C, Chen Y, Xu L, Miao M, Li Y, Yu C. Serum complement C3 levels are associated with nonalcoholic fatty liver disease independently of metabolic features in Chinese population. Sci Rep. 2016;6:23279. doi:10.1038/srep23279.

322. Wlazlo N, van Greevenbroek MMJ, Ferreira I, Jansen EHJM, Feskens EJM, van der Kallen CJH, et al. Activated complement factor 3 is associated with liver fat and liver enzymes: the CODAM study. Eur J Clin Invest. 2013;43:679–88. doi:10.1111/eci.12093.

323. Guo Z, Fan X, Yao J, Tomlinson S, Yuan G, He S. The role of complement in nonalcoholic fatty liver disease. Front Immunol. 2022;13:1017467. doi:10.3389/fimmu.2022.1017467.

324. Gershov D, Kim S, Brot N, Elkon KB. C-Reactive protein binds to apoptotic cells, protects the cells from assembly of the terminal complement components, and sustains an antiinflammatory innate immune response: implications for systemic autoimmunity. J Exp Med. 2000;192:1353–64. doi:10.1084/jem.192.9.1353.

325. Merle NS, Church SE, Fremeaux-Bacchi V, Roumenina LT. Complement System Part I - Molecular Mechanisms of Activation and Regulation. Front Immunol. 2015;6:262. doi:10.3389/fimmu.2015.00262.

326. Hu W, Wang M, Yin C, Li S, Liu Y, Xiao Y. Serum complement factor 5a levels are associated with nonalcoholic fatty liver disease in obese children. Acta Paediatr. 2018;107:322–7. doi:10.1111/apa.14106.

327. Al-Salihi M, Bornikoel A, Zhuang Y, Stachura P, Scheller J, Lang KS, Lang PA. The role of ADAM17 during liver damage. Biol Chem. 2021;402:1115–28. doi:10.1515/hsz-2021-0149.

328. Cardone J, Le Friec G, Kemper C. CD46 in innate and adaptive immunity: an update. Clin Exp Immunol. 2011;164:301–11. doi:10.1111/j.1365-2249.2011.04400.x.

329. Liszewski MK, Kemper C, Price JD, Atkinson JP. Emerging roles and new functions of CD46. Springer Semin Immunopathol. 2005;27:345–58. doi:10.1007/s00281-005-0002-3.

330. Mellinger JL. Epidemiology of Alcohol Use and Alcoholic Liver Disease. Clin Liver Dis (Hoboken). 2019;13:136–9. doi:10.1002/cld.806.

331. Osna NA, Donohue TM, Kharbanda KK. Alcoholic Liver Disease: Pathogenesis and Current Management. Alcohol Res. 2017;38:147–61.

332. Liangpunsakul S, Qi R, Crabb DW, Witzmann F. Relationship between alcohol drinking and aspartate aminotransferase:alanine aminotransferase (AST:ALT) ratio, mean corpuscular volume (MCV), gamma-glutamyl transpeptidase (GGT), and apolipoprotein A1 and B in the U.S. population. J Stud Alcohol Drugs. 2010;71:249–52. doi:10.15288/jsad.2010.71.249.

333. Giorda R, Hagiya M, Seki T, Shimonishi M, Sakai H, Michaelson J, et al. Analysis of the structure and expression of the augmenter of liver regeneration (ALR) gene. Mol Med. 1996;2:97–108.

334. Dayoub R, Wagner H, Bataille F, Stöltzing O, Spruss T, Buechler C, et al. Liver regeneration associated protein (ALR) exhibits antimetastatic potential in hepatocellular carcinoma. Mol Med. 2011;17:221–8. doi:10.2119/molmed.2010.00117.

335. Vodovotz Y, Prelich J, Lagoa C, Barclay D, Zamora R, Murase N, Gandhi CR. Augmenter of liver regeneration (ALR) is a novel biomarker of hepatocellular stress/inflammation: in vitro, in vivo and in silico studies. Mol Med. 2013;18:1421–9. doi:10.2119/molmed.2012.00183.

336. Gandhi CR, Murase N, Starzl TE. Cholera toxin-sensitive GTP-binding protein-coupled activation of augmenter of liver regeneration (ALR) receptor and its function in rat kupffer cells. J Cell Physiol. 2010;222:365–73. doi:10.1002/jcp.21957.

337. Gandhi CR, Chaillet JR, Nalesnik MA, Kumar S, Dangi A, Demetris AJ, et al. Liver-specific deletion of augmenter of liver regeneration accelerates development of steatohepatitis and hepatocellular carcinoma in mice. Gastroenterology. 2015;148:379-391.e4. doi:10.1053/j.gastro.2014.10.008.

338. Tanigawa K, Sakaida I, Masuhara M, Hagiya M, Okita K. Augmenter of liver regeneration (ALR) may promote liver regeneration by reducing natural killer (NK) cell activity in human liver diseases. J Gastroenterol. 2000;35:112–9. doi:10.1007/s005350050023.

339. Jastrzębska I, Zwolak A, Szczyrek M, Wawryniuk A, Skrzydło-Radomańska B, Daniluk J. Biomarkers of alcohol misuse: recent advances and future prospects. Prz Gastroenterol. 2016;11:78–89. doi:10.5114/pg.2016.60252.

340. Grønbaek H, Sandahl TD, Mortensen C, Vilstrup H, Møller HJ, Møller S. Soluble CD163, a marker of Kupffer cell activation, is related to portal hypertension in patients with liver cirrhosis. Aliment Pharmacol Ther. 2012;36:173–80. doi:10.1111/j.1365-2036.2012.05134.x.

341. Etzerodt A, Moestrup SK. CD163 and inflammation: biological, diagnostic, and therapeutic aspects. Antioxid Redox Signal. 2013;18:2352–63. doi:10.1089/ars.2012.4834.

342. Gaïni S, Pedersen SS, Koldkaer OG, Pedersen C, Moestrup SK, Møller HJ. New immunological serum markers in bacteraemia: anti-inflammatory soluble CD163, but not proinflammatory high mobility group-box 1 protein, is related to prognosis. Clin Exp Immunol. 2008;151:423–31. doi:10.1111/j.1365-2249.2007.03586.x.

343. Onofre G, Koláčková M, Jankovičová K, Krejsek J. Scavenger Receptor CD163 and Its Biological Functions. Acta Med. (Hradec Kralove, Czech Repub.). 2009;52:57–61. doi:10.14712/18059694.2016.105.

344. Costa-Hurtado M, Olvera A, Martinez-Moliner V, Galofré-Milà N, Martínez P, Dominguez J, Aragon V. Changes in macrophage phenotype after infection of pigs with Haemophilus parasuis strains with different levels of virulence. Infect Immun. 2013;81:2327–33. doi:10.1128/IAI.00056-13.

345. Møller HJ, Kazankov K, Rødgaard-Hansen S, Nielsen MC, Sandahl TD, Vilstrup H, et al. Soluble CD163 (sCD163): Biomarker of Kupffer Cell Activation in Liver Disease. In: Patel VB, Preedy VR, editors. Biomarkers in liver disease. Dordrecht: Springer; 2017. p. 321–348. doi:10.1007/978-94-007-7675-3_40.

346. Seki E, Schwabe RF. Hepatic inflammation and fibrosis: functional links and key pathways. Hepatology. 2015;61:1066–79. doi:10.1002/hep.27332.

347. Oh Y, Park O, Swierczewska M, Hamilton JP, Park J-S, Kim TH, et al. Systemic PEGylated TRAIL treatment ameliorates liver cirrhosis in rats by eliminating activated hepatic stellate cells. Hepatology. 2016;64:209–23. doi:10.1002/hep.28432.

348. Tomita K, Tamiya G, Ando S, Ohsumi K, Chiyo T, Mizutani A, et al. Tumour necrosis factor alpha signalling through activation of Kupffer cells plays an

essential role in liver fibrosis of non-alcoholic steatohepatitis in mice. Gut. 2006;55:415–24. doi:10.1136/gut.2005.071118.

349. Gobejishvili L, Vatsalya V, Mohammad MK, Barve S, McClain CJ. Sa1656 Serum TRAIL Levels Inversely Correlate With MELD Scores in Severe Alcoholic Hepatitis Patients. Gastroenterology. 2016;150:S1087-S1088. doi:10.1016/S0016-5085(16)33670-8.

350. Senior JR. Drug Hepatotoxicity from a Regulatory Perspective. Clinics in Liver Disease. 2007;11:507–24. doi:10.1016/j.cld.2007.06.002.

351. Alempijevic T, Zec S, Milosavljevic T. Drug-induced liver injury: Do we know everything? World J Hepatol. 2017;9:491–502. doi:10.4254/wjh.v9.i10.491.

352. Fu S, Wu D, Jiang W, Li J, Long J, Jia C, Zhou T. Molecular Biomarkers in Drug-Induced Liver Injury: Challenges and Future Perspectives. Front Pharmacol. 2019;10:1667. doi:10.3389/fphar.2019.01667.

353. Björnsson ES. Hepatotoxicity by Drugs: The Most Common Implicated Agents. Int J Mol Sci. 2016;17:224. doi:10.3390/ijms17020224.

354. Njoku DB. Drug-induced hepatotoxicity: metabolic, genetic and immunological basis. Int J Mol Sci. 2014;15:6990–7003. doi:10.3390/ijms15046990.

355. Sgro C, Clinard F, Ouazir K, Chanay H, Allard C, Guilleminet C, et al. Incidence of drug-induced hepatic injuries: a French population-based study. Hepatology. 2002;36:451–5. doi:10.1053/jhep.2002.34857.

356. Björnsson ES. Incidence and outcomes of DILI in Western patients. Clin Liver Dis (Hoboken). 2014;4:9–11. doi:10.1002/cld.368.

357. Chalasani NP, Maddur H, Russo MW, Wong RJ, Reddy KR. ACG Clinical Guideline: Diagnosis and Management of Idiosyncratic Drug-Induced Liver Injury. Am J Gastroenterol. 2021;116:878–98. doi:10.14309/ajg.0000000000001259.

358. Weinberg S, Sequeira W, Jolly M. 37 - Gastrointestinal and Hepatic Systems. In: Wallace DJ, Hahn BH, editors. Dubois' Lupus Erythematosus and Related Syndromes (Ninth Edition). London: Elsevier; 2019. p. 457–472. doi:10.1016/B978-0-323-47927-1.00037-2.

359. Babai S, Auclert L, Le-Louët H. Safety data and withdrawal of hepatotoxic drugs. Therapies. 2021;76:715–23. doi:10.1016/j.therap.2018.02.004.

360. Jaeschke H, Ramachandran A, Chao X, Ding W-X. Emerging and established modes of cell death during acetaminophen-induced liver injury. Arch Toxicol. 2019;93:3491–502. doi:10.1007/s00204-019-02597-1.

361. Yuan L, Kaplowitz N. Mechanisms of drug-induced liver injury. Clinics in Liver Disease. 2013;17:507-18, vii. doi:10.1016/j.cld.2013.07.002.

362. Church RJ, Watkins PB. The transformation in biomarker detection and management of drug-induced liver injury. Liver Int. 2017;37:1582–90. doi:10.1111/liv.13441.

363. Yu M, Wang H, Ding A, Golenbock DT, Latz E, Czura CJ, et al. HMGB1 signals through toll-like receptor (TLR) 4 and TLR2. Shock. 2006;26:174–9. doi:10.1097/01.shk.0000225404.51320.82.

364. Dear JW, Clarke JI, Francis B, Allen L, Wraight J, Shen J, et al. Risk stratification after paracetamol overdose using mechanistic biomarkers: results from two prospective cohort studies. Lancet Gastroenterol Hepatol. 2018;3:104–13. doi:10.1016/S2468-1253(17)30266-2.

365. Antoine DJ, Dear JW, Lewis PS, Platt V, Coyle J, Masson M, et al. Mechanistic biomarkers provide early and sensitive detection of acetaminophen-induced acute liver injury at first presentation to hospital. Hepatology. 2013;58:777–87. doi:10.1002/hep.26294.

366. Church RJ, Kullak-Ublick GA, Aubrecht J, Bonkovsky HL, Chalasani N, Fontana RJ, et al. Candidate biomarkers for the diagnosis and prognosis of drug-induced liver injury: An international collaborative effort. Hepatology. 2019;69:760–73. doi:10.1002/hep.29802.

367. Diao H, Iwabuchi K, Li L, Onoe K, van Kaer L, Kon S, et al. Osteopontin regulates development and function of invariant natural killer T cells. Proc. Natl. Acad. Sci. U.S.A. 2008;105:15884–9. doi:10.1073/pnas.0806089105.

368. Wang X, Sun R, Wei H, Tian Z. High-mobility group box 1 (HMGB1)-Toll-like receptor (TLR)4-interleukin (IL)-23-IL-17A axis in drug-induced damage-associated lethal hepatitis: Interaction of γδ T cells with macrophages. Hepatology. 2013;57:373–84. doi:10.1002/hep.25982.

369. Antoniades CG, Quaglia A, Taams LS, Mitry RR, Hussain M, Abeles R, et al. Source and characterization of hepatic macrophages in acetaminophen-induced acute liver failure in humans. Hepatology. 2012;56:735–46. doi:10.1002/hep.25657.

370. Atallah E, Freixo C, Alvarez-Alvarez I, Cubero FJ, Gerbes AL, Kullak-Ublick GA, Aithal GP. Biomarkers of idiosyncratic drug-induced liver injury (DILI) - a systematic review. Expert Opin Drug Metab Toxicol. 2021;17:1327–43. doi:10.1080/17425255.2021.1999410.

371. Khoja L, Kibiro M, Metser U, Gedye C, Hogg D, Butler MO, et al. Patterns of response to anti-PD-1 treatment: an exploratory comparison of four radiological

response criteria and associations with overall survival in metastatic melanoma patients. Br J Cancer. 2016;115:1186–92. doi:10.1038/bjc.2016.308.

372. Oyesola OO, Tait Wojno ED. Prostaglandin regulation of type 2 inflammation: From basic biology to therapeutic interventions. Eur J Immunol. 2021;51:2399–416. doi:10.1002/eji.202048909.

373. Lazaridis N, Tsochatzis E. Current and future treatment options in non-alcoholic steatohepatitis (NASH). Expert Rev Gastroenterol Hepatol. 2017;11:357–69. doi:10.1080/17474124.2017.1293523.

374. Cotter TG, Charlton M. Nonalcoholic Steatohepatitis After Liver Transplantation. Liver Transpl. 2020;26:141–59. doi:10.1002/lt.25657.

375. Montalbano M, Neff GW, Yamashiki N, Meyer D, Bettiol M, Slapak-Green G, et al. A retrospective review of liver transplant patients treated with sirolimus from a single center: an analysis of sirolimus-related complications. Transplantation. 2004;78:264–8. doi:10.1097/01.tp.0000128628.31556.b1.

376. McCaughan GW, Bowen DG, Bertolino PJ. Induction Phase of Spontaneous Liver Transplant Tolerance. Front Immunol. 2020;11:1908. doi:10.3389/fimmu.2020.01908.

377. Vionnet J, Sánchez-Fueyo A. Biomarkers of immune tolerance in liver transplantation. Hum Immunol. 2018;79:388–94. doi:10.1016/j.humimm.2018.02.010.

378. Yu Y-Y, Ji J, Zhou G-W, Shen B-Y, Chen H, Yan J-Q, et al. Liver biopsy in evaluation of complications following liver transplantation. World J Gastroenterol. 2004;10:1678–81. doi:10.3748/wjg.v10.i11.1678.

379. van Ha TG. Liver biopsy in liver transplant recipients. Semin Intervent Radiol. 2004;21:271–4. doi:10.1055/s-2004-861561.

380. Minguela A, García-Alonso AM, Marín L, Torio A, Sánchez-Bueno F, Bermejo J, et al. Evidence of CD28 upregulation in peripheral T cells before liver transplant acute rejection. Transplant Proc. 1997;29:499–500. doi:10.1016/s0041-1345(96)00226-6.

381. Elvington M, Liszewski MK, Atkinson JP. CD46 and Oncologic Interactions: Friendly Fire against Cancer. Antibodies (Basel) 2020. doi:10.3390/antib9040059.

382. Kinugasa N, Higashi T, Nouso K, Nakatsukasa H, Kobayashi Y, Ishizaki M, et al. Expression of membrane cofactor protein (MCP, CD46) in human liver diseases. Br J Cancer. 1999;80:1820–5. doi:10.1038/sj.bjc.6690604.

383. Bohne F, Londoño M-C, Benítez C, Miquel R, Martínez-Llordella M, Russo C, et al. HCV-induced immune responses influence the development of operational

tolerance after liver transplantation in humans. Sci Transl Med. 2014;6:242ra81. doi:10.1126/scitranslmed.3008793.

384. Davey MS, Willcox CR, Baker AT, Hunter S, Willcox BE. Recasting Human Vδ1 Lymphocytes in an Adaptive Role. Trends Immunol. 2018;39:446–59. doi:10.1016/j.it.2018.03.003.

385. Zhao X, Li Y, Ohe H, Nafady-Hego H, Uemoto S, Bishop GA, Koshiba T. Intragraft Vδ1 γδ T cells with a unique T-cell receptor are closely associated with pediatric semiallogeneic liver transplant tolerance. Transplantation. 2013;95:192–202. doi:10.1097/TP.0b013e3182782f9f.

386. Li L, Wozniak LJ, Rodder S, Heish S, Talisetti A, Wang Q, et al. A common peripheral blood gene set for diagnosis of operational tolerance in pediatric and adult liver transplantation. Am J Transplant. 2012;12:1218–28. doi:10.1111/j.1600-6143.2011.03928.x.

387. Bohne F, Martínez-Llordella M, Lozano J-J, Miquel R, Benítez C, Londoño M-C, et al. Intra-graft expression of genes involved in iron homeostasis predicts the development of operational tolerance in human liver transplantation. J Clin Invest. 2012;122:368–82. doi:10.1172/JCI59411.

388. Kato H, Kuriyama N, Duarte S, Clavien P-A, Busuttil RW, Coito AJ. MMP-9 deficiency shelters endothelial PECAM-1 expression and enhances regeneration of steatotic livers after ischemia and reperfusion injury. J Hepatol. 2014;60:1032–9. doi:10.1016/j.jhep.2013.12.022.

389. Pinci F, Gaidt MM, Jung C, Kuut G, Jackson MA, Bauernfried S, Hornung V. C-tag TNF: a reporter system to study TNF shedding. J Biol Chem. 2020;295:18065–75. doi:10.1074/jbc.RA120.015248.

390. Kobayashi T, Kim H, Liu X, Sugiura H, Kohyama T, Fang Q, et al. Matrix metalloproteinase-9 activates TGF-β and stimulates fibroblast contraction of collagen gels. Am J Physiol Lung Cell Mol Physiol. 2014;306:L1006-15. doi:10.1152/ajplung.00015.2014.

391. Hazuda DJ, Strickler J, Simon P, Young PR. Structure-function mapping of interleukin 1 precursors. Cleavage leads to a conformational change in the mature protein. J Biol Chem. 1991;266:7081–6.

392. Fabriek BO, Møller HJ, Vloet RPM, van Winsen LM, Hanemaaijer R, Teunissen CE, et al. Proteolytic shedding of the macrophage scavenger receptor CD163 in multiple sclerosis. J Neuroimmunol. 2007;187:179–86. doi:10.1016/j.jneuroim.2007.04.016.

393. Duarte S, Baber J, Fujii T, Coito AJ. Matrix metalloproteinases in liver injury, repair and fibrosis. Matrix Biol. 2015;44-46:147–56. doi:10.1016/j.matbio.2015.01.004.

8. Publications

Yang Zhou J, Werner JM, Glehr G, Geissler EK, Hutchinson JA, Kronenberg K. Identification and Isolation of Type II NKT Cell Subsets in Human Blood and Liver. Front Immunol. 2022;13:898473. doi:10.3389/fimmu.2022.898473.

Yang Zhou J. Innate immunity and early liver inflammation. Front. Immunol. 2023. doi:10.3389/fimmu.2023.1175147.

Glehr G, Riquelme P, **Yang Zhou J**, Cordero L, Schilling H-L, Kapinsky M, et al. External validation of biomarkers for immune-related adverse events after immune checkpoint inhibition. Front Immunol. 2022;13:1011040. doi:10.3389/fimmu.2022.1011040. ***Publication in Appendix***

- Published Article –

Published in: Frontiers in Immunology. 2022 September;

https://doi.org/10.3389/fimmu.2022.1011040

8.1 Annex: External validation of biomarkers for immune-related adverse events after immune checkpoint inhibition

Gunther Glehr,* Paloma Riquelme,* Jordi Yang Zhou,*,† Laura Cordero,*

Hannah-Lou Schilling,* Michael Kapinsky,‡ Hans J. Schlitt,*

Edward K. Geissler,* Ralph Burkhardt,§ Barbara Schmidt,¶

Sebastian Haferkamp,‖ James A. Hutchinson* and Katharina Kronenberg*

*Department of Surgery, University Hospital Regensburg, Regensburg, Germany

†Leibniz Institute for Immunotherapy, Regensburg, Germany

‡Beckman Coulter Life Sciences, Krefeld, Germany

§Institute of Clinical Chemistry and Laboratory Medicine, University Hospital Regensburg, Regensburg, Germany

¶Institute of Clinical Microbiology and Hygiene, University Hospital Regensburg, Regensburg, Germany

‖Department of Dermatology, University Hospital Regensburg, Regensburg, Germany

Grant support: This work was supported by Bristol-Myers Squibb (BMS) Immune Oncology Foundation (Award FA19-009).

Authorship: GG performed statistical evaluation and wrote the manuscript. JYZ performed literature search. PR and LC analyzed data and revised the manuscript. HLS revised the manuscript. MK provided expert flow cytometry advice. HJS, EKG and RB provided infrastructural support and critical feedback. BS provided expert virological opinion. SH provided clinical samples and expert dermatological opinion. JAH designed study and wrote the manuscript. KK performed experiments, analyzed data and wrote the manuscript. All authors contributed to the article and approved the submitted version.

Non-standard abbreviations: Area-under-the-curve (AUC); body mass index (BMI); cytomegalovirus (CMV); Epstein-Barr virus (EBV); false discovery rate (FDR); gamma-glutamyltransferase (γ-GT); glutamic oxaloacetic transaminase (GOT); glutamic pyruvic transaminase (GPT); human herpesvirus (HHV); Immune Checkpoint Inhibitor (ICI); immune-related adverse event (irAE); Kaposi's sarcoma-associated virus (KSHV); lactate dehydrogenase (LDH); leave-one-out cross-validation (LOOCV); monocyte-to-lymphocyte ratio (MLR); receiver operating characteristic (ROC)

Abstract

Immune checkpoint inhibitors have revolutionized treatment of advanced melanoma, but commonly cause serious immune-mediated complications. The clinical ambition of reserving more aggressive therapies for patients least likely to experience immune-related adverse events (irAE) has driven an extensive search for predictive biomarkers. Here, we externally validate the performance of 59 previously reported markers of irAE risk in a new cohort of 110 patients receiving Nivolumab (anti-PD1) and Ipilimumab (anti-CTLA-4) therapy. Alone or combined, the discriminatory value of these routine clinical parameters and flow cytometry biomarkers was poor. Unsupervised clustering of flow cytometry data returned four T cell subsets with higher discriminatory capacity for colitis than previously reported populations, but they cannot be considered as reliable classifiers. Although mechanisms predisposing some patients to particular irAEs have been described, we are presently unable to capture adequate information from pre-therapy flow cytometry and clinical data to reliably predict risk of irAE in most cases.

Introduction

Combined checkpoint blockade with anti-PD-1 (Nivolumab) and anti-CTLA-4 (Ipilimumab) antibodies is now a standard treatment for inoperable metastatic melanoma. The clinical efficacy of dual therapy is evident from the excellent clinical response rate, progression-free survival and overall survival (1-3). However, immune-related adverse events (irAEs) complicate immune checkpoint inhibitor (ICI) treatment in a high proportion of patients, which significantly impacts their quality of life (4). Although life-threatening irAEs are infrequent, even moderate reactions lead to interruption of immunotherapy, multidisciplinary management and treatment with immunosuppressive medication (5). Disruption of ICI treatment and costs associated with monitoring or treatment of irAEs are burdensome; therefore, reliable prognostic methods to assess an individual's risk of irAE prior to therapy would greatly impact patient care.

Factors predisposing individual patients to irAE are incompletely understood. ICI therapy can worsen autoimmune conditions and patients with pre-existing autoimmune diseases stand a greater risk of developing other immune-mediated adverse reactions after treatment (6-8). Immunogenetics also play a role in irAE susceptibility (9-11). Prior exposure to viruses has recently surfaced as a significant predisposing factor in some patients (12). Infection with human herpesviruses (HHV) may play a particularly important role in the context of malignant melanoma. Our own studies revealed that chronic or recurrent cytomegalovirus (CMV; HHV-5) reactivation drives proliferation of virus-specific $CD4^+$ effector memory T cells (T_{EM}) in patients with metastatic melanoma before starting immunotherapy. These expanded T_{EM} cells are responsible for hepatitis after combined Nivolumab and Ipilimumab treatment (13-15). Similarly, others have implicated Epstein-Barr virus (EBV; HHV-4)-specific memory T cells in a case of fatal encephalitis after anti-PD-1 therapy (16). An unexpectedly high rate of seropositivity against Kaposi's sarcoma-associated virus (KSHV; HHV-8) has been reported in Stage IV melanoma patients, hinting at a peculiar susceptibility to HHV infections (17). Beyond ICI therapy, autoimmunity may be triggered

by persistent T cell immunity against various herpesgroup viruses; for example, Hashimoto's thyroiditis has been associated with seroconversion to roseolovirus (HHV-6) (18, 19).

Recently, many groups have reported biomarkers associated with irAE risk, which include leucocyte subsets measured in peripheral blood by flow cytometry. We systematically searched for these reports to independently assess the discriminatory value of biomarkers they identified. We found 20 relevant articles published between 2006 and 2022 that examined a range of tumor entities, treatment strategies and analytical methods (20-39). Here, we tested the general validity of these biomarkers by asking whether they predicted irAEs in a related, but non-identical clinical setting. Specifically, we asked whether any reported biomarkers measured prior to starting combined Ipilimumab and Nivolumab therapy predicted the incidence of hepatitis, colitis or thyroiditis in patients with advanced melanoma.

Materials and methods

Patients. This single-center, non-interventional clinical study was conducted in accordance with the Declaration of Helsinki and all applicable German and European laws and ethical standards. Blood samples were obtained from patients with Stage III/IV melanoma enrolled in an observational trial authorized by the Ethics Committee of the University of Regensburg (approval 16-101-0125) and registered with clinicaltrials.gov (NCT04158544). All participants gave full, informed written consent. The first reported case was recruited in OCT-2016 and the last reported case was recruited in JUN-2021. Patients received standard-of-care treatment according to local guidelines. Patients with unresectable metastatic disease who received first- or second-line checkpoint inhibitor therapy were initially treated with Nivolumab (αPD-1; 1 mg/kg; Bristol-Myers Squibb) plus Ipilimumab (αCTLA-4; 3 mg/kg; Bristol-Myers Squibb) for four cycles at 3 week intervals. Thereafter, patients received 3 mg/kg Nivolumab monotherapy at 3 week intervals.

irAE grading. All irAE were assessed by an expert Dermatological Oncologist (Supplemental Figure 1A). ICI-related hepatitis was diagnosed when: (i) GOT, GPT, γ-GT or total bilirubin substantially deviated from pretreatment values; (ii) this change was not attributable to other causes, such as co-medication or viral disease; and (iii) liver injury was sufficiently severe that ICI therapy was suspended or stopped, or immunosuppression was given. Colitis was diagnosed according to stool frequency and consistency, abdominal discomfort, suspension or cessation of ICI therapy, and introduction of immunosuppressive treatment. Thyroiditis was diagnosed based on decreased T3/T4 and elevated TSH levels measured at routine clinic visits.

Routine investigations. Hematological, Biochemical and Microbiological investigations were performed by accredited diagnostic laboratories at University Hospital Regensburg.

Literature Search. We searched Medline at the National Library of Medicine through the NCBI website on 11-JUN-2022. Our search terms were ‘immunotherapy’, ‘immune checkpoint inhibitor’, ‘irAEs’, ‘biomarkers’, ‘prediction’ and synonyms. We followed-up on relevant citations from articles

returned in our original search. We identified 20 articles (Supplemental Table I) describing 59 unique biomarkers (Supplemental Table II).

Flow cytometry. Step-by-step protocols for preparing and analyzing clinical samples by flow cytometry can be accessed through Nature Protocol Exchange (40). Briefly, blood was collected into EDTA-vacutainers by peripheral venepuncture before delivery to the immune monitoring lab at ambient temperature. Samples were stored at 4°C for up to 4 h until processing. Whole blood samples were stained using DURAClone reagents (DURAClone IM Phenotyping Basic Tube, B53309; DURAClone IM T Cell Subsets Tube, B53328; DURAClone IM TCRs Tube, B53340; DURAClone IM Treg Tube, B53346; DURAClone IM B Cell Tube, B53318; DURAClone IM Dendritic Cell Tube, B53351; DURAClone IM Granulocytes Tube, B88651; all from Beckman Coulter, Krefeld, Germany). For the flow cytometry anaylsis of exhausted T cells the following liquid antibodies were used (EXH_CD8 panel): CD49b FITC, 359306, BioLegend, Amsterdam, Netherlands; CD160 PE, IM3657; CD27 ECD, B26603; CD244 PC5.5, B21171; CD279 (PD-1) PC7, A78885; CD127 APC, B42026; CD8 AA700, B49181; CD3 AA750, A94680; CD4 PB, B49197 and CD45 KrO, B36294; all from Beckman Coulter, Krefeld, Germany. Data were collected with a Navios^{TM} cytometer running Cytometry List Mode Data Acquisition and Analysis Software version 1.3 (Beckman Coulter). An experienced operator performed blinded analyses of all datasets in Kaluza version 2.1, as far as possible replicating gating strategies described in the original reports.

Statistics. Our main dataset comprised 110 samples and 59 features extracted from publications and 9 routine clinical parameters; one missing value for GOT was imputed with the median “25” from all other 109 samples. In the extended analysis of DURAClone IM Tube panels, we extracted 80 cell population frequencies by manual gating. Additionally we included 8 clinical parameters, 9 clinical biochemistry values and 18 cell counter values in this extended feature set. One missing value of the presence of liver metastases was imputed with the median “no presence” from all

other samples. Univariate analysis was performed for each condition per feature. P-values were calculated using a two-sample Wilcoxon test using a significance level of 0.05 (41). For false discovery rate (FDR) correction (42) of the p-values we used a significance level of 0.1. Discriminatory capability of the features was additionally assessed using ROC-curves and the corresponding area under the curves (AUCs). We report features with AUC > 0.65 as discriminatory. All calculations and plots were made with R 4.2.0 (43).

Models were built in leave-one-out cross-validation and the predictions for each left-out sample were gathered to report the final performance of each model. The penalized logistic regression models were built with glmnet (44) using the elastic-net (45) with an alpha=0.9, and 250 lambda steps in inner cross-validation. The random forest model was built using mlr3 (46) for each binary classification problem with alpha=0.5, num.trees=500, replace=True and splitrule=gini. We also assessed ROC-curves and the AUCs here. AUC $\simeq$ 0 were obtained when penalization of the linear model excluded all features in multiple cross-validation steps, leading to a null-model of only the intercept.

Clustering was performed using FlowSOM (47) in CytoBank on $CD45^+$ $CD3^+$ T cells (DURAClone IM T Cell Subsets Tube) and $CD45^+$ $CD19^+$ B cells (DURAClone IM B Cell Tube). All channels were used as clustering markers except for CD3 or CD19, CD45, FSC, SSC and time. We used hierarchical consensus clustering with 10 metaclusters and 100 (T Cell Tube) or 49 (B Cell Tube) clusters. Feature standardization was applied.

Results

Reported biomarkers are weak predictors of irAE

Our first objective was to test the predictive performance of reported biomarkers of irAE risk in our cohort of 110 metastatic melanoma patients treated with dual checkpoint blockade. Patient characteristics are shown in Table I. Reviewing the literature, we catalogued 20 publications that reported associations between irAE risk and the frequencies of 55 unique cell populations in peripheral blood or 4 routine clinical parameters (Supplemental Table I) (20-39). In addition, we selected another 9 routine clinical parameters with possible prognostic relevance – namely, sex, CMV seropositivity, GOT, GPT, γ-GT, total bilirubin, LDH, Protein-S100 and presence of liver metastases. Although many of these biomarkers were identified in different clinical contexts, such as anti-PD-1 monotherapy or other malignancies, we reasoned that any robust, mechanistically relevant biomarker could be reasonably expected to have some predictive capacity in closely related situations. Hence, our aim was not to directly confirm or refute any previous findings through replication, but to test whether they could be generalized.

Table I. Characteristics of study cohort. 110 patients with stage III/IV melanoma were included into the study cohort. For Age and BMI, median values were calculated and minimum and maximum values were given in brackets. Baseline characteristics were obtained before start of Ipi/Nivo therapy.

Patient cohort characteristics	
Total number of cases	110
Female	37 (33.6 %)
Male	73 (66.4 %)
Baseline characteristics	
Age (years)	62 (22-84)
BMI	26.6 (15.4-54.6)
Stage III	8 (7.3 %)
Stage IV	102 (92.7 %)
Liver metastases present	30 (27.3 %)
CMV seropositive	52 (47.3 %)
ANA positive	65 (59.1 %)
Pretreatment	
None	3 (2.7 %)
Surgical excision	102 (92.7%)
Radiosurgery	3 (2.7 %)
Radiation	42 (38.2 %)
Monotherapy	17 (15.5 %)
IFNa therapy	9 (8.2 %)
Braf/Mek inhibitor therapy	21 (19.1 %)
T-VEC therapy	7 (6.4 %)
Chemotherapy	6 (5.5 %)
Rounds of Ipi/Nivo	
1 round	13 (11.8 %)
2 rounds	24 (21.8 %)
3 rounds	20 (18.2 %)
4 rounds	53 (48.2 %)
Complications	
Hepatitis	48 (43.6 %)
Colitis	40 (36.4 %)
Thyroiditis	41 (37.3 %)
No complication	23 (20.9 %)
1 complication	50 (45.5 %)
2 complications	32 (29.1 %)
3 complications	5 (4.5 %)

To externally validate these 55 flow cytometry and 13 clinical features as predictors of irAEs, we performed uni- and multivariate analyses. We particularly focused on 3 common irAE – hepatitis (41 %), colitis (36 %) and thyroiditis (37 %). Each complication was treated as an separate outcome, but we also considered the occurrence of (i) hepatitis and/or colitis, and (ii) hepatitis and/or colitis and/or thyroiditis (henceforth, “any irAE”). Hence, we tested the value of 68 features in predicting 5 clinical outcomes in our dataset of 110 cases (Supplemental Table II).

Considering all five clinical outcomes, significant associations were discovered for 16 features using the Wilcoxon test without correcting for multiple comparison (Supplemental Table IIIA). However, after adjustment for multiple testing using the false discovery rate (FDR) (42), no associations with hepatitis, colitis, thyroiditis, or “hepatitis and/or colitis” were significant. Four features remained significantly associated with “any irAE” – notably, these were all B cell subsets. Next, we assessed the discriminatory capacity of all 68 features using the area under Receiver-Operating-Characteristics (ROC) curves (Figure 1A). An area under the curve (AUC) of 0.5 implies no discrimination, whereas a maximum AUC of 1 implies perfect discrimination. We found 7 features with AUC > 0.65 (Supplemental Table IIIA). Next, we asked whether these discriminatory features were capturing similar information by grouping them into immunologically relevant classes (Figure 1B). The most discriminatory marker for hepatitis was $CD4^+$ T cell frequency (AUC=0.630) (Supplemental Table IV). Discriminatory markers of colitis risk related primarily to T cells, especially the frequency of $CD4^+$ T cells (AUC = 0.652). The most discriminatory feature for thyroiditis risk was the platelet count (AUC = 0.659). The five most discriminatory features of “any irAE” were B cell markers (best AUC = 0.727). Unfortunately, no single biomarker was powerful enough to reliably identify predisposed individuals.

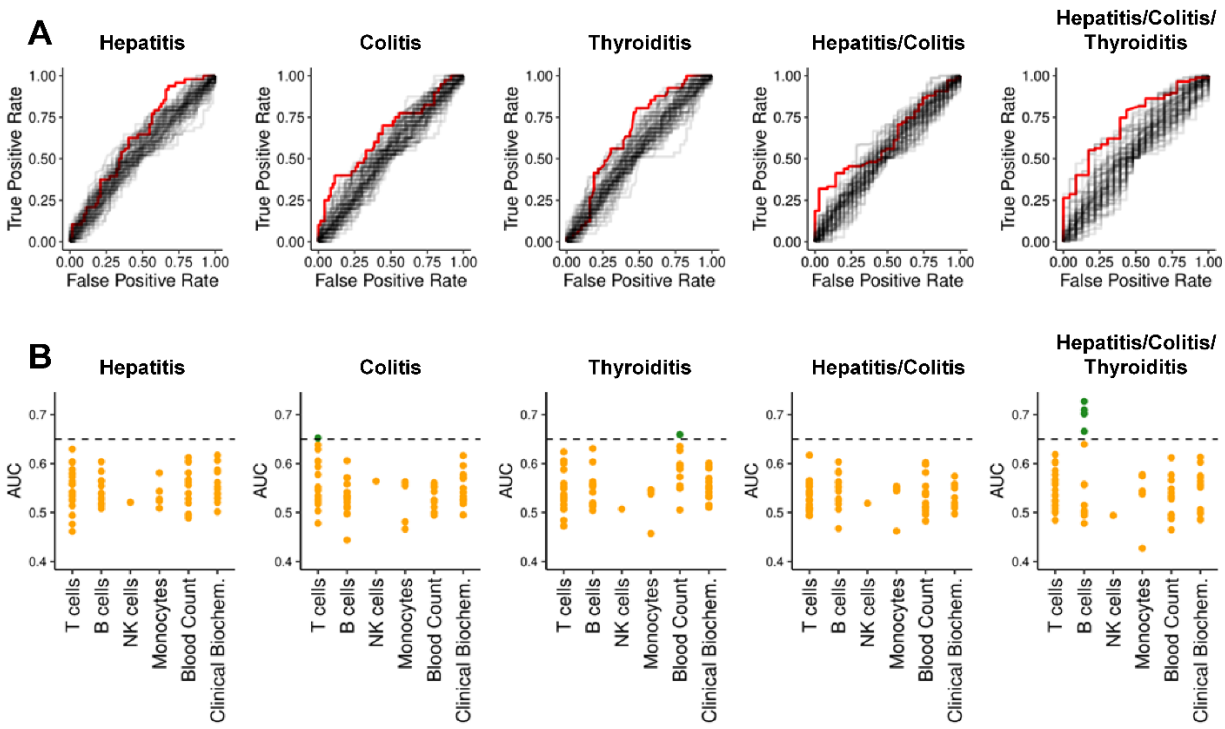

Figue 1. ROC-curves and AUCs for previously reported biomarkers and clinical parameters per condition. (A) ROC-curves for all 68 features regarding each dependent variable are shown. For each dependent variable, the features with highest AUC is highlighted in red. (B) AUCs from ROC-curves in subfigure (A) grouped according to immunological classes. The y-axis represents the AUC. Orange dots denote AUC ≤ 0.65; green dots denote AUC > 0.65.

Combining features does not improve discriminatory power

We next asked whether combining previously reported features predicted irAEs better than single features alone. Therefore, we generated simple penalized logistic regression models (48) and random forest (49) analyses in leave-one-out cross-validation (LOOCV). Neither approach found reliable predictive models (Figure 2). AUC ≃ 0 were obtained when penalization of the linear model excluded all features in multiple cross-validation steps, leading to a null-model of only the intercept. The prediction of each left-out sample is then the mean prediction of all other samples, which always leads to incorrect class prediction.

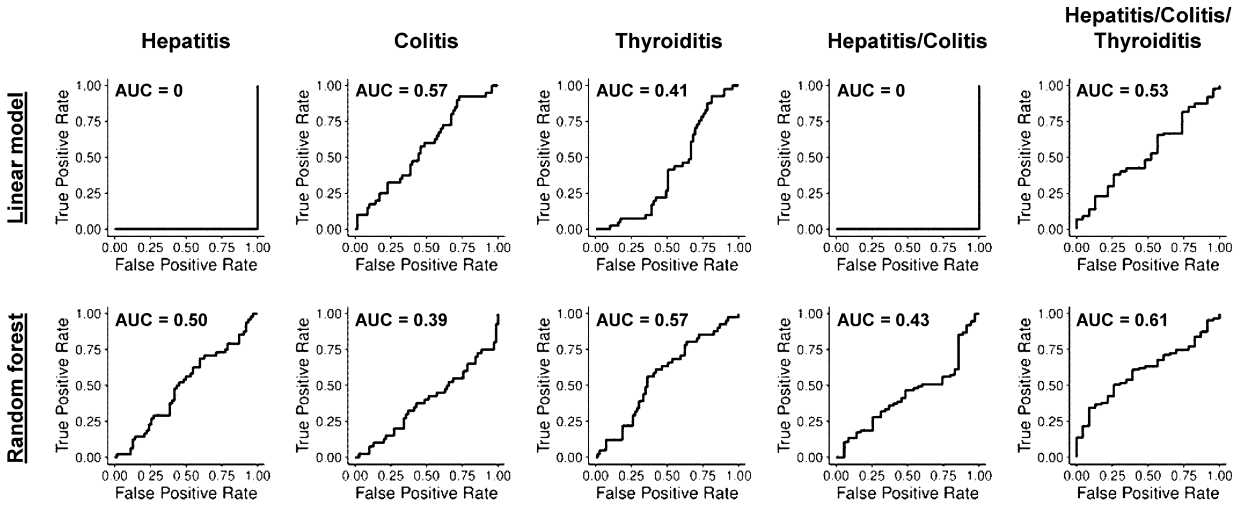

Figure 2. ROC-curves for linear models and random forests with previously reported biomarkers and clinical parameters. ROC-curves in LOOCV for penalized logistic regression and random forest models predicting hepatitis (AUC 0 and 0.50), colitis (AUC 0.57 and 0.39), thyroiditis (AUC 0.41 and 0.57), hepatitis and/or colitis (AUC 0 and 0.43) and hepatitis and/or colitis and/or thyroiditis (AUC 0.53 and 0.61).

Our inability to find a reliable predictive model combining different discriminatory biomarkers could be explained in several ways: (i) There may be no immunological predisposition to particular irAEs; (ii) immunological factors might be only partly responsible for any such predisposition; (iii) hepatitis or colitis may be the end-result of more than one immune aetiology; (iv) although we may be capturing predictive information, we might be unable to extract the signal from background noise; or (v) our selection of biomarkers might not capture all phenotypic information necessary for a reliable prediction. Importantly, the hope of finding predictive biomarkers of irAE risk that could drive personalized treatment decisions rests upon there being measurable predisposing factors of irAE. There is now good mechanistic evidence for immunological predisposition to irAEs in some cases. For instance, our group and others reported that irAE risk is predicted by oligoclonal expansion of T cells prior to immunotherapy, likely as a consequence of chronic or recurrent viral exposure (13, 20).

To investigate whether our selection of features or analytical methods were limiting the performance of our predictive models, we extended our set of biomarkers by making a finer manual re-gating of our flow cytometry data before repeating our uni- and multivariate analyses. After correction for multiple testing, no extended-set features were significantly associated with hepatitis, colitis, thyroiditis or “hepatitis and/or colitis” risk. However, three B cell subpopulations were significant markers of “any irAE” (Supplemental Table IIIB). The extended-set feature that returned the highest AUCs in prediction of hepatitis was $CD4^+$ T_{EM} (AUC = 0.677), whereas colitis was weakly predicted by immature neutrophils (AUC = 0.670) (Supplemental Table IV). Unfortunately, combining the extended-set features did not return a more stable predictive model for any of the outcomes (Supplemental Figure 1B).

ICI-related hepatitis may have more than one cause

We previously reported that $CD4^+$ T_{EM} expansion in CMV-seropositive patients before therapy is a strong predictor of hepatitis risk after combined Nivolumab and Ipilimumab treatment (13). We were able to rederive this result in a subset of patients comprising the validation set from our original publication (n=45) plus an additional 30 patients added in this study: The AUC for $CD4^+$ T_{EM} (%) was 0.729. In addition, we used the full dataset to discover another 12 markers of CMV IgG^+ hepatitis with AUC > 0.65, which were mainly T cell subsets (Supplemental Table IIIC). Interestingly, for the CMV IgG^- samples, monocyte frequency (AUC = 0.705) and absolute numbers (AUC = 0.657) predicted hepatitis risk, suggesting there may be more than one aetiological route to ICI-related liver inflammation (Supplemental Table IIID & Supplemental Table IV).

Unsupervised clustering returns new predictive features

It is conceivable our flow cytometry dataset captured predictive information about irAE risk, but that our manual gating strategy failed to identify the most informative cell subsets. Therefore, we applied an unsupervised clustering algorithm (FlowSOM) to samples stained with B cell or T cell markers, then used clusterwise cell abundances as predictive features (47). Univariate analyses after clustering of B cell markers identified no new features with greater discriminatory value than previously considered features (Supplemental Table IIIE & IIIF). Furthermore, the top-performing models after combining B cell (meta-)clusters in LOOCV were not superior to single features alone (Supplemental Table IV, Supplemental Figure 2A & 2B).

Likewise, clustering T cells revealed no better discriminatory features for hepatitis, thyroiditis, "hepatitis or colitis" or "any irAE" (Supplemental Table IIIG & IIIH, Supplemental Table IV & Supplemental Figure 2C). Surprisingly, 4 clusters (C45, C50, C56 and C63) were significantly associated with colitis after FDR correction. These clusters returned AUCs of 0.690, 0.709, 0.711 and 0.713, respectively – hence, they showed greater discriminatory value than previously considered features (Supplemental Table IIIH). Unfortunately, combining C45, C50, C56 and C63 in LOOCV did not improve their predictive performance (Supplemental Figure 2D).

We next asked why these particular T cell clusters might encode more information about colitis risk than other T cell subsets. C63, C56 and C45 were $CD4^+$ memory T cells with a $CD45RA^-$ $CCR7^{int/-}$ $CD27^+$ $CD28^+$ $CD57^-$ phenotype, possibly representing transitional states between recently activated central memory (T_{CM}) and T_{EM} cells (Figure 3). Apart from CCR7 expression, these T cell clusters differed only in PD-1 expression. C50 was a minor population of $CD8^+$ $CD45RA^+$ $CCR7^-$ $CD27^+$ $CD28^-$ $PD\text{-}1^-$ $CD57^+$ T_{EMRA} cells. We speculate that C50 overlaps with a non-exhausted, recirculating subset of $CD8^+$ T_{EMRA} cells that others have reported as important for maintaining anti-viral immunity (50). Our results suggest that patients at risk of ICI-related colitis might have on-going immune responses – possibly against subclinical viral infections – and that our predictive features actually capture information about the rate of T_{CM} to T_{EM} differentiation.

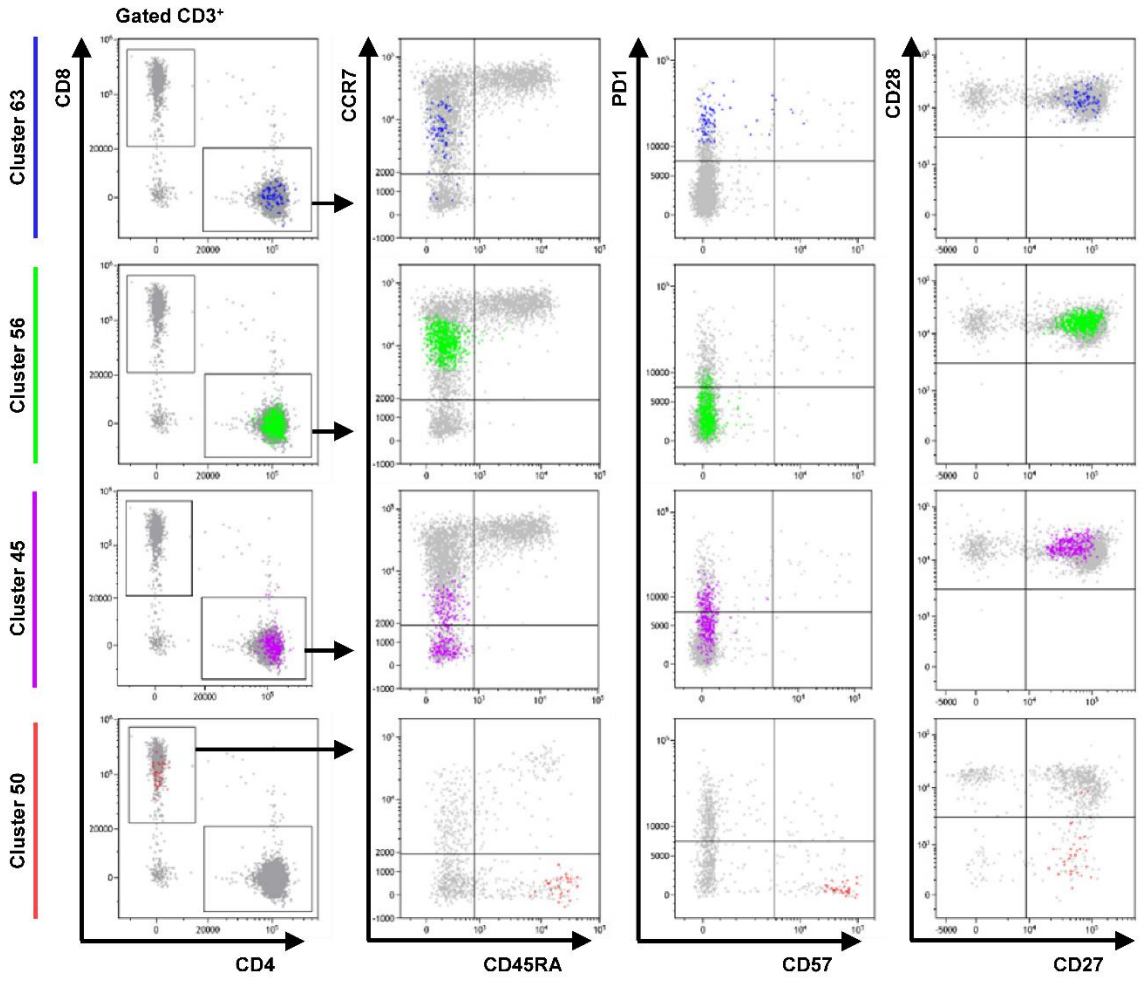

Figure 3. Phenotype of cells in FlowSOM clusters associated with colitis. Dot plots show the phenotype of the cells in each cluster (color) and all gated cells for reference (grey). Clusters 63 and 56 are $CD4^+$ $CD45RA^-$ $CCR7^{int}$ $CD27^+$ $CD28^+$ $CD57^-$ T cells that differ only in expression of PD-1. Cluster 45 is $CD4^+$ $CD45RA^-$ $CCR7^{low/-}$ $PD\text{-}1^{int}$ $CD27^+$ $CD28^+$ $CD57^-$ T cell population. Cluster 50 represents a $CD8^+$ $CD45RA^+$ $CCR7^-$ $CD27^+$ $CD28^-$ $PD\text{-}1^-$ $CD57^+$ T_{EMRA} subpopulation. Data from one representative patient.

Discussion

Reproducibility studies using external data are an important validation step in clinical biomarker development. Here, we showed that previously reported flow cytometry-based biomarkers of irAE are not generally reliable enough to predict hepatitis, colitis or thyroiditis as a basis for clinical decision-making. Promisingly, however, unsupervised clustering revealed four T cell

subpopulations associated with risk of colitis that returned AUC > 0.65, which we take as a sign that better predictions of irAE risk might be possible with a refined marker selection and more sophisticated computational methods. We conclude that deeper phenotyping of monocytes and $CD4^+$ memory T cells transitioning between T_{EM} and T_{CM} might lead to more informative biomarkers in future.

Acknowledgements

The authors are grateful to The Bristol Myers Squibb Foundation for Immuno-Oncology (Award FA-19-009) for funding this work. L.C. is a Marie Skłodowska-Curie Research Fellow affiliated with INsTRuCT and receives funding from the European Union's Horizon 2020 research and innovation programme (Award 860003). We are very grateful for Beckman Coulter Life Sciences' continuing support of our research. This work would not have been possible without the outstanding technical support of Erika Ostermeier and Joachim Schweimer.

Disclosures

M.K. is a Beckman Coulter Life Sciences associate. S.H. has received consulting fees and speaker's honoraria from BMS and Merck Sharp & Dohme (MSD). Other authors have no conflict-of-interest to declare.

References

1. Larkin, J., V. Chiarion-Sileni, R. Gonzalez, J. J. Grob, P. Rutkowski, C. D. Lao, C. L. Cowey, D. Schadendorf, J. Wagstaff, R. Dummer, P. F. Ferrucci, M. Smylie, D. Hogg, A. Hill, I. Marquez-Rodas, J. Haanen, M. Guidoboni, M. Maio, P. Schoffski, M. S. Carlino, C. Lebbe, G. McArthur, P. A. Ascierto, G. A. Daniels, G. V. Long, L. Bastholt, J. I. Rizzo, A. Balogh, A. Moshyk, F. S. Hodi, and J. D. Wolchok. 2019. Five-Year Survival with Combined Nivolumab and Ipilimumab in Advanced Melanoma. *N Engl J Med* 381: 1535-1546.

2. Robert, C., A. Ribas, J. Schachter, A. Arance, J. J. Grob, L. Mortier, A. Daud, M. S. Carlino, C. M. McNeil, M. Lotem, J. M. G. Larkin, P. Lorigan, B. Neyns, C. U. Blank, T. M. Petrella, O. Hamid, S. C. Su, C. Krepler, N. Ibrahim, and G. V. Long. 2019. Pembrolizumab versus ipilimumab in advanced melanoma (KEYNOTE-006): post-hoc 5-year results from an open-label, multicentre, randomised, controlled, phase 3 study. *Lancet Oncol* 20: 1239-1251.

3. Hodi, F. S., V. Chiarion-Sileni, R. Gonzalez, J. J. Grob, P. Rutkowski, C. L. Cowey, C. D. Lao, D. Schadendorf, J. Wagstaff, R. Dummer, P. F. Ferrucci, M. Smylie, A. Hill, D. Hogg, I. Marquez-Rodas, J. Jiang, J. Rizzo, J. Larkin, and J. D. Wolchok. 2018. Nivolumab plus ipilimumab or nivolumab alone versus ipilimumab alone in advanced melanoma (CheckMate 067): 4-year outcomes of a multicentre, randomised, phase 3 trial. *Lancet Oncol* 19: 1480-1492.

4. Wolchok, J. D., V. Chiarion-Sileni, R. Gonzalez, P. Rutkowski, J. J. Grob, C. L. Cowey, C. D. Lao, J. Wagstaff, D. Schadendorf, P. F. Ferrucci, M. Smylie, R. Dummer, A. Hill, D. Hogg, J. Haanen, M. S. Carlino, O. Bechter, M. Maio, I. Marquez-Rodas, M. Guidoboni, G. McArthur, C. Lebbé, P. A. Ascierto, G. V. Long, J. Cebon, J. Sosman, M. A. Postow, M. K. Callahan, D. Walker, L. Rollin, R. Bhore, F. S. Hodi, and J. Larkin. 2017. Overall Survival with Combined Nivolumab and Ipilimumab in Advanced Melanoma. *N Engl J Med* 377: 1345-1356.

5. Kähler, K. C., J. C. Hassel, L. Heinzerling, C. Loquai, K. M. Thoms, S. Ugurel, L. Zimmer, and R. Gutzmer. 2020. Side effect management during immune checkpoint blockade using CTLA-4 and PD-1 antibodies for metastatic melanoma - an update. *J Dtsch Dermatol Ges* 18: 582-609.

6. Johnson, D. B., R. J. Sullivan, P. A. Ott, M. S. Carlino, N. I. Khushalani, F. Ye, A. Guminski, I. Puzanov, D. P. Lawrence, E. I. Buchbinder, T. Mudigonda, K. Spencer, C. Bender, J. Lee, H. L. Kaufman, A. M. Menzies, J. C. Hassel, J. M. Mehnert, J. A. Sosman, G. V. Long, and J. I. Clark. 2016. Ipilimumab Therapy in Patients With Advanced Melanoma and Preexisting Autoimmune Disorders. *JAMA Oncol* 2: 234-240.

7. Menzies, A. M., D. B. Johnson, S. Ramanujam, V. G. Atkinson, A. N. M. Wong, J. J. Park, J. L. McQuade, A. N. Shoushtari, K. K. Tsai, Z. Eroglu, O. Klein, J. C.

Hassel, J. A. Sosman, A. Guminski, R. J. Sullivan, A. Ribas, M. S. Carlino, M. A. Davies, S. K. Sandhu, and G. V. Long. 2017. Anti-PD-1 therapy in patients with advanced melanoma and preexisting autoimmune disorders or major toxicity with ipilimumab. *Ann Oncol* 28: 368-376.

8. Young, A., Z. Quandt, and J. A. Bluestone. 2018. The Balancing Act between Cancer Immunity and Autoimmunity in Response to Immunotherapy. *Cancer Immunol Res* 6: 1445-1452.

9. Shahabi, V., D. Berman, S. D. Chasalow, L. Wang, Z. Tsuchihashi, B. Hu, L. Panting, M. Jure-Kunkel, and R. R. Ji. 2013. Gene expression profiling of whole blood in ipilimumab-treated patients for identification of potential biomarkers of immune-related gastrointestinal adverse events. *J Transl Med* 11: 75.

10. Jing, Y., J. Liu, Y. Ye, L. Pan, H. Deng, Y. Wang, Y. Yang, L. Diao, S. H. Lin, G. B. Mills, G. Zhuang, X. Xue, and L. Han. 2020. Multi-omics prediction of immune-related adverse events during checkpoint immunotherapy. *Nat Commun* 11: 4946.

11. Gibney, G. T., L. M. Weiner, and M. B. Atkins. 2016. Predictive biomarkers for checkpoint inhibitor-based immunotherapy. *Lancet Oncol* 17: e542-e551.

12. Hauschild, A. 2021. Could controlling occult cytomegalovirus reactivation with prophylactic valganciclovir prevent immune checkpoint blockade-Related complications? *Eur J Cancer* 153: 72-73.

13. Hutchinson, J. A., K. Kronenberg, P. Riquelme, J. J. Wenzel, G. Glehr, H. L. Schilling, F. Zeman, K. Evert, M. Schmiedel, M. Mickler, K. Drexler, F. Bitterer, L. Cordero, L. Beyer, C. Bach, J. Koestler, R. Burkhardt, H. J. Schlitt, D. Hellwig, J. M. Werner, R. Spang, B. Schmidt, E. K. Geissler, and S. Haferkamp. 2021. Virus-specific memory T cell responses unmasked by immune checkpoint blockade cause hepatitis. *Nat Commun* 12: 1439.

14. Schilling, H. L., G. Glehr, M. Kapinsky, N. Ahrens, P. Riquelme, L. Cordero, F. Bitterer, H. J. Schlitt, E. K. Geissler, S. Haferkamp, J. A. Hutchinson, and K. Kronenberg. 2021. Development of a Flow Cytometry Assay to Predict Immune Checkpoint Blockade-Related Complications. *Front Immunol* 12: 765644.

15. Schilling, H. L., J. A. Hutchinson, and S. Haferkamp. 2022. Prediction of immune checkpoint blockade-related hepatitis in metastatic melanoma patients. *J Dtsch Dermatol Ges*.

16. Johnson, D. B., W. J. McDonnell, P. I. Gonzalez-Ericsson, R. N. Al-Rohil, B. C. Mobley, J. E. Salem, D. Y. Wang, V. Sanchez, Y. Wang, C. A. Chastain, K. Barker, Y. Liang, S. Warren, J. M. Beechem, A. M. Menzies, M. Tio, G. V. Long, J. V. Cohen, A. C. Guidon, M. O'Hare, S. Chandra, A. Chowdhary, B. Lebrun-Vignes, S. M. Goldinger, E. J. Rushing, E. I. Buchbinder, S. A. Mallal, C. Shi, Y. Xu, J. J. Moslehi, M. E. Sanders, J. A. Sosman, and J. M. Balko. 2019. A case report of

clonal EBV-like memory CD4(+) T cell activation in fatal checkpoint inhibitor-induced encephalitis. *Nat Med* 25: 1243-1250.

17. Kronenberg, K., J. Wenzel, B. Schmidt, J. A. Hutchinson, and S. Haferkamp. 2022. Unexpectedly high seroprevalance of Kaposi's sarcoma-associated herpesvirus (HHV-8) in patients with stage IV melanoma. *Eur J Cancer* 172: 51-52.

18. Caselli, E., M. C. Zatelli, R. Rizzo, S. Benedetti, D. Martorelli, G. Trasforini, E. Cassai, E. C. degli Uberti, D. Di Luca, and R. Dolcetti. 2012. Virologic and immunologic evidence supporting an association between HHV-6 and Hashimoto's thyroiditis. *PLoS Pathog* 8: e1002951.

19. Broccolo, F., L. Fusetti, and L. Ceccherini-Nelli. 2013. Possible role of human herpesvirus 6 as a trigger of autoimmune disease. *ScientificWorldJournal* 2013: 867389.

20. Lozano, A. X., A. A. Chaudhuri, A. Nene, A. Bacchiocchi, N. Earland, M. D. Vesely, A. Usmani, B. E. Turner, C. B. Steen, B. A. Luca, T. Badri, G. S. Gulati, M. R. Vahid, F. Khameneh, P. K. Harris, D. Y. Chen, K. Dhodapkar, M. Sznol, R. Halaban, and A. M. Newman. 2022. T cell characteristics associated with toxicity to immune checkpoint blockade in patients with melanoma. *Nat Med* 28: 353-362.

21. Reschke, R., P. Gussek, A. Boldt, U. Sack, U. Köhl, F. Lordick, T. Gora, M. Kreuz, K. Reiche, J. C. Simon, M. Ziemer, and M. Kunz. 2021. Distinct Immune Signatures Indicative of Treatment Response and Immune-Related Adverse Events in Melanoma Patients under Immune Checkpoint Inhibitor Therapy. *Int J Mol Sci* 22.

22. Shi, Y., X. Liu, J. Liu, D. Zhang, X. Liu, Y. Yue, Q. Zhou, X. Gao, M. Chen, Y. Xu, J. Zhao, W. Zhong, M. Provencio, J. Jassem, T. M. Williams, A. Seeber, F. Kocher, and M. Wang. 2021. Correlations between peripheral blood biomarkers and clinical outcomes in advanced non-small cell lung cancer patients who received immunotherapy-based treatments. *Transl Lung Cancer Res* 10: 4477-4493.

23. Michailidou, D., A. R. Khaki, M. P. Morelli, L. Diamantopoulos, N. Singh, and P. Grivas. 2021. Association of blood biomarkers and autoimmunity with immune related adverse events in patients with cancer treated with immune checkpoint inhibitors. *Sci Rep* 11: 9029.

24. Isono, T., N. Kagiyama, K. Takano, C. Hosoda, T. Nishida, E. Kawate, Y. Kobayashi, T. Ishiguro, Y. Takaku, K. Kurashima, T. Yanagisawa, and N. Takayanagi. 2021. Outcome and risk factor of immune-related adverse events and pneumonitis in patients with advanced or postoperative recurrent non-small cell lung cancer treated with immune checkpoint inhibitors. *Thorac Cancer* 12: 153-164.

25. Kurimoto, C., H. Inaba, H. Ariyasu, H. Iwakura, Y. Ueda, S. Uraki, K. Takeshima, Y. Furukawa, S. Morita, Y. Yamamoto, S. Yamashita, M. Katsuda, A. Hayata, H.

Akamatsu, M. Jinnin, I. Hara, H. Yamaue, and T. Akamizu. 2020. Predictive and sensitive biomarkers for thyroid dysfunctions during treatment with immune-checkpoint inhibitors. *Cancer Sci* 111: 1468-1477.

26. Kim, K. H., J. Y. Hur, J. Cho, B. M. Ku, J. Koh, J. Y. Koh, J. M. Sun, S. H. Lee, J. S. Ahn, K. Park, M. J. Ahn, and E. C. Shin. 2020. Immune-related adverse events are clustered into distinct subtypes by T-cell profiling before and early after anti-PD-1 treatment. *Oncoimmunology* 9: 1722023.

27. Eun, Y., I. Y. Kim, J. M. Sun, J. Lee, H. S. Cha, E. M. Koh, H. Kim, and J. Lee. 2019. Risk factors for immune-related adverse events associated with anti-PD-1 pembrolizumab. *Sci Rep* 9: 14039.

28. Abolhassani, A. R., G. Schuler, M. C. Kirchberger, and L. Heinzerling. 2019. C-reactive protein as an early marker of immune-related adverse events. *J Cancer Res Clin Oncol* 145: 2625-2631.

29. Pavan, A., L. Calvetti, A. Dal Maso, I. Attili, P. Del Bianco, G. Pasello, V. Guarneri, G. Aprile, P. Conte, and L. Bonanno. 2019. Peripheral Blood Markers Identify Risk of Immune-Related Toxicity in Advanced Non-Small Cell Lung Cancer Treated with Immune-Checkpoint Inhibitors. *Oncologist* 24: 1128-1136.

30. Toi, Y., S. Sugawara, J. Sugisaka, H. Ono, Y. Kawashima, T. Aiba, S. Kawana, R. Saito, M. Aso, K. Tsurumi, K. Suzuki, H. Shimizu, Y. Domeki, K. Terayama, A. Nakamura, S. Yamanda, Y. Kimura, and Y. Honda. 2019. Profiling Preexisting Antibodies in Patients Treated With Anti-PD-1 Therapy for Advanced Non-Small Cell Lung Cancer. *JAMA Oncol* 5: 376-383.

31. Stroud, C. R., A. Hegde, C. Cherry, A. R. Naqash, N. Sharma, S. Addepalli, S. Cherukuri, T. Parent, J. Hardin, and P. Walker. 2019. Tocilizumab for the management of immune mediated adverse events secondary to PD-1 blockade. *J Oncol Pharm Pract* 25: 551-557.

32. Nakamura, Y., R. Tanaka, H. Maruyama, Y. Ishitsuka, N. Okiyama, R. Watanabe, M. Fujimoto, and Y. Fujisawa. 2019. Correlation between blood cell count and outcome of melanoma patients treated with anti-PD-1 antibodies. *Jpn J Clin Oncol* 49: 431-437.

33. Diehl, A., M. Yarchoan, A. Hopkins, E. Jaffee, and S. A. Grossman. 2017. Relationships between lymphocyte counts and treatment-related toxicities and clinical responses in patients with solid tumors treated with PD-1 checkpoint inhibitors. *Oncotarget* 8: 114268-114280.

34. Fujisawa, Y., K. Yoshino, A. Otsuka, T. Funakoshi, T. Fujimura, Y. Yamamoto, H. Hata, M. Gosho, R. Tanaka, K. Yamaguchi, Y. Nonomura, I. Hirai, S. Furudate, H. Okuhira, K. Imafuku, M. Aoki, and S. Matsushita. 2017. Fluctuations in routine

blood count might signal severe immune-related adverse events in melanoma patients treated with nivolumab. *J Dermatol Sci* 88: 225-231.

35. Das, R., N. Bar, M. Ferreira, A. M. Newman, L. Zhang, J. K. Bailur, A. Bacchiocchi, H. Kluger, W. Wei, R. Halaban, M. Sznol, M. V. Dhodapkar, and K. M. Dhodapkar. 2018. Early B cell changes predict autoimmunity following combination immune checkpoint blockade. *J Clin Invest* 128: 715-720.

36. Chaput, N., P. Lepage, C. Coutzac, E. Soularue, K. Le Roux, C. Monot, L. Boselli, E. Routier, L. Cassard, M. Collins, T. Vaysse, L. Marthey, A. Eggermont, V. Asvatourian, E. Lanoy, C. Mateus, C. Robert, and F. Carbonnel. 2017. Baseline gut microbiota predicts clinical response and colitis in metastatic melanoma patients treated with ipilimumab. *Ann Oncol* 28: 1368-1379.

37. Khoja, L., E. G. Atenafu, A. Templeton, Y. Qye, M. A. Chappell, S. Saibil, D. Hogg, M. O. Butler, and A. M. Joshua. 2016. The full blood count as a biomarker of outcome and toxicity in ipilimumab-treated cutaneous metastatic melanoma. *Cancer Med* 5: 2792-2799.

38. Damuzzo, V., S. Solito, L. Pinton, E. Carrozzo, S. Valpione, J. Pigozzo, R. Arboretti Giancristofaro, V. Chiarion-Sileni, and S. Mandruzzato. 2016. Clinical implication of tumor-associated and immunological parameters in melanoma patients treated with ipilimumab. *Oncoimmunology* 5: e1249559.

39. Jaber, S. H., E. W. Cowen, L. R. Haworth, S. L. Booher, D. M. Berman, S. A. Rosenberg, and S. T. Hwang. 2006. Skin reactions in a subset of patients with stage IV melanoma treated with anti-cytotoxic T-lymphocyte antigen 4 monoclonal antibody as a single agent. *Arch Dermatol* 142: 166-172.

40. Kronenberg, K., P. Riquelme, and J. A. Hutchinson. 2019. Standard protocols for immune profiling of peripheral blood leucocyte subsets by flow cytometry using DuraClone IM reagents. *Protocol Exchange*.

41. Hollander, M., D. A. Wolfe, and E. Chicken. 2014. *Nonparametric statistical methods*. Wiley, Hoboken, N.J.

42. Benjamini, Y., and Y. Hochberg. 1995. Controlling the False Discovery Rate: A Practical and Powerful Approach to Multiple Testing. *Journal of the Royal Statistical Society. Series B (Methodological)* 57: 289–300.

43. Team, R. C. R: A language and environment for statistical computing. *R Foundation for Statistical Computing, Vienna, Austria* 2021.

44. Friedman, J., T. Hastie, and R. Tibshirani. 2010. Regularization Paths for Generalized Linear Models via Coordinate Descent. *Journal of statistical software* 33: 1–22.

45. Zou, H., and T. Hastie. 2005. Regularization and variable selection via the elastic net. *Journal of the Royal Statistical Society: Series B (Statistical Methodology)* 67: 301–320.

46. Lang, M., M. Binder, J. Richter, P. Schratz, F. Pfisterer, S. Coors, Q. Au, G. Casalicchio, L. Kotthoff, and B. Bischl. 2019. mlr3: A modern object-oriented machine learning framework in R. *Journal of Open Source Software* 4: 1903.

47. Van Gassen, S., B. Callebaut, M. J. Van Helden, B. N. Lambrecht, P. Demeester, T. Dhaene, and Y. Saeys. 2015. FlowSOM: Using self-organizing maps for visualization and interpretation of cytometry data. *Cytometry A* 87: 636-645.

48. Friedman, J., T. Hastie, and R. Tibshirani. 2010. Regularization Paths for Generalized Linear Models via Coordinate Descent. *J Stat Softw* 33: 1-22.

49. Wright, M. N., and A. Ziegler. 2017. ranger : A Fast Implementation of Random Forests for High Dimensional Data in C++ and R. *Journal of Statistical Software* 77.

50. Tian, Y., M. Babor, J. Lane, V. Schulten, V. S. Patil, G. Seumois, S. L. Rosales, Z. Fu, G. Picarda, J. Burel, J. Zapardiel-Gonzalo, R. N. Tennekoon, A. D. De Silva, S. Premawansa, G. Premawansa, A. Wijewickrama, J. A. Greenbaum, P. Vijayanand, D. Weiskopf, A. Sette, and B. Peters. 2017. Unique phenotypes and clonal expansions of human CD4 effector memory T cells re-expressing CD45RA. *Nat Commun* 8: 1473.

9. Acknowledgement

I would like to express my appreciation to everyone who has contributed to the completion of this Ph.D. thesis. Your support, guidance and encouragement have been invaluable throughout these years. I would like to extend my gratitude to Professor Edward Geissler for bringing me this opportunity. I would also like to acknowledge the academic members and staff who helped me throughout this journey, especially my institution, Leibniz Institute for Immunotherapy (LIT), for funding me. Your contributions, big or small, have made a significant impact on this work. Thank you all for being a part of this academic endeavor and for making this Ph.D. journey an enriching and memorable experience.